Synthesis of Polymer Brushes as Smart Materials for Surface Modification

Anca Mateescu

A thesis

submitted to the University of Crete

in fulfillment of the requirements for the degree

of doctor of Philosophy in Chemistry

Department of Chemistry

University of Crete

&

Foundation for Research and Technology

Institute of Electronic Structure and Laser

2009

Περίληψη

Στην παρούσα εργασία περιγράφεται η σύνθεση πολυμερικών ψηκτρών από επίπεδες επιφάνειες με την τεχνική του ριζικού πολυμερισμού μεταφοράς ατόμου (ATRP) από επιφάνεια. Τα πολυμερικά υμένια που παρασκευάστηκαν χαρακτηρίστηκαν με ελλειψομετρία, μικροσκοπία ατομικών δυνάμεων (AFM), φασματοσκοπία υπερύθρου εσωτερικής ανακλαστικότητας (ATR-FTIR) καθώς και με μετρήσεις γωνίας επαφής.

Στο πρώτο μέρος της εργασίας, περιγράφεται ο εκκινούμενος από επιφάνεια χρυσού πολυμερισμός αποκρινόμενων ομοπολυμερικών και συσταδικών συμπολυμερικών ψηκτρών. Συγκεκριμένα, χρησιμοποιήθηκαν τρία ευαίσθητο-αποκρινόμενα μεθακρυλικά μονομερή, ο μεθακρυλικός 2-(διμεθυλαμινο)αιθυλεστέρας (DMAEMA), ο οποίος είναι υδρόφιλος και ιονιζόμενος, ο μεθακρυλικός 2-(διαιθυλαμινο)αιθυλεστέρας (DEAEMA), που είναι υδρόφοβος και ευαίσθητος στο pH, και το μεθακρυλικό τετραϋδροπυράνιο (THPMA), που είναι υδρόφοβος μεθακρυλικός εστέρας, ο οποίος μπορεί εύκολα να υδρολυθεί σε μεθακρυλικό οξύ (MAA), που είναι υδρόφιλο και ιονιζόμενο μονομερές. Επιπρόσθετα, συντέθηκαν πολυμερικά υμένια αποτελούμενα από ουδέτερες ομάδες, ολιγο(αιθλυλενογλυκόλη) μεθακρυλικού εστέρα (OEGMA). Σε όλα τα παραπάνω πολυμερικά υμένια πραγματοποιήθηκε μελέτη της ικανότητας διαβροχής. Επιπλέον, μελετήθηκε η pH εξαρτώμενη διόγκωση των πολυμερικών ψηκτρών του PDMAEMA. Στην συνέχεια συντέθηκαν επιτυχώς συσταδικές συμπολυμερικές ψήκτρες, γεγονός που αποδεικνύει τον ζωντανό χαρακτήρα των πολυμερισμών. Στις ψήκτρες αυτές πραγματοποιήθηκε μελέτη της ικανότητας διαβροχής σε διάφορους διαλύτες.

Στο δεύτερο τμήμα της διατριβής, παρουσιάζεται η σύνθεση και ο χαρακτηρισμός πολυμερικών ψηκτρών σε τραχείες επιφάνειες πυριτίου. Συγκεκριμένα, πολυμερικές ψήκτρες ευαίσθητες σε μεταβολές του pH, αποτελούμενες από επαναλαμβανόμενες μονάδες του μονομερούς μεθακρυλικός 2-(διισοπρόπυλαμινο)αιθυλεστέρας (DPAEMA) αγκυροβολήθηκαν πάνω σε τραχείες επιφάνειες πυριτίου καθιστώντας τις επιφάνειες ικανές να μετατρέπονται αντιστρεπτά από υδρόφιλες σε χαμηλό pH, σε υπέρ-υδρόφοβες σε υψηλό pH. Οι τραχείες επιφάνειες πυριτίου παρουσιάζουν τραχύτητα σε μίκρο- και νάνο- κλίμακα, μορφολογία παρόμοια με αυτή επιφανειών που συναντώνται στην φύση και έχουν την ικανότητα να απομακρύνουν το νερό. Η ικανότητα διαβροχής των

επιφανειών, στην υπέρ υδρόφοβη κατάσταση χαρακτηρίστηκε με μετρήσεις στατικής γωνίας επαφής και με μελέτες υστέρησης γωνίας επαφής. Επιπλέον διερευνήθηκε ο συντελεστής απόδοσης της ελαστικότητας της ανάκρουσης σταγόνων νερού από τις υπερυδρόφοβες επιφάνειες συναρτήσει της ταχύτητας πρόσκρουσης.

Στο τελευταίο μέρος της εργασίας παρουσιάζεται η άμεση σύνθεση ομοπολυμερικών ψηκτρών υψηλής πυκνότητας σύνδεσης αποτελούμενες από παράγωγα σακχαριτών μεθακρυλικού εστέρα. Συγκεκριμένα, συντέθηκαν ομοπολυμερικες ψήκτρες βασιζόμενες στο μεθακρυλικό (γλυκοαιθυλ)αμίδιο (GAMA), που φέρει μια ομάδα γλυκόζης και στο μεθακρυλικό 2-(λακτοαιθυλ)αμίδιο (LAMA) που φέρει μια ομάδα γαλακτόζης. Σε επιφάνειες χρυσού, πυριτίου/γυαλιού παρασκευάστηκαν πολυμερικά υμένια σακχάρων διαφορετικού πάχους με αλλαγή στις συνθήκες και στον χρόνο πολυμερισμού. Τα πολυμερικά υμένια που συντέθηκαν παρουσιάζουν ισχυρή αλληλεπίδραση δέσμευσης με συγκεκριμένες λεκτίνες γεγονός που επιβεβαιώνεται με μελέτες διέγερσης επιφανειακών πλασμονίων (SPR). Επιπλέον, εξετάστηκε η αλληλεπίδραση ανθρώπινων ηπατικών κυττάρων και κυττάρων του συνδετικού ιστού από ποντίκια με τις γλυκοπολυμερικές ψήκτρες. Τέλος, μελετήθηκε η επίδραση της μοριακής δομής και του πάχους των πολυμερικών υμενίων στην εναπόθεση των κυττάρων.

Abstract

The synthesis of advanced functional materials with well-defined compositions, architectures and functionalities offers a route for tuning the surface properties of materials. Surface-attached polymers became increasingly attractive as reliable means for tailoring the surface properties and their study has received a lot of attention in the last decade. The "grafting from" technique in tandem with controlled surface-initiated polymerizations offers numerous possibilities in designing well-defined grafted polymer layers.

This thesis describes the synthesis of polymer brushes on flat substrates by the "grafting from" technique using atom transfer radical polymerization (ATRP). This polymerization is one of the most robust controlled/"living" radical polymerizations used for the synthesis of polymer brushes as it allows the accurate control of the molecular weight or thickness of the brush while maintaining a low polydispersity. The prepared polymer films were characterized by ellipsometry, atomic force microscopy (AFM), attenuated total reflectance (ATR)-FTIR spectroscopy and contact angle measurements.

The surface-initiated polymerization of responsive homopolymer and block copolymer brushes on gold substrates is described. Three stimuli-responsive methacrylate monomers were used, namely 2-(dimethylamino)ethyl methacrylate (DMAEMA), hydrophilic and ionizable, 2-(diethylamino)ethyl methacrylate (DEAEMA), hydrophobic and pH-sensitive, tetrahydropyranyl methacrylate (THPMA), a hydrophobic methacrylate ester that can be easily hydrolyzed to methacrylic acid (MAA) which is hydrophilic and ionizable. Grafted polymer films comprising of neutral oligo(ethylene glycol) methacrylate (OEGMA) moieties were also synthesized. The wettability of the prepared films and the pH dependent swelling of the PDMAEMA brushes were studied. The living character of the polymerizations was demonstrated by the successful synthesis of block copolymer brushes. The wetting properties of the block copolymer brushes upon solvent treatment were investigated.

pH-responsive polymer brushes comprising of 2-(diisopropylamino)ethyl methacrylate (DPAEMA) monomer repeat units were grafted onto roughened silicon substrates to give surfaces which can reversibly switch between superhydrophilicity at low pH and superhydrophobicity at high pH. The roughened silicon substrates exhibit

hierarchical micro- and nano-roughness, which mimics the morphology of natural water repellent surfaces. The water repellency of the prepared surfaces in their superhydrophobic state was characterized by static contact angle measurements and contact angle hysteresis studies. Moreover, the restitution coefficient of water droplets bouncing off the superhydrophobic surfaces as a function of their impact velocity was investigated.

The direct synthesis of sugar methacrylate-based homopolymer brushes of high grafting densities based on D-gluconamidoethyl methacrylate (GAMA) carrying a glucose functionality and 2-lactobionamidoethyl methacrylate (LAMA) which possesses a galactose group is presented. Glycopolymer films with various thicknesses were prepared on gold, silicon and glass substrates by varying the reaction conditions and the polymerization time. The synthesized glycopolymer films exhibited strong binding interactions with specific lectins via the “glycocluster” effect as verified by surface plasmon resonance (SPR). The interactions of human hepatocyte and mouse fibroblast cell lines with the glycopolymer brushes were investigated and the influence of the glycopolymer molecular structure and film thickness on the cell deposition was studied.

Aim and Outline of the Thesis

This thesis focuses on the synthesis of polymer brushes with well-defined compositions and controlled functionality for altering the surface properties of flat substrates. Polymer brushes refer to an assembly of polymer molecules tethered by one end to a surface or interface. If the grafting density of the polymer molecules is high enough that the individual coils overlap, the polymer chains will stretch away form the substrate in order to avoid overlapping. The synthesis of tethered polymer chains has received a lot of attention in the last decade due to their unique properties and applications. Grafted polymer layers have emerged as potential candidates for the fabrication of novel biomaterials for tissue engineering, cell adhesion and protein recognition. Adhesion, wetting, microfluidics, chemical gating or molecular recognition are among other areas in which these materials will have a great impact. Well-defined polymer brushes with control over the thickness, composition, chain architecture and grafting density can be prepared by a combination of surface-initiated polymerizations (SIP) with modern controlled polymerization methods. By using surface-initiated atom transfer radical polymerization (ATRP), polymer brushes of various structures, compositions and molecular weight were synthesized onto different substrates. In addition, in order to probe the surface properties, optical, spectroscopic and microscopic methods were used for the characterization of the prepared polymer films.

The thesis is organized in to seven chapters. **Chapter 1** aims to give a short introduction on polymer brushes and the methods used for their synthesis focusing on surface-initiated ATRP. The experimental section of the thesis is presented in **Chapter 2. Chapter 3** describes the synthesis of stimuli-responsive polymer brushes from modified gold substrates by surface-initiated ATRP. The surface-initiated polymerization of there different stimuli-responsive methacrylate monomers: 2-(dimethylamino)ethyl methacrylate (DMAEMA), 2-(diethylamino)ethyl methacrylate (DEAEMA) and tetrahydropyranyl methacrylate (THPMA) a methacrylate ester easily hydrolyzed to methacrylic acid (MAA) was investigated. Polymer chains comprising of hydrophilic oligo(ethylene glycol) methacrylate (OEGMA) monomer repeat units were also synthesized. The active chain ends of the prepared homopolymer brushes were used as macroinitiators for the synthesis of block copolymer end-tethered chains. **Chapter 4**

presents a methodology to prepare artificial pH-responsive surfaces which can reversibly switch between superhydrophilicity and superhydrophobicity. Such surfaces were achieved by grafting 2-(diisopropylamino)ethyl methacrylate (DPAEMA) brushes onto micro- and nano- scale roughened silicon substrates. Results on the characterization of the contact angle hysteresis of a superhydrophobic polymer surface based on sliding angle and bouncing drop elasticity measurements are also presented. **Chapter 5** presents the direct synthesis of well defined sugar methacrylate-based homopolymer brushes of high grafting densities based on D-gluconamidoethyl methacrylate (GAMA) and 2-lactobionamidoethyl methacrylate (LAMA) from functionalized gold substrates by surface-initiated ATRP. The synthesis of PGAMA and PLAMA brushes by direct ATRP on glass and silicon substrates is also presented. The protein recognition properties of the prepared glycopolymer films were investigated. The adhesion and spreading behaviour of human hepatocyte and mouse fibroblast cell lines onto the glycopolymer brushes was studied. The conclusions and outlook of this thesis are presented in **Chapter 6**. Finally, **Chapter 7** describes briefly the main experimental techniques used in this study: ellipsometry, atomic force microscopy (AFM), attenuated total reflectance ATR-FTIR spectroscopy, contact angle measurements, surface plasmon resonance (SPR) and gel-permeation chromatography (GPC).

Keywords: surface-initiated ATRP, stimuli-responsive polymer brushes, superhydrophobicity, superhydrophilicity, glycopolymer brushes, lectin recognition, cell adhesion and spreading behavior.

Contents

CHAPTER 1

Introduction

1. 1. Polymer Brushes: Applications and General Features

Thin organic coatings applied on the surface of materials can influence drastically the surface properties of materials. The coating can serve as a barrier against chemical or photochemical degradation or as means to control the interactions between the material and the surrounding environment. Traditional coatings are based on colloidal dispersions such as paint, which create a coating that is thick and not chemically adhered onto the surface. There are more sophisticated ways to prepare coatings and a current employed strategy is the use of self assembled monolayers (SAM). These small molecules posses a reactive head group and can be immobilized onto different substrates. Examples are silanes on oxide surfaces, thiols on gold surfaces, and phosphates on metals. Some limitations of such layers are the inability to control the film thickness and the grafting density of the chains. A new pathway in preparing functional surfaces with control over the film thickness and the grafting density is the tethering of long-chain macromolecules by one end to a surface. If the polymer chains are grafted densely onto a substrate in such a way that the chains become crowded and stretch away from the surface the result is a polymer brush.[1] Due to their robust mechanical and chemical nature, high distribution of functional groups and the possibility to tailor their properties by the brush composition and structure, polymer brushes attracted a lot of interest for potential application in different areas of science and technology. Polymer brushes attracted attention in 1950s when it was found that grafting polymer chains onto colloidal particles was a very effective way to prevent flocculation. Subsequently, it was realized that polymer brushes could be of interest in other applications such as surface modification, new adhesive materials, lubricants and protein resistant biosurfaces. Tailoring materials with “smart” polymer brushes which respond to external stimuli have been employed as biomolecular diagnostics and biosensors, scaffolds for tissue engineering, high capacity ion exchange materials for specific binding or separation, chemical gating and supports for protein immobilization. Some of these applications are schematically represented in Figure 1.

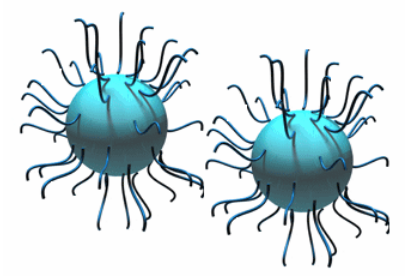

Colloid stabilization

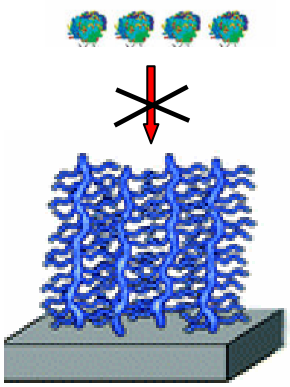

Protein-resistant surfaces

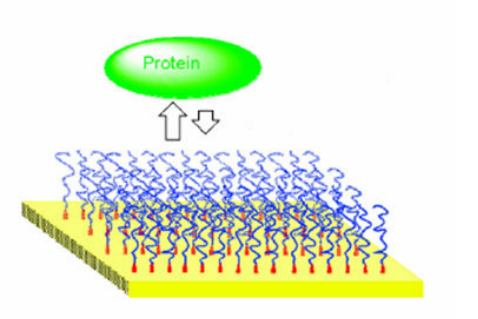

Protein immobilization

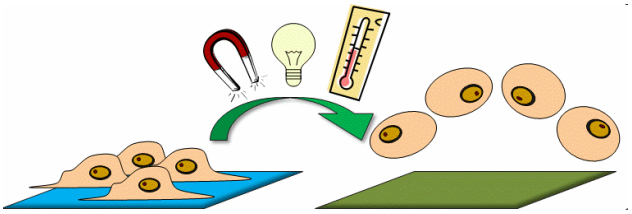

Scaffolds for tissue engineering

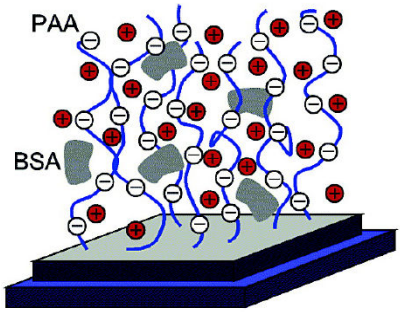

Ion exchange materials

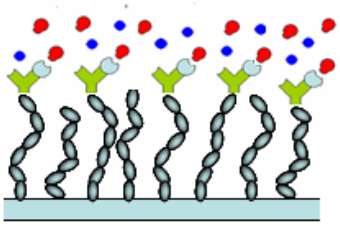

Biosensors

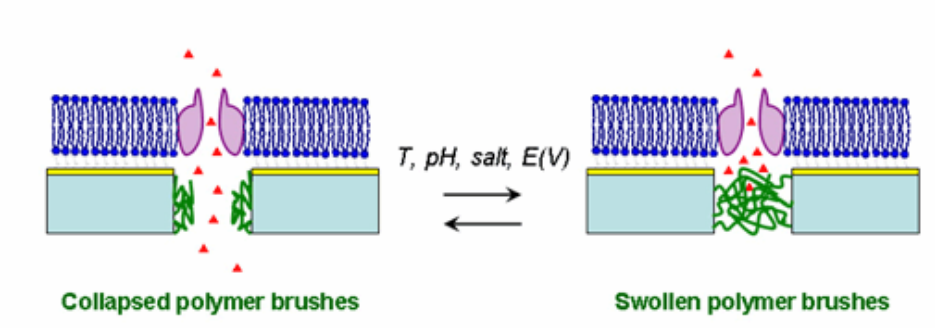

Chemical gating

Figure 1. *Schematic illustration of different applications of polymer brushes.*

Polymer chains can be grafted onto both organic and inorganic materials with either flat or curved surfaces. These may result in planar brushes for flat substrates (Figure 2a), cylindrical brushes for fiber- or rod-like substrates (Figure 2b) or spherical brushes for substrates of spherical shape (Figure 2c).

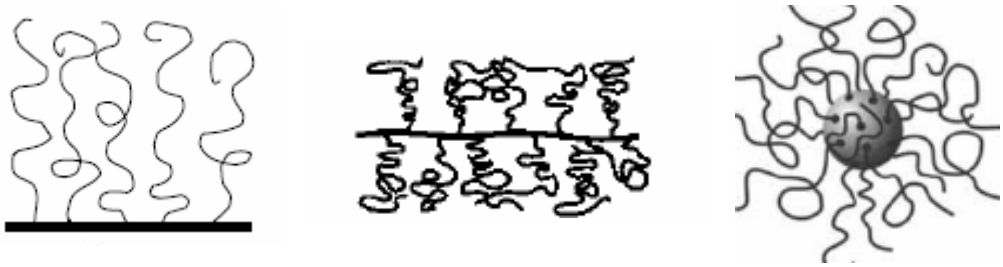

a) **b)** **c)**

Figure 2*. Planar homopolymer brushes (a), cylindrical homopolymer bushes (b) and spherical homopolymer brushes (c).*

In terms of polymer chemical composition, polymer brushes can be divided into homopolymer brushes consisting of one type of monomer repeat unit, mixed homopolymer brushes consisting of two or more types of homopolymer chains, random copolymer brushes consisting of two different monomer repeat units randomly distributed along the polymer chain and block copolymer brushes. Block copolymer brushes refer to an assembly of tethered polymer chains consisting of two or more homopolymer chains covalently connected to each other by one end.

The extension of tethered polymer chains is determined by the dimensionless distance between two grafting points (d) calculated as $2R_g\sigma^{1/2}$, where R_g is the radius of gyration that a free chain would have in solution and σ is the grafting density. The grafted polymer layer forms a brush if the following condition is satisfied: $2R_g\sigma^{1/2} > 1$. Outside this condition ($2R_g\sigma^{1/2} < 1$) the grafted layers are in the so called "mushroom regime" (Figure 3).

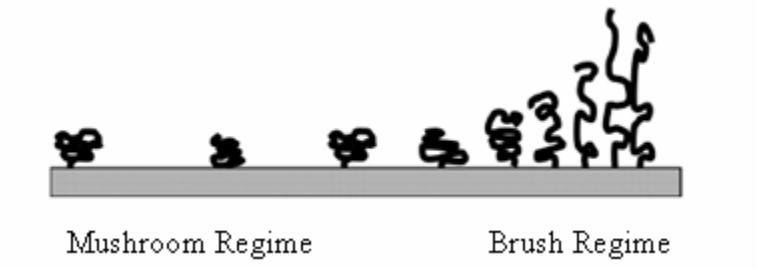

Figure 3. *Schematic representation of the "mushroom regime" and the "brush regime".*

The molecular shape that polymer brushes assume are far from the typical random coil conformation that polymer molecules presume in solution. The chains are strongly stretched and the thickness of the polymer brush increases as the distance between chains decreases. Tethering the chains in close proximity to each other forces the polymer chains to stretch in the direction normal to the plane of grafting in order to minimize segment-segment interactions and to avoid overlapping. The first description of a brush system was first attempted by Alexander. Monodisperse chains consisting of N segments attached to a flat surface with the distance between the anchor points much smaller than the radius of gyration of the free unperturbed chains have been used as a model. The conformation of the brushes is determined by the energy balance between the elastic free energy of the stretched chain and the energy of the interaction between statistical segments (Equation 1. 1):[2, 3]

$$F = F_{int} + F_{el} \qquad 1.\ 1$$

where, F_{int} is the energy difference between stretched and unstretched polymer chains and F_{el} is the elastic free energy.

In a good solvent, the brush height scales with the degree of polymerization/molecular weight of the polymer molecules (N) and the grafting density following Equation 1. 2:

$$h \sim N \times \sigma^{1/3} \qquad 1.\ 2$$

In a poor solvent, the exponent describing the influence of the grafting density is given by Equation 1. 3:

$$h \sim N \times \sigma^{1/2} \qquad 1.\ 3$$

A distinctive characteristic of polymer brushes is that the equilibrium thickness varies linearly with the degree of polymerization, which is different than the size of a polymer coil in solution, where the radius of gyration scales with $R_g \sim N^{0.59}$ for a polymer in a good solvent and $R_g \sim N^{0.50}$ for solutions in poor solvents. This finding, revels that densely tethered polymer chains are deformed. More sophisticated theoretical models, such as numerical and analytical self-consistent field (SCF) theories have been used to better understand the structure of polymer brushes.[4-6] A general result of the SCF calculations is that the polymer chain ends may be located at any distance from the interface onto which the chain is tethered, which means that the segment density profile is parabolic.

1. 2. Synthesis of Polymer Brushes

Polymer brushes are typically synthesised using either of the two techniques physisorption or covalent attachment. Covalent attachment can be achieved by the "grafting to" or "grafting from" techniques.

1. 2. 1. Preparation of polymer brushes by physisorption. Polymer physisorption involves absorption of block copolymers onto a substrate, where one block interacts strongly with the surface and the other block forms the brush layer (Figure 4). Very often the anchoring block has a hydrophobic or an electrostatic interaction with the substrate. Due to the physical nature of the tethering points, the polymer layers are thermally and solvolytically unstable. Additionally, the control of the grafting density is poor.

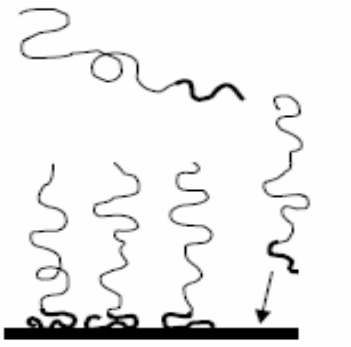

Figure 4. *Preparation of polymer brushes by physisorption.*

1. 2. 2. Preparation of polymer brushes by covalent attachment. "Grafting to" approach. In the "grafting to" approach, preformed end-functionalized polymer chains

react with the surface functionalities of a suitable substrate under appropriate conditions (Figure 5). The polymer molecules must diffuse from the solution through the existing polymer film in order to reach the reactive sites on the surface, thus the technique leads to polymer brushes of low grafting density and low film thickness.

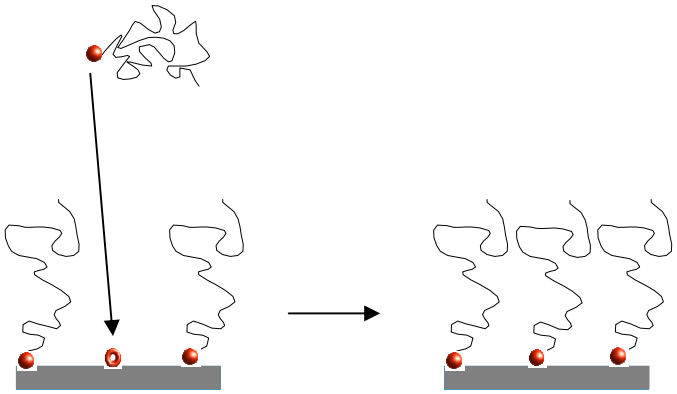

Figure 5. *Preparation of polymer brushes by the "grafting to" technique.*

"Grafting from" approach. The "grafting from" technique involves the immobilizing of initiator molecules onto a substrate followed by in situ surface-initiated polymerization (Figure 6). The surface modification can be performed using Langmuir-Blodgett techniques or SAM deposition. This approach allows the synthesis of uniform polymer brush layers of high grafting density, with tunable brush thicknesses via molecular weight control because in this case a small monomer molecule must diffuse to the chains ends.

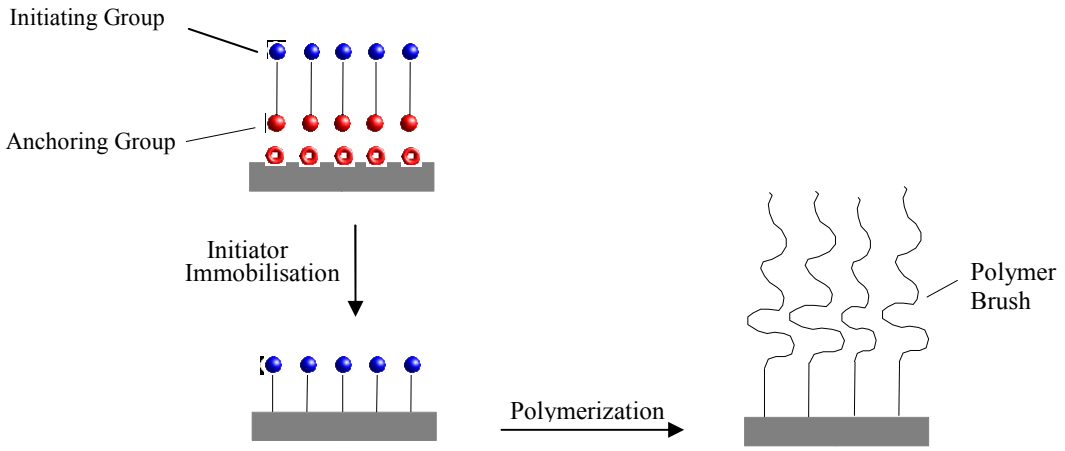

Figure 6. *Preparation of polymer brushes by the "grafting from" approach.*

A. Synthesis of tethered polymer brushes by conventional radical polymerization. There are many reports in the literature on the synthesis of polymer brushes by the "grafting from" technique using the conventional radical polymerization mechanism. Different groups reported the synthesis of polymer brushes using a series of steps. An anchor molecule was immobilized on the substrate, followed by the linkage of the initiating species.[7-9] One major disadvantage of this procedure is the low grafting density of the initiators and grafted polymers if the reactions are not quantitative. To circumvent this problem, a strategy which involves the attachment of the initiator molecule in one step by SAM techniques was implemented.[10, 11] The surface polymerization can be started either thermally through a chemical process or photochemically. An azo free radical initiator is usually employed in the synthesis of the polymer brushes. Under the above conditions thick polymer brushes up to 2000 nm can be prepared.[12, 13]

B. Synthesis of tethered polymer brushes by controlled polymerization techniques. Controlled polymerization techniques are of major interest as they allow the preparation of well-defined uniform polymer brushes with control over the polymer molecular weight and the molecular weight distribution while possessing a variety of functionalities. Additionally, by using a controlled polymerization novel materials such as block copolymer brushes can be successfully prepared. Controlled/living polymerizations techniques, such as anionic and cationic polymerization have been employed for the synthesis of polymer brushes. However, using these techniques, the reaction condition must be very strict and typically the polymer thickness is no greater then 30 nm.[14, 15] "Living" radical polymerization (LRP) techniques including nitroxide mediated polymerization (NMP)[16], atom transfer radical polymerization (ATRP) [17-19] and reversible addition-fragmentation chain transfer (RAFT)[20, 21] have also been used to synthesize polymer brushes. The basic mechanism common to all the mentioned techniques is the alternating activation-deactivation process of the growing chain (Scheme 1). The dormant specie P-X is activated to the polymer radical $P^{\bullet}$, which in the presence of the monomer M will undergo propagation until it is deactivated back to the dormant specie. The cycle is repeated enough times to give every "living" chain an equal chance to grow. The reaction conditions in LRP are more tolerant to impurities than the

ionic systems and also aqueous polymerizations, which afford the preparation of thick polymer brushes, are possible in some of the polymerization techniques.

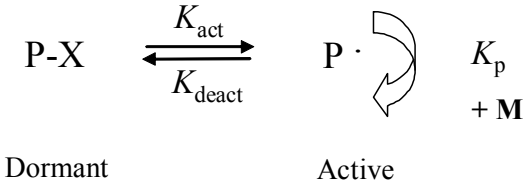

Scheme 1*. General scheme of the reversible activation-deactivation of the polymer chains.*

1. 3. Atom Transfer Radical Polymerization (ATRP)

ATRP is one of the most employed controlled/"living" radical techniques to prepare polymer brushes. It is tolerant to traces of impurities such as water, oxygen, inhibitor, and is readily applicable to industrial processes. ATRP can be carried out either in bulk, in solution, or in emulsion or suspension at temperatures ranging from -20 ° C to 130 °C.

The mechanism of ATRP is shown in Scheme 2. Controlled ATRP is achieved by establishing an equilibrium between the propagating species (the radicals) and the dormant species (the halogen-capped radicals, R-X) with the copper complexes acting as reversible halogen atom-transfer reagents. This process occurs with a rate constant of activation, K_{act}, and deactivation K_{deact}. The growth of polymer chains is achieved by the addition of radicals to the monomer with the rate constant of propagation, K_p. The reactivation of the dormant species allows the polymer chains to reinitiate the growth, only to be deactivated later. This results in polymer chains that steadily grow and have a well-defined group at their end. The reaction equilibrium is shifted to the left side, thus the free radical concentration is kept very low during the polymerization. As a consequence, the contribution of termination (K_t) to the overall reaction is greatly reduced. In a controlled polymerization, besides a low termination rate, a uniform growth of the polymer chains is needed and can be achieved through a fast initiation and fast exchange between the dormant and growing species.[22]

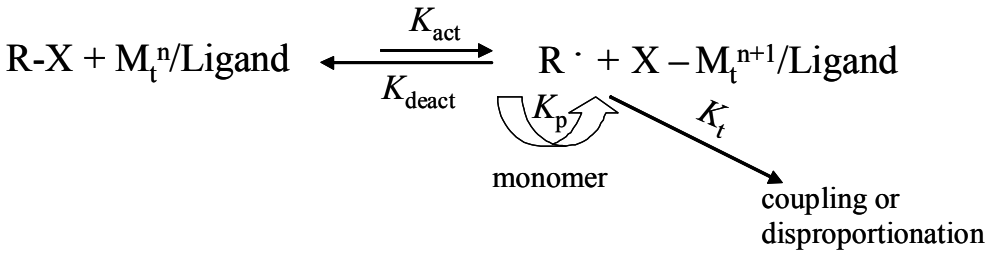

Scheme 2. *General mechanism of ATRP.*

Experimental kinetic studies of ATRP of various monomers,[23-25] using soluble catalyst systems suggest that the rate of polymerization is first order with respect to monomer, initiator and the concentration of the lower oxidation state metal complex and second order with respect to concentration of the higher oxidation state metal complex (Equation 1. 4):

$$R_p = K_p[P^{\cdot}][M] = K_p K_{eq}[I][Me^n][M]/[Me^{n+1}X] \qquad 1.4$$

where, K_p is the rate constant of propagation, $[P^{\cdot}]$ is the radical concentration, [M] is the monomer concentration, K_{eq} is the rate constant of equilibrium, [I] is the initiator concentration, $[Me^n]$ is the transition metal concentration in the lower oxidation state and $[Me^{n+1}X]$ is the transition metal concentration in the higher oxidation state. The rate constant of equilibrium is given by Equation 1. 5:

$$K_{eq} = \frac{K_{act}}{K_{deact}} = \frac{[P^{\cdot}][Me^{n+1}X]}{[Me^n][I]} \qquad 1.5$$

At the beginning of the polymerization, the initial deactivator concentration (transition metal in the higher oxidation state) is not sufficient to ensure a fast rate of deactivation and the coupling of radicals will take place. The radical termination will lead to an increase in the deactivator concentration until a sufficient amount of deactivator is formed, while the radical concentration remains low. At this point, the rate at which radicals combine will become slower then the rate at which radicals react with the deactivator complex and in this way a controlled polymerization is obtained. Only a very small fraction of the growing polymer chains (~5%) will be terminated in the beginning of the polymerization. The proportion of terminated polymer chains can be reduced if an amount of deactivator is added in the beginning of the polymerization.

Similar to a living polymerization, the theoretical molecular weight or the degree of polymerization can be calculated from Equation 1. 6:

$$DP = [M]_o/[I] \times \text{conversion} \qquad 1.6$$

where, $[M]_o$ is the initial monomer concentration. Low molecular weight distribution or polydispersity (M_w/M_n) can be achieved by using ATRP polymerization. Polydispersities lower than 1.10 can be accomplished under certain reaction conditions. In the absence of significant chain termination and transfer, the polydispersity becomes lower with conversion (p) as showed in Equation 1. 7:

$$M_w/M_n = 1 + \left(\frac{[I]K_p}{K_{deact}[Me^{n+1}X]}\right)\left(\frac{2}{p} - 1\right) \qquad 1.7$$

As predicted by Equation 1. 7, for the same monomer, a lower polydispesity can be achieved if the catalyst system deactivates the growing chains faster or if the deactivator concentration is increased.

As remarked above an ATRP system is formed of a monomer, an initiator molecule and a catalyst system composed of a transition metal species with any suitable ligand.

Monomers. A wide range of vinyl monomers have been polymerized by ATRP, including styrenes, (meth)acrylates, (meth)acrylamides, and acrylonitrile. However, up till now acrylic and methacrylic acid cannot be polymerized in a controlled fashion with the available ATRP catalysts. These monomers react rapidly with the metal complexes and form metal carboxylates which are inefficient deactivators for ATRP.

Initiators. In ATRP the initiation is fast and the transfer and termination reactions are negligible. As a consequence, during the polymerization the number of growing chains remains constant and equal to the initial initiator concentration, affording well-defined polymers with narrow molecular weight distributions. Any alkyl halide (RX) such as aryl, carbonyl or allyl groups, can potentially be used as ATRP initiators. For a fast initiation the halide group must undergo a fast interchange between the growing polymer chains and the metal complex. Up to now, best control of the polymerization was obtained when using bromine or chlorine as the halide group.

Catalyst Systems. The catalyst system is based on a transition metal and an appropriate ligand and regulates the polymerization rate and the polydispersity. *(a) Transition Metals.* A large number of transition-metal complexes have been studied as potential ATRP catalysts. Until now, copper-based catalysts have been successfully adapted for the controlled/"living" polymerization of different monomers including styrenes, acrylates, methacrylates, and acrylonitrile. Iron-based catalysts were successfully used for the ATRP of styrenes and methacrylates, while nickel catalysts have been shown to give good results for methacrylate based monomers.

(b) Ligands. The role of the ligand is to solubilize the transition-metal salt in the reaction mixture and adjust the atom transfer equilibrium constant. Different nitrogen, phosphorus, oxygen and sulfur based ligands have been successfully used for ATRP. For copper-mediated ATRP, nitrogen-based ligands were found to work particularly well. A variety of multidentate nitrogen based ligands have been prepared and the most effective are the ones based on 2,2'bipyridine, alkyl substituted bipyridines, linear, branched and cyclic amines.

Due to the control over the end group functionality and the ability to use a range of different monomers, ATRP can be used to synthesize a large variety of new polymeric materials by varying the polymer microstructure (linear, branched or multi-armed star-shaped polymers) and/or the composition (random, alternating, gradient and block copolymers which are synthesized by using the ATRP homopolymers as macroinitiators).

1. 3. 1. ATRP form flat surfaces. ATRP can be used to prepare well-defined polymer brushes for tailoring the surface properties on different types of substrates such as planar surfaces, inorganic particles/colloids or polymer chains. Surface confined polymerization brings about some differences compared to solution polymerization, which comes from the immobilization of initiating (dormant) species and tethering and crowding of polymer chains on the surface. As mentioned earlier, for a good control of the polymerization a sufficient amount of deactivator must be present in the polymerization. In solution ATRP the required deactivator is formed by the termination of a few percent of the polymer chains in the early stages of the reaction. However, in systems where initiator groups are adsorbed on a very low surface area such as a flat substrate, the low concentration of the

initiator is insufficient to form the desired deactivator complex to control the polymerization.[26] Two different approaches have been used to control the growth of polymer brushes and to ensure the presence of a sufficient amount of deactivator throughout the course of the polymerization. One approach involves the addition of untethered small molecule initiators, the so called free or "sacrificial" initiator in the reaction mixture.[27,28] This leads to the formation of the required deactivator concentration by the termination of a few percent of the polymer chains via redox reactions in solution. By using this approach, the molecular weight of the free polymer can serve as a measure of the molecular weight and molecular weight distribution of the polymer chains grown on the surface. However, this approach limits the maximum thickness of the polymer layer, as most of the monomer is consumed by the polymer formed in solution.[29] The other method requires the addition of deactivator with the catalyst system at the beginning of the polymerization.[17] This facilitates exchange reactions between the active radicals and the dormant species. Surface-initiated ATRP performed without the addition of deactivator at the beginning of the reaction results in fast polymerizations and termination of the tethered polymer chains. If a sufficient amount of deactivator is added in the reaction mixture a linear increase of the polymer film thickness with time is obtained.

1. 4. References

1. B. Zhao; W. J. Brittain, *Prog. Polym. Sci.* **2000,** *25*, 677-710.
2. S. Alexander, *J. Phys.* **1977,** *38*, 983-987.
3. S. T. Milner, *Science* **1991,** *251*, 905-914.
4. E. B. Zhulina; O. V. Borisov; V. A. Pryamitsyn; T. M. Birshtein, *Macromolecules* **1991,** *24*, 140-149.
5. C. M. Wijmans; J. M. H. M. Scheutjens; E. B. Zhulina, *Macromolecules* **1992,** *25*, 2657-2665.
6. S. T. Milner; T. A. Witten; M. E. Cates, *Macromolecules* **1988,** *21*, 2610-2619.
7. T. Sugawara; T. Matsuda, *Macromolecules* **1994,** *27*, 7809-7814.
8. N. Tsubokawa; A. Kogure; K. Maruyama; Y. Sone; M. Shimomura, *Polym. J.* **1990,** *22*, 827-833.

9. A. Sidorenko; S. Minko; K. Schenk-Meuser; H. Duschner; M. Stamm, *Langmuir* **1999,** *15*, 8349-8355.
10. O. Prucker; J. Rühe, *Langmuir* **1998,** *14*, 6893-6898.
11. M. Biesalski; J. Rühe, *Macromolecules* **1999,** *32*, 2309-2316.
12. M. Biesalski; D. Johannsmann; J. Rühe, *J. Chem. Phys.* **2002,** *117*, 4988-4994.
13. M. Biesalski; J. Rühe, *Macromolecules* **2003,** *36*, 1222-1227.
14. R. Advincula; Q. Zhou; M. Park; S. Wang; J. Mays; G. Sakellariou; S. Pispas; N. Hadjichristidis, *Langmuir* **2002,** *18*, 8672-8684.
15. R. Jordan; A. Ulman, *J. Am. Chem. Soc.* **1998,** *120*, 243-247.
16. X. Guo; A. Weiss; M. Ballauff, *Macromolecules* **1999,** *32*, 6043-6046.
17. K. Matyjaszewski; P. J. Miller; N. Shukla; B. Immaraporn; A. Gelman; B. B. Luokala; T. M. Siclovan; G. Kickelbick; T. Valiant; H. Hoffmann; T. Pakula, *Macromolecules* **1999,** *32*, 8716-8724.
18. M. Ejaz; S. Yamamoto; K. Ohno; Y. Tsujii; T. Fukuda, *Macromolecules* **1998,** *31*, 5934-5936.
19. C. Perruchot; M. A. Khan; A. Kamitsi; S. P. Armes; T. Von Werne; T. E. Patten, *Langmuir* **2001,** *17*, 4479-4481.
20. M. Baum; W. J. Brittain, *Macromolecules* **2002,** *35*, 610-615.
21. Y. Tsujii; M. Ejaz; K. Sato; A. Goto; T. Fukuda, *Macromolecules* **2001,** *34*, 8872-8878.
22. K. Matyjaszewski; J. Xia, *Chem. Rev.* **2001,** *101*, 2921-2990.
23. K. Matyjaszewski; T. E. Patten; J. Xia, *J. Am. Chem. Soc.* **1997,** *119*, 674-680.
24. J. L. Wang; T. Grimaud; K. Matyjaszewski, *Macromolecules* **1997,** *30*, 6507-6512.
25. V. Percec; B. Barboiu; H. J. Kim, *J. Am. Chem. Soc.* **1998,** *120*, 305-316.
26. J. Pyun; T. Kowalewski; K. Matyjaszewski, *Macromolecular Rapid Communications* **2003,** *24*, 1043-1059.
27. M. Ejaz; S. Yamamoto; K. Ohno; Y. Tsujii; T. Fukuda, *Macromolecules* **1998,** *31,* , 5934-5936.

28. M. Husseman; E. E. Malmström; M. McNamara; M. Mate; D. Mecerreyes; D. G. Benoit; J. L. Hedrick; P. Mansky; E. Huang; T. P. Russell; C. J. Hawker, *Macromolecules* **1999,** *32*, 1424-1431.
29. Q. Yang; J. Tian; M. X. Hu; Z. K. Xu, *Langmuir* **2007,** *23*, 6684-6690.

CHAPTER 2

Experimental Section

2. 1. Materials

2-(dimethylamino)ethyl methacrylate (DMAEMA, 98%, Aldrich), 2-(diethylamino)ethyl methacrylate (DEAEMA, 99%, Aldrich), oligo(ethylene glycol) methacrylate, (OEGMA, M_n ~ 526, Aldrich), poly(ethylene glycol) methyl ether methacrylate (MeOEGMA, M_n ~ 475, Aldrich) were passed through neutral alumina column before use. 2-(diisopropylamino)ethyl methacrylate (DPAEMA, Scientific Polymer Products) was passed through an inhibitor-removing column DHR-4 before use. Copper (I) bromide (CuBr, 99.999%, Aldrich), copper (II) chloride ($CuCl_2$, 99.999%, Aldrich), 2,2'- bipyridyl (Bpy, ≥ 98%, Fluka), 1,1,4,7,10,10-hexamethyltriethylenetetramine (HMTETA, 97%, Aldrich), *N*,*N*,*N*′,*N*′-tetramethylethylenediamine (TMEDA, 99%, Fluka), 11-mercapto-1-undecanol (97%, Aldrich), ethyl 2-bromoisobutyrate (EBIB, 98%, Aldrich), 3-aminopropyltrimethoxysilane (≥ 97%, Fluka), allyl alcohol (99%, Sigma-Aldrich), triethoxysilane (≥ 97%, Fluka), Karstedt catalyst solution (platinum(0)-1-3-divinyl-1,1,3,3-tetramethyldisiloxane complex, 2% Pt Aldrich), magnesium sulfate ($MgSO_4$, ≥ 99.5%, Sigma-Aldrich) were used as received without further purification. Pyridine (≥ 99%, Sigma), 2-bromoisobutyryl bromide (98%, Aldrich) and triethylamine (TEA, 99%, Sigma-Aldrich) were freshly distilled before use. Concanavalin A (Con A) (isolated from Jack bean) and *Ricinus communis* agglutinin (RCA_{120}) were purchased from Sigma. Dulbecco's modified Eagle's medium (DMEM) and phosphate buffer solution (PBS) were purchased from Wako Pure Chemicals Co. (Tokyo, Japan) and Sigma Aldrich. Paraformaldehyde (PFA) was purchased from Wako Pure Chemicals Co. (Tokyo, Japan). Tissue culture grade polystyrene (TCPS) dishes were purchased from Iwaki (Chiba, Japan). Hep G2 cells, fetal bovine serum (FBS) and antibiotics (penicillin and streptomycin) were purchased from Sigma Aldrich. Other chemicals and solvents were used as received. D-gluconamidoethyl methacrylate (GAMA) and 2-lactobionamidoethyl methacrylate (LAMA) were synthesized according to the method reported previously by

Narain et al.[1-3] Tetrahydropyranyl methacrylate (THPMA) was synthesized according to Lowe et al.[4]

2. 2. Analytical Methods

The synthesized polymer films were characterized by ellipsometry, atomic force microscopy (AFM), attenuated total reflectance ATR-FTIR spectroscopy and contact angle measurements. A variable angle spectroscopic ellipsometer (model VASE, J. A. Woollam Co., Inc.) was used to determine the thickness and the refractive index of the polymeric films. The measurements were performed at three different angles of incidence 60^o, 70^o and 75^o in the wavelength range 450 – 1200 nm. AFM studies were performed at ambient conditions on a multimode Nanoscope III instrument (Digital Instruments, Veeco) operating in tapping mode at 1 Hz scan rate. Silicon tips with a spring constant of 20 N/m and frequency of 267 – 348 KHr were used. For the AFM experiments carried out in liquid cell, tips with a spring constant of 2.8 N/m and frequency of 30 – 60 KHr were used. The root-mean square roughness was evaluated using the integrated software. ATR-FTIR spectra were measured on a Nicolet 6700 optical spectrometer. For each spectrum 200 scans were collected in the range of 400 - 4000 cm^{-1} with a resolution of 4 cm^{-1}. The static contact angles were determined by the sessile drop method on a homemade instrument using a 2 μL drop of nanopure water (18.2 MΩ). Images of the droplet on the substrate were recorded using a camera and the contact angles were calculated from these images using the appropriate software. For each sample, at least three measurements from different surface locations were averaged. Successive measurements were reproducible within ±1°. A tilt stage assembly, with an extendable lever arm that permitted continuous inclination of the surface from horizontal, was used in order to determine the angle at which a drop starts to move (the sliding angle). Depending on the variability of the data, a mean sliding angle value was calculated from five to ten individual measurements. The advancing and receding angles were determined from the drop-snapshot just before slippage occurred; on a drop about to slide, the wetting angle on the lower edge is the advancing angle, whereas that on the upper edge is the receding angle. The dynamic behavior of water droplets free falling on flat or patterned surfaces was followed using a high-speed camera at a frame rate of up to

1000Hz. The velocities before and after each shock were calculated either from the distance traveled between successive snapshots (at high impact speeds) or from the corresponding maximum heights attained (at low impact speeds).

The molecular weight of the polymers synthesized in solution by the free initiator was determined by gel permeation chromatography (GPC) (Thermo Finnigan, equipped with two columns, Mixed-D and Mixed-E) using tetrahydrofuran (THF) as the mobile phase. Aqueous GPC was used to characterize the molecular weight of the glycopolymers synthesized in the presents of free initiator. Chromatograms were recorded from a conventional Viscotek GPC system using two Waters WAT011545 columns and 0.1 M sodium nitrate as eluent at a flow rate of 1.0 mL/min, at room temperature. Seven near-monodisperse Pullulan standards (M_w = 5,900 - 404,000 g mol^{-1}) were used for calibration.

The interactions of the synthesized glycopolymer layers with different lectines were monitored by surface plasmon resonance (SPR) measurements using an IBIS II instrument. All measurements were performed at 25 °C.

2. 3. Synthesis of Stimuli-Responsive Homopolymer and Block Copolymer Brushes on Gold Substrates

2. 3. 1. Synthesis of the surface initiator ω-mercaptoundecyl bromoisobutyrate. The surface-bound initiator was synthesized using the procedure developed by Huck and co-workers (Scheme 1).[5] Briefly, the thiol initiator was synthesized by dissolving mercaptoundecanol (0.75 g, 3.67 mmol) and pyridine (0.27 mL, 3.34 mmol) in a flask containing freshly distilled dichloromethane (DCM) (15 mL) under nitrogen. Bromoisobutyryl bromide (0.41 mL, 3.34 mmol) was added dropwise to the stirred solution at 0 °C. The reaction was stirred at 0 °C for 1 h and then at room temperature for 18 h. Water was added and the product was extracted with ether, which was removed afterwards under reduced pressure. The white extract was redissolved in ether, washed with saturated ammonium chloride, and dried over $MgSO_4$. The volatiles were evaporated under reduced pressure. The product was then distilled in a Büchi Kugharal equipment to give the final product as a colorless oil (230 mg, 0.65 mmol). ^{1}H NMR ($CDCl_3$): δ 4.15 (t,

2H, OCH_2), 2.45 (q, 2H, SCH_2), 1.92 (s, 6H, CH_3), 1.57-1.68 (m, 4H, CH_2), 1.27-1.35 (m, 14H, CH_2).

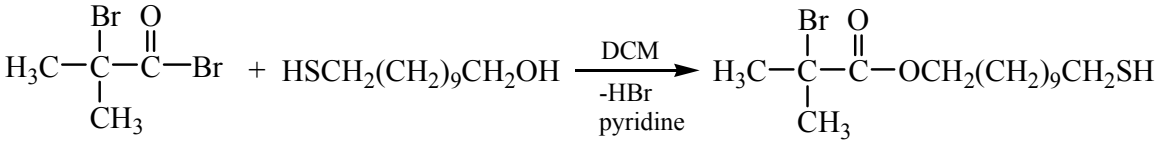

2- bromoisobutyryl bromide | mercaptoundecanol | mercaptoundecyl bromoisobutyrate

Scheme 1. *Chemical diagram describing the synthesis of the ATRP initiator ω-mercaptoundecyl bromoisobutyrate.*

2. 3. 2. Initiator self-assembly. The self-assembled monolayer (SAM) was formed by immersing the gold-coated silicon wafer (45 nm of gold sputtered on 2 nm of chromium on a silicon wafer) in a vial containing an ethanolic solution of the ATRP initiator, ω-mercaptoundecyl bromoisobutyrate, for 24 h. After the incubation period the substrate was rinsed extensively with ethanol, dried under a stream of nitrogen and transferred to the polymerization flask.

2. 3. 3. Surface-initiated polymerization of homopolymer brushes on gold substrates. Surface-initiated polymerizations of DMAEMA, DEAEMA, THPMA and OEGMA were carried out in various solvents at room temperature. Table 1 summarize the ATRP reaction conditions used for the synthesis of PDMAEMA grafted polymer films, while Table 2 summarizes the reaction condition used for the synthesis of PDEAEMA and PTHPMA brushes. The reaction conditions used for the synthesis of POEGMA and PMeOEGMA films are presented in Table 3. Table 4 lists the ATRP reaction conditions used for the synthesis of polymer brushes in the presence of free initiator EBIB.

Details for a typical protocol are given below for DMAEMA in 4/1 v/v methanol/water mixture. An initiator coated gold substrate was placed in a reaction flask under nitrogen atmosphere. In a separate flask, DMAEMA (10 g, 64 mmol) was dissolved in a 4/1 methanol/water mixture (10 mL). Copper (I) bromide (0.1435 g, 1 mmol), 2,2'- bipyridyl (0.32 g, 2 mmol) and copper (II) chloride (0.0135 g, 0.1 mmols) were added next and the solution was purged with nitrogen. After stirring for 20 minutes at room temperature the dark brown solution was transferred to the flask containing the

substrate. The polymerization was allowed to proceed for a predetermined period of time before the reaction was quenched by exposure to air. The ungrafted polymer was removed from the substrate by washing extensively with methanol and water, followed by washing in the ultrasonic bath. For the polymerizations carried out in the absence of copper(II), EBIB free initiator (16.48 μL, 0.11 mmols) was added to ensure the controlled synthesis of the polymer chains. In this case, the ATRP catalyst was removed from the reaction medium by passing the solution through a basic alumina column. Excess solvent was removed using a rotary evaporator before the polymer was precipitated in *n*-hexane. The obtained solid product was dried in a vacuum oven at RT and was characterized by GPC.

Table 1. Reaction conditions used for the synthesis of PDMAEMA homopolymer brushes

Monomer	Polymerization conditions	Solvent (v/v)	Reaction time (h)
DMAEMA	10 g (64 mmol) DMAEMA 0.32 g (2 mmol) Bpy 0.1435 g (1mmol) $Cu^{I}Br$	$MeOH/H_2O$ = 3/2	0.25
			0.5
			1
			2
	10 g (64 mmol) DMAEMA 0.32 g (2 mmol) Bpy 0.1435 g (1 mmol) $Cu^{I}Br$ 0.0135 g (0.1 mmol) $Cu^{II}Cl$	$MeOH/H_2O$ = 4/1	0.25
			0.5
			1
			2
			3
		MeOH	2
			5
			24
	10 g (64 mmol) DMAEMA 0.23 g (2 mmol) TMEDA 0.1435 g (1 mmol) $Cu^{I}Br$	acetone	2
			10
		THF	2
			10

Table 2. Reaction conditions used for the synthesis of PDEAEMA and PTHPMA homopolymer brushes

Monomer	Polymerization conditions	Solvent (v/v)	Reaction time (h)
DEAEMA	10 g (54 mmol) DEAEMA 230 µL (0.84 mmol) HMTETA 0.121 g (0.84 mmol) $Cu^{I}Br$	MeOH	0.5
			3
			24
	10 g (54 mmol) DEAEMA 0.27 g (1,68 mmol) Byp 0.121 g (0.84 mmol) $Cu^{I}Br$	MeOH	6
			24
	10 g (54 mmol) DEAEMA 0.27 g (1,68 mmol) Byp 0.121 g (0.84 mmol) $Cu^{I}Br$ 0.0114 g (mmol 0.084) $Cu^{II}Br$	MeOH	3
			6
			24
THPMA	5 g (29.4 mmol) THPMA 0.066 g (0.46 mmol) $Cu^{I}Br$ 125 µL (0.46 mmol) HMTETA	MeOH	2
			4
		o-dichlorobenzene	6
			24

Table 3. Reaction conditions used for the synthesis of POEGMA and PMeOEGMA homopolymer brushes

Monomer	Polymerization conditions	Solvent (v/v)	Reaction time (h)
OEGMA	10 g (19 mmols) OEGMA 0.094 g (0.6 mmol) Bpy 0.043 g (0.3 mmol) $Cu^{I}Br$ 0.0043 g (0.03 mmol) $Cu^{II}Cl$	H_2O	0.25
			0.5
			1
		$MeOH/H_2O$ = 4/1	0.25
			0.5
			1
MeOEGMA	10 g (21 mmols) OEGMA 0.1 g (0.66 mmol) Bpy 0.047 g (0.33 mmol) $Cu^{I}Br$ 0.0047g (0.033mmol) $Cu^{II}Cl$	$MeOH/H_2O$ = 4/1	1.5

.

Table 4. Reaction conditions used for the synthesis polymer brushes in the presence of EBIB

Monomer	Polymerization conditions	Reaction time (h)
DMAEMA	0.1435 g (1 mmol) $Cu^{I}Br$ 16.48 µL (0.11 mmol) EBIB $MeOH/H_2O$ = 4/1	18
	0.0117 g (0.12 mmol) $Cu^{I}Cl$ 8.8 µL (0.06 mmol) EBIB Bulk	20
DEAEMA	0.121 g (0.84 mmol) $Cu^{I}Br$ 13.9 µL (0.093 mmol) EBIB MeOH	24
THPMA	0.066 g (0.46 mmol) $Cu^{I}Br$ 7.6 µL (0.051 mmol) EBIB MeOH	5
MeOEGMA	0.047 g (0.33 mmol) $Cu^{I}Br$ 5.4 µL (0.036 mmol) EBIB $MeOH/H_2O$ = 4/1	3

2. 3. 4. Surface-initiated polymerization of block copolymer brushes. For the synthesis of the block copolymer brushes the above procedure was repeated using a polymer coated substrate immersed in a solution of a second monomer. Two homopolymer brushes were prepared in the same reaction flask, one of which was used for the characterization of the homopolymer film, while the second was used as the substrate onto which the second block was grown. Details for a typical protocol are given below for a PDMAEMA-*b*-POEGMA diblock copolymer brush. First, a PDMAEMA brush was prepared in a 4/1 methanol/water mixture in the presence of copper (II). The polymerization was stopped after 30 min of reaction time and a second block consisting of POEGMA was synthesized next. In a separate flask OEGMA (10 g, 19 mmols) was dissolved in water (10 mL). Copper (I) bromide (0.043 g, 0.3 mmols), 2,2'- bipyridyl (0.094 g, 0.6 mmols) and copper (II) chloride (0.0043 g, 0.03 mmols) were added next and the solution was purged with nitrogen. After stirring for 20 minutes at room temperature the solution was transferred to a degassed flask containing the PDMAEMA modified substrate. The polymerization was allowed to proceed for another 30 min after which the reaction was quenched by exposure to air. After the polymerization, the substrate was removed from the polymerization solution and rinsed extensively with methanol and water, followed by washing in the ultrasonic bath. Table 5 summarizes the ATRP reaction conditions used for the synthesis of the block copolymer brushes.

Table 5. Reaction conditions used for the synthesis of diblock copolymer brushes

Sample		Reaction conditions	Reaction time (h)
PDMAEMA-*b*-POEGMA	Thetered block	Cu(I)/Cu(II)/Bpy MeOH/H_2O = 4/1	0.5
	Outer block	Cu(I)/Cu(II)/Bpy H_2O	0.5
POEGMA-b-PDMAEMA	Thetered block	Cu(I)/Cu(II)/Bpy H_2O	0.5
	Outer block	Cu(I)/Cu(II)/Bpy MeOH/H_2O = 4/1	0.5
POEGMA-b-PDMAEMA	Thetered block	Cu(I)/Cu(II)/Bpy MeOH/H_2O = 3/2	1
	Outer block	Cu(I)/Cu(II)/Bpy MeOH/H_2O = 4/1	2
POEGMA-b-PDMAEMA	Thetered block	Cu(I)/Cu(II)/Bpy MeOH/H_2O = 4/1	1
	Outer block	Cu(I)/Cu(II)/Bpy MeOH/H_2O = 4/1	2
PMeOEGMA-*b*-PDMAEMA	Thetered block	Cu(I)/Cu(II)/Bpy MeOH/H_2O = 4/1	1.5
	Outer block	Cu(I)/Cu(II)/Bpy MeOH/H_2O = 4/1	2
PDMAEMA-*b*-PDEAEMA	Thetered block	Cu(I)/Cu(II)/Bpy MeOH/H_2O = 4/1	2
	Outer block	Cu(I)/HMTETA MeOH	1
PDEAEMA-*b*-PDMAEMA	Thetered block	Cu(I)/HMTETA MeOH	0.5
	Outer block	Cu(I)/Cu(II)/Bpy MeOH/H_2O = 4/1	3
PDEAEMA-*b*-PDMAEMA	Thetered block	Cu(I)/Cu(II)/Bpy MeOH/H_2O = 4/1	3
	Outer block	Cu(I)/Cu(II)/Bpy MeOH/H_2O = 4/1	2
PDEAEMA-*b*-PDMAEMA	Thetered block	Cu(I)/Cu(II)/HMTETA MeOH	0.5
	Outer block	Cu(I)/Cu(II)/Bpy MeOH/H_2O = 4/1	2

Table 5. Continued

Sample		Reaction conditions	Reaction time (h)
PDMAEMA-*b*-PTHPMA	Thetered block	Cu(I)/Cu(II)/Bpy MeOH/H_2O = 4/1	3
	Outer block	Cu(I)/HMTETA o-dichlorobenzene	24
PTHPMA-*b*-PDMAEMA	Thetered block	Cu(I)/Cu(II)/Bpy MeOH	5
	Outer block	Cu(I)/Cu(II)/Bpy MeOH/H_2O = 4/1	2
PTHPMA-*b*-PDMAEMA	Thetered block	Cu(I)/HMTETA o-dichlorobenzene	24
	Outer block	Cu(I)/Cu(II)/Bpy MeOH/H_2O = 4/1	2
PTHPMA-*b*-PDMAEMA	Thetered block	Cu(I)/Bpy MeOH	2
	Outer block	Cu(I)/Cu(II)/Bpy MeOH/H_2O = 4/1	2
PTHPMA-*b*-PDMAEMA	Thetered block	Cu(I)/Bpy THF	20
	Outer block	Cu(I)/Cu(II)/Bpy MeOH/H_2O = 4/1	2
PTHPMA-*b*-PDMAEMA	Thetered block	Cu(I)/HMTETA THF	20
	Outer block	Cu(I)/Cu(II)/Bpy MeOH/H_2O = 4/1	2
PTHPMA-*b*-PDMAEMA	Thetered block	Cu(I)/HMTETA MeOH	2
	Outer block	Cu(I)/Cu(II)/Bpy MeOH/H_2O = 4/1	2

2. 4. Synthesis of Stimuli Responsive Polymer Brushes on Flat and Artificially Structured Silicon Substrates

2. 4. 1. Synthesis of the surface initiator 3-(2-bromoisobutyramido) propyl(trimethoxy)silane. The surface-bound initiator was synthesized using the procedure developed by Klok and co-workers (Scheme 2).[6] In a flask containing 3-aminopropyltrimethoxysilane (3.5 mL, 20 mmol) were added 30 mL of anhydrous tetrahydrofuran (THF) and freshly distilled triethylamine (3.35 mL, 24 mmol). 2-bromoisobutyrylbromide (3 mL, 24 mmol) was added next under ice cooling. The

solution was allowed to warm to room temperature and stirring was continued for an additional 3 h. The triethylammonium bromide salt was removed by filtration and the excess solvent was evaporated under vacuum. Residual triethylammonium bromide that precipitated upon evaporation was removed by filtration and the product was evaporated to dryness. In order to remove all the side products the oily residue was stirred under vacuum at 50 °C for 5 h. The final product (5.68 g, 17.29 mmol) was stored at 4 °C under a nitrogen atmosphere. ^{1}H NMR ($CDCl_3$): δ 6.85 (s, 1H, NH), 3.48 (s, 9H, Si-O-CH_3), 3.24 (m, 2H, CH_2), 1.95 (s, 6H, CH_3), 1.62 (m, 2 H, CH_2), 0.64 (t, 2H, Si-CH_2).

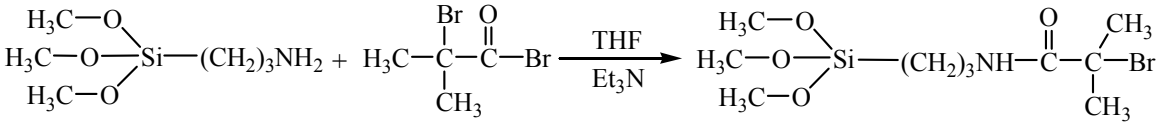

3-aminopropyltri-methoxysilane

2- bromoisobutyryl bromide

3-(2-bromoisobutyramido)propyl (trimethoxy)silane

Scheme 2. *Reaction scheme for the synthesis of the surface attached initiator 3-(2-bromoisobutyramido)propyl(trimethoxy)silane.*

2. 4. 2. Initiator self-assembly. SAM were formed by immersing overnight a thermally oxidized silicon substrate in a vial containing a 40 mM solution of the 3-(2-bromoisobutyramido)propyl(trimethoxy)silane initiator in anhydrous THF. After the incubation period, the substrate was rinsed extensively with anhydrous THF, dried under a stream of nitrogen and transferred to the polymerization flask.

2. 4. 3. Surface-initiated polymerization of stimuli-responsive brushes on silicon substrates. Surface-initiated ATRP of DEAEMA and DPAEMA monomers was carried out from the initiator-modified silicon substrates. A typical polymerization protocol for the growth of the DPAEMA brushes is given below. A flat and a rough silicon substrate modified with the ATRP initiator were placed in a reaction flask under a nitrogen atmosphere. In a separate flask DPAEMA (2 g, 9.345 mmol) was dissolved in DMF (10 ml). Copper (I) bromide (0.0717 g, 0.499 mmol) and HMTETA (136 μL, 0.499 mmol) were added next and the solution was purged with nitrogen. After stirring for 20 minutes at room temperature the solution was transferred to the flask containing the substrates. EBIB free initiator (8.16 μL, 0.055 mmol) was also added to the polymerization mixture,

which resulted in the formation of free polymer in solution. The polymerization was allowed to proceed for 24 h at 70 °C before the reaction was quenched by exposure to air. The substrates were cleaned by extensive washing with DMF and acetone, followed by sonication in an ultrasonic bath. The ATRP catalyst was removed from the reaction medium by passing the solution through a basic alumina column. Excess solvent was evaporated using a rotary evaporator before the polymer was precipitated in water. A similar protocol was employed for the ATRP of DEAEMA in methanol at room temperature, using copper(I) bromide and HMTETA as the catalyst system.

2. 5. Synthesis of Glycopolymer Brushes on Gold Substrates

2. 5. 1. Surface-initiated polymerization of glycopolymers. The ω-mercaptoundecyl bromoisobutyrate modified gold substrate and the free initiator EBIB (0.0042 mmol) were placed in a flask under a nitrogen atmosphere. In a separate flask, GAMA (0.5 g, 1.62 mmol) was dissolved in a 4/1 methanol/water mixture (5 mL). The solution was heated at 70 ^{o}C to facilitate the monomer dissolution. Copper (I) bromide (0.01 g, 0.07 mmol) and 2,2'- bipyridyl (0.022 g, 0.14 mmol) were added next and the solution was purged with nitrogen. For the polymerizations carried out in the absence of free initiator, 0.1 mol% of Cu(II) deactivator relative to Cu(I) was also added with the catalyst system to ensure the controlled growth of the glycopolymer chains. After stirring for 20 minutes at room temperature the solution was transferred to the flask containing the substrate. The polymerization was allowed to proceed for a predetermined period of time before the reaction was quenched by exposure to air. After the polymerization, the substrate was removed and rinsed extensively with water and ethanol and was dried under a nitrogen flow. The ATRP catalyst was removed from the reaction medium by passing the solution through a basic alumina column and next the solvent was removed under vacuum using a rotary evaporator. The solid product was dried in a vacuum oven at RT for 3 days. The obtained polymer was characterized by aqueous GPC. A similar protocol was used for the ATRP synthesis of end-grafted GAMA and LAMA homopolymer chains in water and in a 3/2 methanol/water mixture. For the LAMA polymerization the following amounts of reagents were used: 0.5 g (1.065 mmol) LAMA, 0.014 g (0.092 mmol) Bpy, 0.006 g

(0.046 mmol) $Cu^{I}Br$ and 0.0028 mmol of EBIB. Table 6 summarizes the ATRP reaction conditions used for the synthesis of the glycopolymer brushes.

Table 6. Reaction conditions used for the synthesis of the glycopolymer brushes

Monomer	Catalyst system	Solvent (v/v)	Reaction time (h)
GAMA	0.5 g (1.62 mmol) GAMA 0.022 g (0.14 mmol) Bpy 0.01 g (0.07 mmol) $Cu^{I}Br$	1-methyl-2-pyrolidinone	2
			24
	0.5 g (1.62 mmol) GAMA 0.022 g (0.14 mmol) Bpy 0.01 g (0.07 mmol) $Cu^{I}Br$ 0. 001 g (0.007 mmol) $Cu^{II}Cl$	$MeOH/H_2O$ = 3/2	24
		$MeOH/H_2O$ = 4/1	5
			24
		H_2O	5
			24
LAMA	0.5 g (1.065 mmol) LAMA, 0.014 g (0.092 mmol) Bpy, 0.006 g (0.046 mmol) $Cu^{I}Br$	1-methyl-2-pyrolidinone	2
			24
	0.5 g (1.065 mmol) LAMA, 0.014 g (0.092 mmol) Bpy, 0.006 g (0.046 mmol) $Cu^{I}Br$ 0.0006 g (0.0046 mmol) $Cu^{II}Cl$	H_2O	5
			24
		$MeOH/H_2O$ = 3/2	5
			24

2. 6. Synthesis of Glycopolymer Brushes on Glass and Silicon Substrates

2. 6. 1. Synthesis of the surface initiator (3-(2-bromoisobutyryl) propyl)triethoxysilane. The surface initiator was synthesized in a two-step reaction. *First step*: Freshly distilled bromoisobuyryl bromide (4 mL, 32.5 mmol) was added dropwise to a cold solution of allyl alcohol (1.85 mL, 27 mmol) in anhydrous THF (60 mL) with triethylamine (4.55 mL, 32 mmol) at 0 °C (Scheme 3). The mixture was allowed to stir for 3 h at 0 °C and for another 12 h at room temperature. The reaction mixture was filtered and the filtrate was evaporated to dryness under reduced pressure. The residue was purified using a Büchi Kughoral equipment. The product, allyl 2-bromoisobutyrate (1.8 g, 8.69 mmol) was diluted with chloroform and washed twice with a saturated sodium hydrogen carbonate ($NaHCO_3$) aqueous solution and twice with water

and finally dried over $MgSO_4$. ^1H NMR ($CDCl_3$): δ 5.9 (1H, m, H_2C=C*H*), 5.23 (2H,dd, *H_2*C=CH), 4.63 (2H, d, CH_2O), 1.94 (6H, s, CH_3).

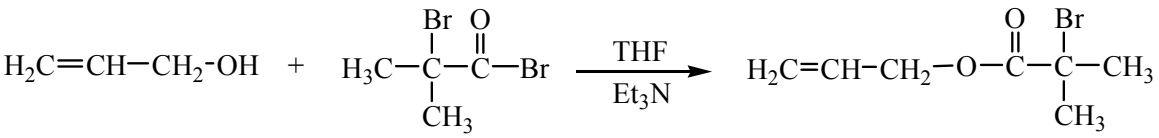

allyl alcohol | 2- bromoisobutyryl bromide | allyl 2-bromoisobutyrate

Scheme 3. *Reaction Scheme for the synthesis of allyl 2-bromoisobutyrate.*

Second step: Ally 2-bromoisobutyrate (1.8 g, 8.69 mmol) and anhydrous toluene (5 mL) were charged into a round bottom flask equipped with a stirrer bar. Triethoxysilane (3.23 ml, 17.44 mmol) was added dropwise into the flask and the Karstedt's catalyst solution (90 μL) was added next. The reaction mixture was stirred under a nitrogen atmosphere overnight at 60 °C (Scheme 4). The unreacted triethoxysilane and the solvent were removed under vacuum to yield the initiator (3-(2-bromoisobutyryl)propyl)triethoxysilane as a light yellow liquid (0.4 g, 1.08 mmol) ^1H NMR ($CDCl_3$): δ 0.68 (2H, t, $SiCH_2$), 1,20 (9H, t, C*H_3*CH_2OSi), 1.93 (6H, s, CH_3), 3.71 (6H, q, CH_3C*H_2*OSi), 4,12 (2H,t, C*H_2*O), 1.80 (2H, CH_2).

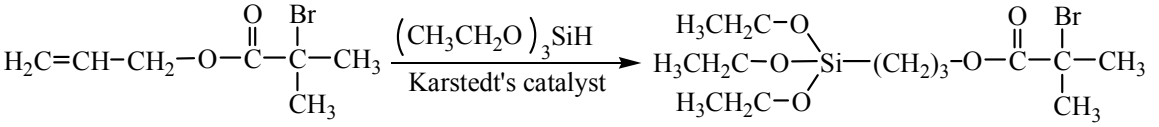

allyl 2-bromoisobutyrate | (3-(2-bromoisobutyryl)propyl)triethoxysilane

Figure 4. *The synthesis of the initiator (3-(2-bromoisobutyryl)propyl)triethoxysilane.*

2. 6. 2. Initiator self-assembly. Silicon wafers were immersed in piranha solution (1 : 3 mixture of 30% H_2O_2 aqueous solution and 98% H_2SO_4) followed by heating to 100-135 °C to remove any organic residues and to create silanol groups on the surface. After 30 minutes the substrates were removed form the solution and rinsed extensively with water. The silicon substrates were dried under nitrogen and placed under vacuum for 1 h. The SAM of the initiator was formed by immersing overnight silicon and glass substrates in a vial containing a 27 mM solution of the (3-(2-bromoisobutyryl)propyl)triethoxy

silane initiator in anhydrous THF. After the incubation period, the substrate was rinsed extensively with anhydrous THF and dried under a stream of nitrogen.

2. 6. 3. Surface-initiated polymerization of glycopolymer brushes. A similar polymerization procedure to that used for the synthesis of the glycopolymer brushes on gold substrates was followed for the synthesis of the PGAMA and the PLAMA chains on glass and silicon substrates in the presence of free initiator. Table 7 summarizes the ATRP reaction conditions used for the synthesis of the glycopolymer brushes.

Table 7. Reaction conditions used of the glycopolymer brushes

Monomer	**Catalyst system**	**EBIB (mmol)**	**Solvent (v/v)**
0.5 g (1.62 mmol) GAMA	0.022 g (0.14 mmol) Bpy 0.01 g (0.07 mmol) $Cu^{I}Br$	0.035	$MeOH/H_2O$ = 4/1
		0.0077	
	0.022 g (0.14 mmol) Bpy 0.01 g (0.07 mmol) $Cu^{I}Br$ 0.001 g (0.007 mmol) $Cu^{II}Cl$	–	
0.5 g (1.065 mmol) LAMA	0.014 g (0.092 mmol) Bpy, 0.0066 g (0.046 mmol) $Cu^{I}Br$	0.023	$MeOH/H_2O$ = 3/2
		0.0051	
		0.0028	

2. 7. SPR Measurements

2. 7. 1. BSA adsorption. The sensor chips employed for the measurements of the BSA adsorption were modified with the ATRP initiator followed by the surface-initiated polymerization of the DMAEMA monomer. DMAEMA was polymerized in a 4/1 methanol/water mixture for 2 h of reaction time. Under these conditions a 19 nm grafted polymer film was obtained. BSA solution with a concentration of a 0.1 mg/mL at a pH of 5.8 was injected into the SPR cuvette over the PDMAEMA grafted layers. The protein adsorbed amount (mg/m^2) was determined from the SPR sensogram taking in to account that a change of 120 m^o in the resonance angle corresponds to 1 ng/mm^2 protein uptake.

2. 7. 2. Lectin binding. The sensor chips employed for the measurements of the lectin interaction with the glycopolymer brushes were modified with the ATRP initiator followed by the surface-initiated polymerization of GAMA or LAMA. GAMA was polymerized in a 4/1 methanol/water mixture, while the polymerization of LAMA was performed in a 3/2 methanol/water mixture. Both polymerizations were allowed to proceed for 5 h. Under these conditions a 20 nm film was obtained for GAMA and a 30 nm layer for LAMA. A buffer consisting of 0.1 M phosphate buffer saline (PBS), 1 mM $CaCl_2$ and 1 mM $MnCl_2$ at pH = 7.3 was used in the binding process. Con A solutions with concentrations varying between 36 to 80 μM with respect of the protein monomeric form and RCA_{120} solutions with concentrations varying between 0.02 to 0.45 μM were injected into the SPR cuvette mounted on a PGAMA and a PLAMA modified sensor chip, respectively. A non-regenerative protocol was used for the determination of the affinity constant, K_A.

2. 8. Cell Culture on Glycopolymer Films

2. 8. 1. Culture of hepatocyte cells. Hep G2 cells were harvested in a 25 mL flask, using Dubelcco's modified eagle medium (DMEM) supplemented with 10 % fetal bovine serum (FBS) and antibiotics (penicillin 100 U/ml and streptomycin 100 ug/mL) at 37 °C and 5 % CO_2. Upon 80 % confluency, the cells were dislodged from the flask surface, using 2 mL of fresh medium and 200 μL of the cell stock solution were seeded into 6 well plates, containing the glycopolymer functionalized gold substrates. The final volume

of the medium in each well was 2 mL. The cells were incubated for 20 hrs at 37 °C, under a humidified atmosphere of 5 % CO_2 and 95 % H_2O. The morphology of the cells was studied using an Olympus Reflecting microscope BX1-5TRF, and the digital pictures were obtained using a CCD camera.

2. 8. 2. Culture of fibroblast cells. The L929 mouse fibroblast line (ATCC, CCL-1) was incubated in DMEM supplemented with 10 % fetal bovine serum (FBS) at 37 °C in a 5 % CO_2 atmosphere. The fibroblasts were transferred into the wells containing the glycopolymer-functionalized gold surfaces at a concentration of 2.0×10^3 cell/mL. The surfaces were incubated for 24 hrs in 10 % FBS DMEM and then rinsed with PBS to remove nonadherent cells. Adherent cells were fixed for 15 minutes with 100 mL of a 4 % solution of PFA in PBS. The surfaces were next rinsed three times with PBS and were allowed to dry in air. The morphologies of the cultures were observed by scanning electron microscopy (SEM; Keyence VE-8800).

2. 9. References

1. R. Narain, S. P. Armes, *Chem. Commun.* **2002**, 2776-2777.
2. R. Narain, S. P. Armes, *Macromolecules* **2003**, *36*, 4675-4678.
3. R. Narain, S. P. Armes, *Biomacromolecules* **2003**, *4*, 1746-1758.
4. A. B. Lowe, N. C. Billingham, S. P. Armes, *Macromolecules* **1998**, *31*, 5991-5998.
5. D. M. Jones, A. A. Brown, W. T. S. Huck, *Langmuir* **2002**, *18*, 1265-1269.
6. S. Tugulu, A. Arnold, I. Sielaff, K. Johnsson, H. A. Klok, *Biomacromolecules* **2005**, 6, 1602-1607.

CHAPTER 3

Synthesis and Characterization of Stimuli Responsive Homopolymer and Block Copolymer Brushes on Gold Substrates

Chapter 3 presents the synthesis of stimuli-responsive homopolymer and block copolymer brushes from modified gold substrates by surface-initiated ATRP. The surface-initiated polymerization of three different stimuli-responsive methacrylic monomers: 2-(dimethylamino)ethyl methacrylate (DMAEMA), 2-(diethylamino)ethyl methacrylate (DEAEMA) and tetrahydropyranyl methacrylate (THPMA) a methacrylate ester easily hydrolyzed to methacrylic acid (MAA) was investigated. Polymer films comprising of neutral oligo(ethylene glycol) methacrylate (OEGMA) were also synthesized. The active chain ends of the prepared brushes were used as macroinitiators for the synthesis of block copolymers. The wetting properties of the grafted block copolymer films were investigated upon solvent treatment. The swelling of the PDMAEMA homopolymer brushes was studied as a function of pH. Moreover, the interactions of the PDMAEMA brushes with BSA protein were studied. Ellipsometry, atomic force microscopy (AFM), attenuated total reflectance (ATR)-IR spectroscopy and contact angle measurements were employed for the characterization of the grafted polymer layers.

3. 1. Introduction

The control of surface properties is important in many areas of research and in numerous commercially important technologies ranging from biotechnology to advanced microelectronics. One method that has been employed for controlling surface properties is the utilization of densely grafted polymer chains or polymer brushes. A first application of polymer brushes was in colloid particle stabilization. If polymer chains are attached onto the surface of colloid particles, the grafted chains of two approaching particles can resist overlapping and prevent flocculation.[1, 2] The functionalization of flat surfaces with polymeric nanolayers generates materials with enhanced properties for applications in various emerging areas of science and technology. Hydrophilic polymer

brushes based on oligo(ethylene glycol) methacrylate (OEGMA), 2-hydroxyethyl methacrylate (HEMA), acrylamide (AAm) and zwitterionic monomers form a highly hydrated layer in an aqueous medium.[3-11] It is believed that the large excluded volume of the polymer units and the high flexibility of the hydrated chains in water are the reason behind the surface repellent properties. Such polymer brushes have been investigated for their ability to resist non-specific adsorption of proteins and cells. The non-specific adsorption results in biological contamination, which reduces the sensitivity of biosensors and chip-based diagnostic assays and also limits the use of certain materials in implants, food processing equipments and industrial cooling water devices. The thickness and the density of the brush are important parameters in making an efficient non-adhesive coating. Polymer brushes based on poly(thiophene) and poly(ethylenedioxythiophene) grafted onto polyethylene and poly(styrenesulfonic) acid coated substrates have been used to prepare conducting surfaces[12-14] while liquid crystalline polymer brushes have been suggested as an alignment layer in electronic devices with a liquid crystalline active phase.[15]

Polymer chains which are responsive to an environmental stimulus by changing their conformation generate so called "smart" polymer systems. The polymer chains respond to the external stimulus by modifying the conformation and/or location of the backbone, the side chains, as well as the end-groups. Stimuli-responsive polymer chains attached to a solid substrate by one end (brushes) are capable to change the surface properties onto which they are tethered under the influence of physical external stimuli such as temperature, electric or magnetic fields and chemical stimuli such as pH, ionic strength or chemical agents. The reversible ability of the polymer brush to reorganize under the influence of external stimuli can be employed to produce reversible switching of the surface properties.

Stimuli-responsive polymer brushes of different monomers have been synthesized by ATRP to produce temperature-responsive and pH-responsive surfaces. Temperature is one of the most frequent used external stimuli in responsive polymer systems. Poly(N-isopropylacrylamide (PNIPAAm) is the most broadly studied thermo-sensitive polymer. PNIPAAm exhibits a lower critical solution temperature (LCST) of 32-33 °C in aqueous solution[16] and assumes a hydrophilic swollen state below the LCST and a hydrophobic

state above the LCST due to reversible chain hydration and dehydration. Due to this unique property, PNIPAAm brushes have been extensively used for the preparation of temperature-responsive surfaces.[17-19]

Polyelectrolyte (PEL) brushes undergo changes in swelling and contraction in response to pH or ionic strength making them excellent candidates for responsive surfaces. PEL brushes consist of polymers containing ionizable groups along their backbone. The charge density on a polymer chain in a polar solvent depends on the chain constitution and degree of dissociation of the ionizable groups. If the ionizable groups are strong acids or bases (strong PEL) the degree of dissociation is not affected by the environment and as a consequence these brushes are insensitive to local pH. However, if the ionizable groups are weak acids or bases (weak PEL) the degree of dissociation depends on the local pH (Scheme 1). Weak polyacids accept protons at low pH and release them at neutral and high pH when they become negatively charged. Polybases are deprotonated at high pH and become positively charged at neutral and low pH. The structure and the properties of such polymer layers are dominated by the electrostatic interactions. Due to electrostatic interactions the polymer segments are strongly stretched and show physical properties which are very different compared to neutral polymer brushes.

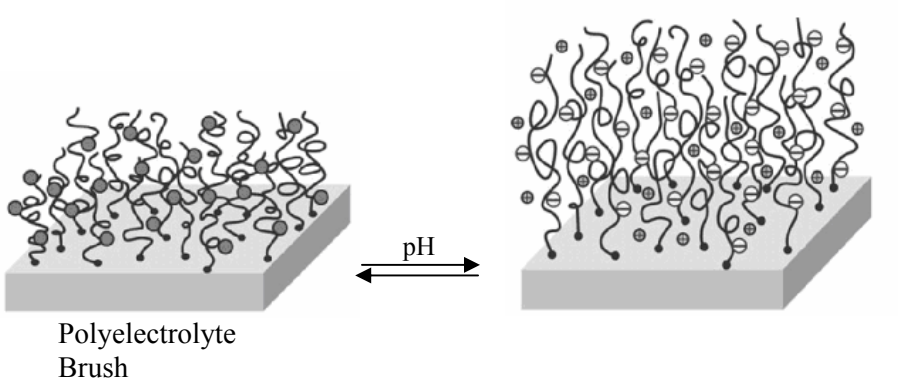

Scheme 1. *Dissociation of weak PEL brushes as a function of pH*

Polyacid brushes possessing carboxylic acid groups such as poly(acrylic acid) (PAA) and poly(methacrylic acid) (PMAA) are being used as weak polyacids. Direct ATRP of polyacid brushes is hindered by the complexation of the monomer with the

catalyst metal complex. As a consequence, polyacid brushes are usually prepared by ATRP of a protected monomer followed by deprotection.[20-22] Polybase brushes bear mostly amine pendant groups along their chains. The amine groups gain protons and become positively charged under neutral and low-pH conditions. 2-(Dimethylamino)ethyl methacrylate (DMAEMA) based brushes prepared by ATRP have been most frequently reported.[23-26]

Responsive polymer brushes have been used for their ability to tune different surface properties using an external stimulus. By grafting stimuli-responsive brushes onto a surface, the adhesion or wetting of the surface could be rapidly changed to switch off and on for capillary flow, protein adsorption, and drug release. Thermo-responsive polymers such as PNIPAAm have been proposed as scaffolds in tissue engineering.[18, 27] The control of cell adhesion and detachment can be regulated using temperature modulation. The cells can adhere, grow and proliferate at 37 °C and spontaneously detach from the hydrophilic grafted polymer film at temperatures below the LCST of the polymer. pH responsive polymer brushes are very promising for applications as high capacity ion exchange materials for specific binding or separation. PAA based brushes have been used for protein immobilization at low ionic strength of the protein solution.[28] PDMAEMA brushes which are cationic at physiological pH can uptake negatively charged proteins, while positively charged proteins are effectively rejected therefore rendering them as charge-selective protein uptake materials.[26, 29] Bimolecular diagnostics and biosensors[30] have been developed using responsive brushes as supports. Coating nanoporous polymeric membranes with stimuli responsive polymers found use in chemical gating.[31, 32]

One of the most interesting architectures produced to date are diblock copolymer brushes containing two or more homopolymer chains covalently connected to each other by one end.[33-35] Block copolymer brushes are interesting due to the fact that vertical phase separation results when the block copolymer chains are tethered by one end to a surface or a substrate. The ability to control the conformation and rearrangement of the tethered blocks affects the morphology and the properties of the polymer film. Recently, a variety of applications of block copolymer brushes were demonstrated. The self-assembly of block copolymer brushes is an easy method to create nanoscale patterns on

polymeric surfaces.[36, 37] Tethered block copolymers can also be used in forming multilayered materials, having the ability to arrange the layers in a predetermined order.[38, 39] Additionally, block copolymer brushes can be employed as responsive surfaces. For instance, selective solvent treatment will expose the polymer block favored by the solvent at the surface. In this way, by changing the solvent medium the surface properties can be switched from one component of the copolymer to the other.[40]

3. 2. Self-Assembly of the ATRP Initiator

A gold-coated silicon substrate was modified with the ATRP initiator ω-mercaptoundecyl bromoisobutyrate and the successful immobilization was verified by ATR-FTIR spectroscopy (Figure 1). The appearance of a characteristic peak at 1739 cm^{-1} corresponding to the C=O stretching vibration of the ester carbonyl group, the peaks at 2967 and 2930 cm^{-1} assigned to the C-H symmetric and asymmetric vibration modes of the $-CH_2-$ groups and the peaks at 1266 and 1167 cm^{-1} due to the C-O stretching in the ATR-FTIR spectrum were attributed to the grafted initiator.

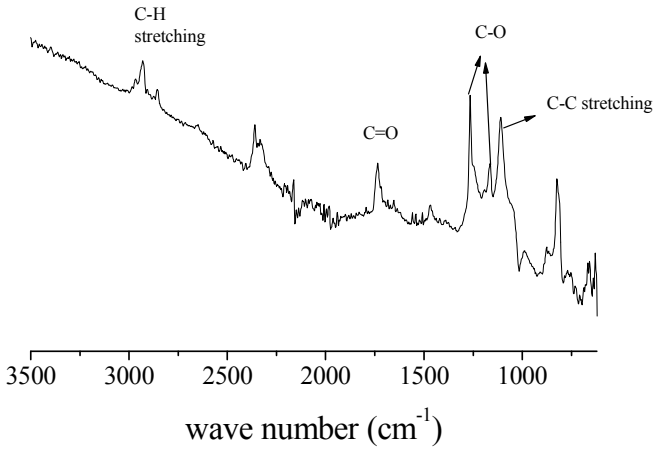

Figure 1. *ATR-FTIR spectra of the immobilized ω-mercaptoundecyl bromoisobutyrate ATRP initiator on a gold substrate.*

3. 3. Synthesis and Characterization of Responsive Homopolymer Brushes

The surface-initiated ATRP of the methacrylate monomers was carried out next from the initiator modified gold substrates (Scheme 2). The polymerizations were performed at 20 °C using Cu(I)Br and/or $Cu(II)Cl_2$ and 2,2'- bipyridyl, HMTETA or

TMEDA as the catalyst system. When copper (II) deactivator was not added at the beginning of the polymerization, free initiator was added to ensure the controlled synthesis of the polymer chains. The polymerizations were allowed to proceed for a predetermined period of time, after which the substrates were removed from the reaction solution, followed by extensive rinsing with solvent and sonication.

Controlled ATRP is achieved by establishing an equilibrium between the radicals (active species) and the inactive form of the polymer, known as the dormant species with the metal complexes acting as a reversible halogen atom-transfer reagent. The reaction equilibrium is shifted to the left side, thus the free radical concentration is kept very low during the polymerization and as a consequence the contribution of termination to the overall reaction is greatly diminished. The reactivation of the dormant species allows the polymer chains to reinitiate the growth, only to be deactivated later. This results in a polymer chain that steadily grows and has a well-defined group at its free end. For a good control of the polymerization a sufficient amount of deactivator must be present in the ATRP process. In solution ATRP the required deactivator is formed by the termination of a few percent of the polymer chains in the early stages of the reaction. However, in systems where initiator groups are adsorbed on a very low surface area such a flat substrate, the low concentration of the initiator is insufficient to form the desired copper (II) deactivator complex to control the polymerization.[41]

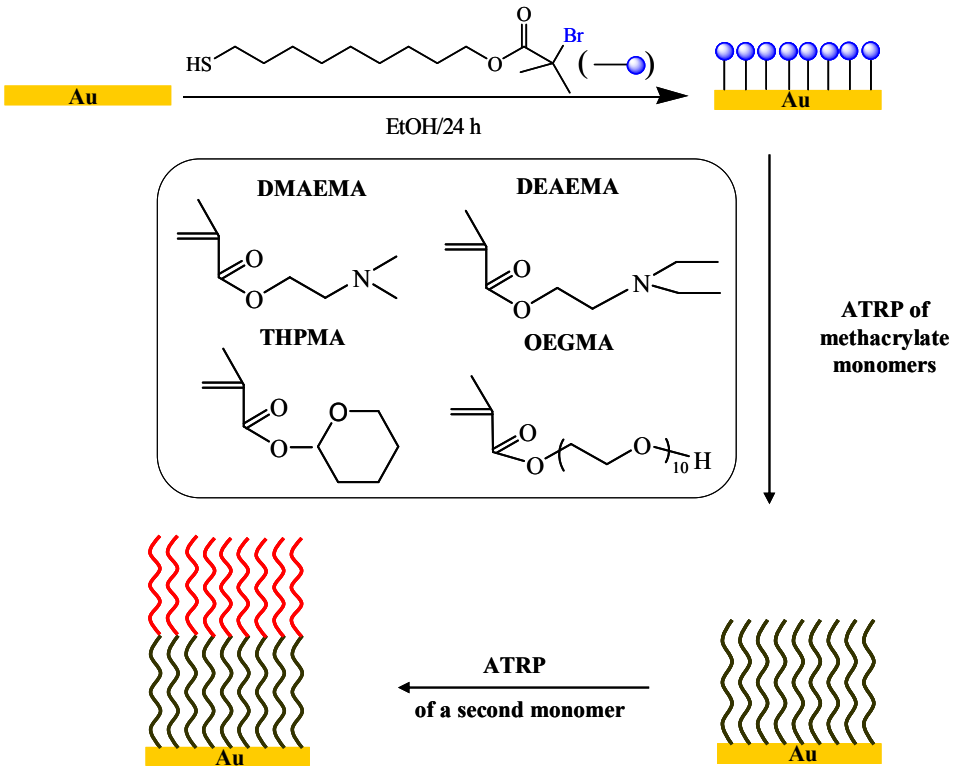

Scheme 2. *Schematic representation of the self-assembly of the ATRP initiator onto the gold substrate and the surface initiated polymerization of various methacrylic monomers.*

Two different approaches have been used to control the growth of polymer brushes and to ensure the presence of a sufficient amount of deactivator throughout the course of the polymerization. One approach involves the addition of free or "sacrificial" initiator in the reaction mixture.[42, 43] This leads to the formation of the required copper (II) species by the termination of a few percent of the polymer chains in solution via redox reactions. By using this approach, the molecular weight of the free polymer can serve as a measure of the molecular weight and molecular weight distribution of the polymer chains grown on the surface. However, this approach limits the maximum thickness of the polymer layer, as most of the monomer is consumed by the polymer formed in solution.[44] The other approach requires the direct addition of deactivator with the catalyst system at the beginning of the polymerization.[45]

Table 1 summarizes the ATRP reaction conditions used for the synthesis of PDMAEMA grafted polymer films and the film characteristics. DMAEMA is a

hydrophilic monomer possessing pH- and temperature- responsive properties. The PDMAEMA brushes can be considered to be neutral in organic solvents and pH-responsive weak polybase brushes in water. At pH values lower than 8, linear PDMAEMA becomes positively charged due to the protonation of the amine groups, while at pH values higher than 8 the chains are neutral. The pH-responsive behavior of the PDMAEMA films is discussed bellow in section 3. 7.

DMAEMA was polymerized in a 3/2 and a 4/1 methanol/water mixture and pure methanol. The catalyst system used in the polymerizations was Cu(I)Br and/or Cu(II)Cl_2 and 2,2' bipyridyl. In the 3/2 methanol/water mixture the polymerization was carried out without the addition of copper (II) at the beginning of the reaction. The substrates were removedfrom the polymerization mixture at various periods of time and the film thickness was measured by ellipsometry. Figure 2 shows the film thickness of the PDMAEMA brushes as a function of the polymerization time. A dry film thickness of 34 nm was observed after only 15 minutes of polymerization in the 3/2 methanol/water mixture. This is an indication of a fast initial growth rate of the polymer chains. Within 30 minutes of reaction time the film thickness reached 66 nm which further increased to 112 nm after 1 h of polymerization. The polymer film thickness continued to increase and after 2 h of polymerization a 200 nm PDMAEMA film was obtained. To slow down the growth rate and to retain control of the reaction, 0.1 mol% of the deactivator relative to copper (I) was added at the begging of the polymerization and also the amount of water in the solvent mixture was reduced. Therefore, the polymerizations were performed in a 4/1 methanol/water mixture and copper (II) deactivator was added in the polymerization solution. Under these conditions a 5 nm film was obtained after 30 minutes of reaction time. Prolonging the reaction time to 1 h, 2 h, and 3 h the PDMAEMA film increased to 10 nm, 19 nm and 25 nm, respectively. This is an indication that a slower polymerization rate was obtained when the copper(II) deactivator was added in the beginning of the polymerization and the water content of the solution mixture was decreased. Moreover, when the water content was further decreased and the polymerization was carried out in a less polar medium such as methanol, a thickness of only 2 nm was obtained after 2 h of reaction, which increased to 5 nm after 5 h. After 24 h of polymerization the thickness of

the grafted film increased to 19 nm, suggesting that the rate of polymerization and therefore the thickness of the prepared films decrease significantly in less polar media.

In order to verify the ellipsometry results, the thickness of the PDMAEMA grafted film prepared in the 4/1 methanol/water mixture for 3 h of polymerization time was measured by AFM. A cut was made very carefully using a scalpel to leave a brush-gold boundary that was then imaged by AFM and the step height was measured. The image of the cut together with the step height are shown in Figure 3. A thickness of 28 nm was found for the PDMAEMA brush by AFM which is in very good agreement with the 25 nm thickness measured by ellipsometry.

The roughness of the polymer films prepared in the 3/2 methanol/water mixture increased form 0.9 nm to 2.7 nm upon increasing the polymer film form 34 nm to 200 nm. For the rest of the prepared brushes, the polymer film thickness does not seem to influence the roughness and smooth polymer films with a roughness below 1 nm were observed (Table 1).

Table 1. Reaction conditions and characteristics of PDMAEMA grafted films

Monomer	**Reaction conditions**	**Reaction time (h)**	**Thickness by ellipsometry (nm)**	**Roughness by AFM (nm)**
DMAEMA	Cu(I)/Bpy MeOH/H_2O = 3/2	0.25	34	0.9
		0.5	66	1.4
		1	112	2.5
		2	200	2.7
	Cu(I)/Cu(II)/Bpy MeOH/H_2O = 4/1	0.25	4	0.7
		0.5	5	0.6
		1	10	0.7
		2	19	0.6
		3	25	0.8
	Cu(I)/Cu(II)/Bpy MeOH	2	2	0.8
		5	5	1
		24	19	0.9

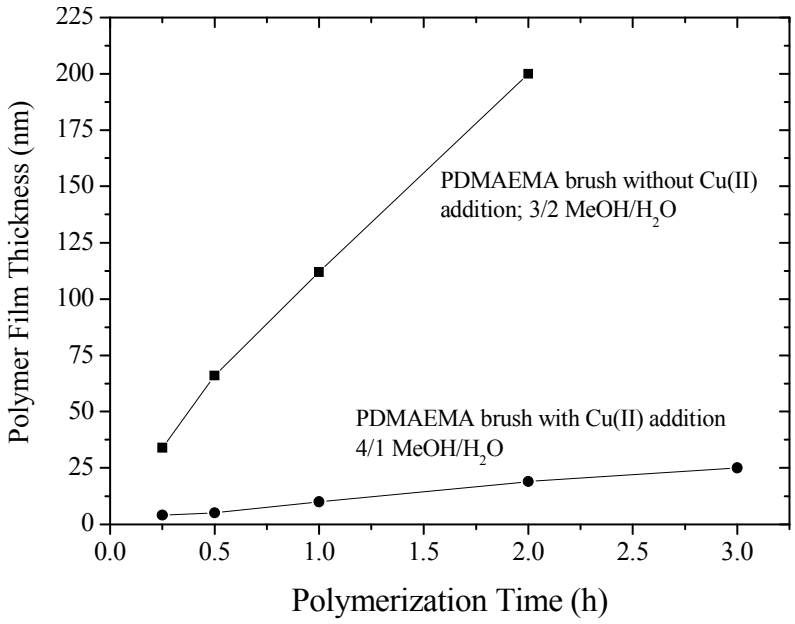

Figure 2. *Evolution of ellipsometric brush thickness with polymerization time for the surface ATRP of DMAEMA in the absence (filled squares) and the presence (filled circles) of copper (II).*

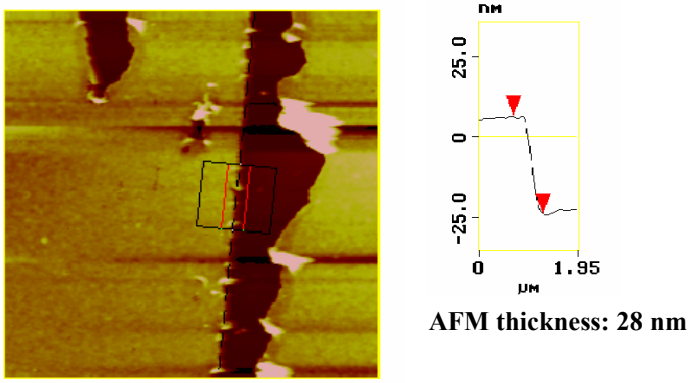

Figure 3. *AFM brush height measurement for a PDMAEMA brush prepared in a 4/1methanol/water mixture for 3h polymerization time.*

For a good control of the polymerization in aqueous solution ATRP a sufficient amount of deactivator must be present in the reaction mixture. It has been found that a very fast polymerization with unsatisfactory control of the reaction takes place in aqueous media when no copper(II) complex was added in the beginning of the polymeriation.[46] We have observed a similar behaviour for the polymerization of DMAEMA in a 3/2 methanol/water mixture with no copper (II) deactivator initially added. Under these

reaction conditions a very fast polymerization was observed and a polymer film with a thickness of ~100 nm was obtained within 1 h of reaction time. As a consequence, in order to obtain grafted polymer films under controlled conditions in aqueous ATRP, copper(II) deactivator, 0.1 wt % relative to copper(I), was added at the beginning of the reaction.

The ATRP of DMAEMA was also investigated in organic solvents such as acetone and THF. Very low polymer film thicknesses (~ 3nm), which did not increase further even after 10 h of reaction time were obtained under these conditions, suggesting that the polymerization rate becomes very slow in organic media (Table 2).

Table 2. Reaction conditions and characteristics of PDMAEMA grafted layers prepared in organic solvents

Monomer	**Reaction conditions**	**Reaction time (h)**	**Thickness by ellipsometry (nm)**	**Roughness by AFM (nm)**
DMAEMA	Cu(I)/TMEDA Acetone	2 h	2	0.8
		10 h	3	0.7
	Cu(I)/TMEDA THF	2 h	1	0.7
		10 h	2	0.7

DEAEMA is another example of a stimuli response monomer. It is a hydrophobic monomer which possesses pH-responsive properties. At pH values higher than 7 linear PDEAEMA is neutral and hydrophobic, while at pH values lower than 7 it become positively charged. All the DEAEMA polymerizations were carried out in methanol. The catalyst system used was Cu(I)Br and/or $Cu(II)Cl_2$ as the metal salt and 2,2' bipyridyl or HMTETA as the ligands. Table 3 summarizes the ATRP reaction conditions used for the synthesis of PDEAEMA grafted polymer films and the film characteristics. A dry polymer film thickness of 18 nm was found by ellipsometry after 6 h of reaction time using the Cu(I)/Bpy as the catalyst system. The film thickness further increased to 31 nm after 24 of polymerization. When $Cu(II)Cl_2$ was added in the reaction mixture the rate of polymerization slowed down and lower film thickness were found. After 3 h of polymerization a PDEAEMA film of 5 nm was found which increased to 7 nm after 6 h of polymerization. The polymer film continued to increase and after 24 h of

polymerization a 26 nm film was obtained. A dry film thickness of 19 nm was obtained after 30 min of reaction time when HMTETA was used as the catalyst system. The polymer film increased to 23 nm and further to 29 nm after 3 h and 24 h of polymerization time. PDEAEMA films, with a roughness below 1nm were synthesized as indicated by the AFM measurements, verifying the preparation of smooth, soft polymer films (Table 3).

Table 3. Reaction conditions and characteristics of PDEAEMA films

Monomer	**Reaction conditions**	**Reaction time (h)**	**Thickness by ellipsometry (nm)**	**Roughness by AFM (nm)**
DEAEMA	Cu(I)/Bpy MeOH	6	18	0.6
		24	31	0.8
	Cu(I)/Cu(II)/Bpy MeOH	3	5	0.7
		6	7	0.8
		24	26	0.7
	Cu(I)/HMTETA MeOH	0.5	19	0.9
		3	23	0.9
		24	29	1.8

The dry film thickness of the PDEAEMA brushes prepared in methanol using C(I)Br and HMTETA as the catalyst system at 30 min of reaction time was also measured by AFM. As mention above, in order to have a step height, cuts were made on the polymer film and then imaged by AFM (Figure 4). A thickness of 19 nm was measured for the PDEAEMA grafted film by AFM. When a second cut was analyzed a value of 21 nm was found. The obtained AFM thicknesses are in very good agreement with the 19 nm film thickness obtained by ellipsometry.

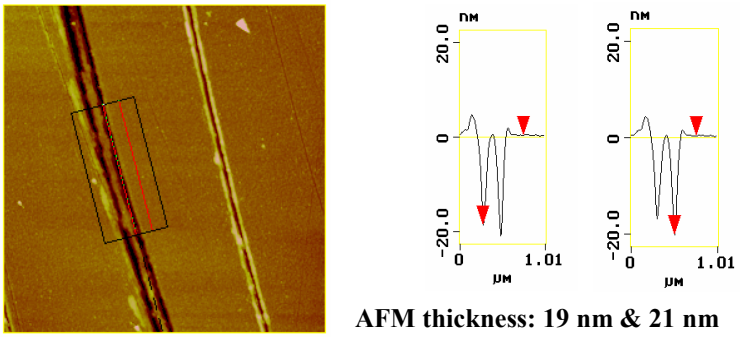

Figure 4. *AFM brush height measurements for PDEAEMA brushes prepared in methanol for 30 min polymerization time.*

A class of monomers which can not yet be polymerized by ATRP includes acidic monomers. The carboxylic acid side groups of the monomer may react with the catalyst metal complexes and hamper the polymerization.[47] A number of authors have synthesized poly((meth)acrylic acid) brushes via SI-ATRP of *tert*-butyl(meth)acrylate, followed by hydrolysis under acidic conditions or pyrolysis at elevated temperatures of the *tert*-butyl ester protective groups.[45, 48, 49] Sometimes the reaction conditions used for the hydrolysis or pyrolysis proved to be too harsh on the polymer brushes and led to the partial cleavage of the polymer chains form the surface.[48] In another study the poly(methacrylic acid) brushes were synthesized by ATRP of 1-ethoxyethyl methacrylate, but once again the hydrolysis of the polymer brushes required high temperatures.[50] We synthesized the acidic brushes using the protected monomer, THPMA, followed by hydrolysis of the polyester brushes under mild conditions. THPMA is a methacrylate ester which contains an acid-labile acetal bond as a side chain and can be easily hydrolyzed to methacrylic acid (MAA). Table 4 lists the reaction conditions used for the synthesis of PTHPMA grafted layers and the film characteristics. The polymerization of THPMA was carried out in methanol and o-dichlorobenzene with Cu(I)Br/HMTETA as the catalyst system. A film thickness of 30 nm was obtained in methanol after 2 h of reaction time, which further increased to 43 nm after 4 h of polymerization. For the polymerization of THPMA in o-dichlorobenzene a 7 nm thick film was obtained after 6 h of reaction, which increased to 26 nm after 24 h, verifying that the rate of polymerization slows down in

organic media as discussed above. The PTHPMA films were imaged by AFM, which showed that the prepared polymer films were smooth with an overall roughness below 1 nm (Table 4).

Table 4. Reaction conditions and characteristics of PTHPMA films

Monomer	Reaction conditions	Reaction time (h)	Thickness by ellipsometry (nm)	Roughness by AFM (nm)
THPMA	Cu(I)/HMTETA MeOH	2	30	1.7
		4	43	-
	Cu(I)/ HMTETA o-dichlorobenzene	6	7	0.9
		24	26	0.7

Next, the THPMA units were converted to MAA units. The PTHPMA modified substrate was immersed in a mixture of THF and water (pH 3) for different periods of time. Unfortunately, the above conditions proved to be too harsh for the polymer film and after only two minutes of immersion time, the thickness of the film decreased to 4 nm while no notable changes were seen in the ATR spectrum of the 4 nm layer, which was associated with the cleavage of the polymer film from the gold substrate. Therefore, in order to avoid the cleavage of the polymer from the substrate, the PTHPMA brush was immersed in pure water for one week at RT and the hydrolysis of the THPMA group was monitored. The successful hydrolysis of the ester group was verified by ATR-FTIR spectroscopy, ellipsometry and contact angle measurements. Following hydrolysis the ATR-FTIR spectrum of PMAA showed a broad band at 3200 cm^{-1} attributed to the –OH group of the PMAA, a broadening of the carbonyl stretch due to the overlapping of the dimeric acid band at 1724 cm^{-1} and the monomeric acid band at 1709 cm^{-1} and the disappearance of the peaks associated with the ring deformation of the tetrahydropyranyl group (900-1000 cm^{-1}), confirming the almost complete hydrolysis of the polymer (Figure 5). Ellipsometry showed that the thickness of 11 nm measured for the PTHPMA modified substrate decreased to 8 nm after the immersion of the substrate for one week in water. The thickness of the grafted polymer layer did not decreased further after the immersion of the substrate in water for longer times.[50] The difference in thickness between the hydrolyzed and unhydrolyzed brushes is an indication that the bulky protecting groups of the THPMA were removed from the polymer chain. This decrease in

the polymer brush thickness is in accordance to literature data and correlates with the lost of the protective group as discussed above.[49, 50] A contact angle of 71 ^{o} was measured for the PTHPMA brush synthesized in methanol. After the immersion of the substrate in water for one week a decrease in contact angle to 43 ^{o} was observed, suggesting the conversion of the PTHPMA brushes to the more hydrophilic PMAA brushes (Figure 6) and verifying the ATR and ellipsometry results. The obtained value is comparable with values found in literature, where a water contact angle of 42 ^{o} was found for a PMAA grafted film after hydrolysis of poly(1-ethoxyethyl methacrylate) brushes[50], while contact angles with values between 32 - 55 ^{o} were found for a PMAA brush depending on the polymerization conditions used.[51]

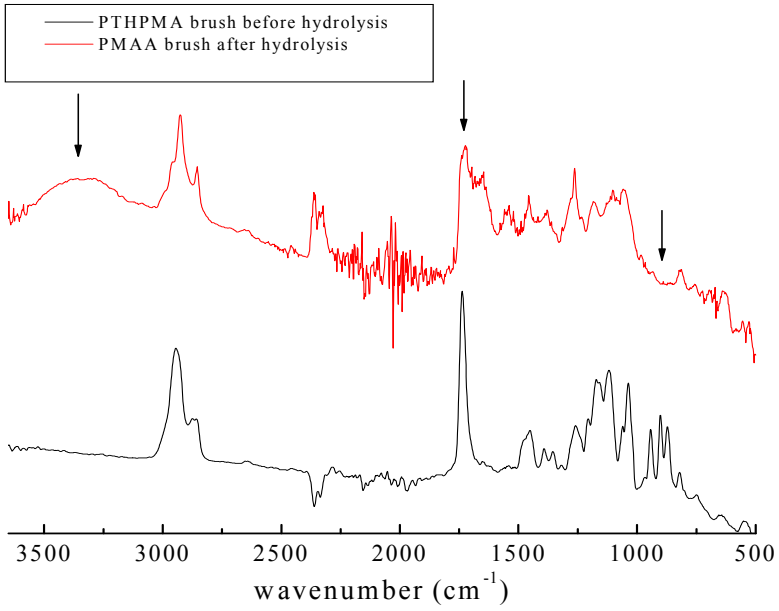

Figure 5. *ATR-FTIR spectra of PTHPMA brush before hydrolysis and PMAA brush after hydrolysis. The arrows indicate the main changes after conversion to PMAA as noted in the text.*

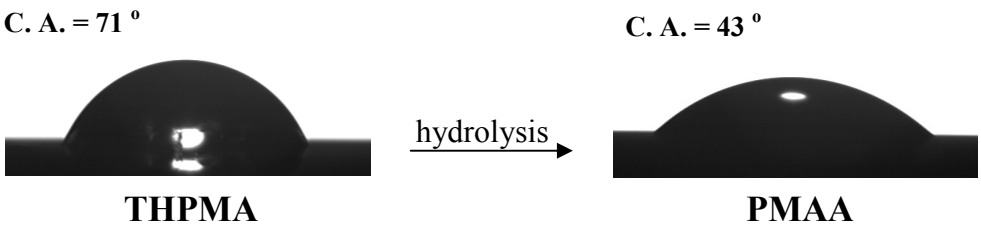

Figure 6. *Contact angle image of a PTHPMA modified substrate and the same substrate after conversion of PTHPMA to PMAA.*

OEGMA-based polymers are among the most important materials which exhibit nonfouling functions being able to reduce protein adsorption and cell attachment and growth.[3-5, 52] OEGMA was polymerized in water and a 4/1 methanol/water mixture using Cu(I)Br/Cu(II)Cl_2/2,2' bipyridyl as the catalyst system. The reaction conditions used for the synthesis of grafted POEGMA films, as well as their characteristics are listed in Table 5. A dry film with a thickness of 23 nm was obtained after 15 min of reaction time using water as a solvent, indicating a fast initial polymerization rate. The thickness of the polymer film further increased to 28 nm and to 43 nm after 30 min and 1 h of reaction time, respectively. In order to diminish the secondary reactions which take place in aqueous ATRP, methanol was added as a cosolvent. A film thickness of 3 nm, 5 nm and 8 nm were obtained after 15 min, 30 min and 1 h of reaction time in a 4/1 methanol/water mixture.

Table 5. Reaction conditions and characteristics of POEGMA grafted films

Monomer	Reaction conditions	Polymerization time (min)	Thickness by ellipsometry (nm)	Roughness by AFM (nm)
OEGMA	Cu(I)/Cu(II)/Bpy H_2O	15	23	0.5
		30	28	0.9
		60	43	0.9
	Cu(I)/Cu(II)/ Bpy MeOH/H_2O = 4/1	15	3	0.8
		30	5	0.7
		60	8	0.9

The above results suggest that the growth rate of the polymer chains slowed down when methanol was added as a cosolvent in the reaction medium. The obtained POEGMA films were very smooth with roughness below 1 nm, as verified by AFM measurements (Table 5).

The thickness of the POEGMA brush prepared in water for 1 h polymerization time was also measured by AFM. A cut was made very carefully leaving a brush-gold boundary. The height found by AFM for the POEGMA grafted film was 41 nm which is in very good agreement with the ellipsometric thickness of 43 nm (Figure 7).

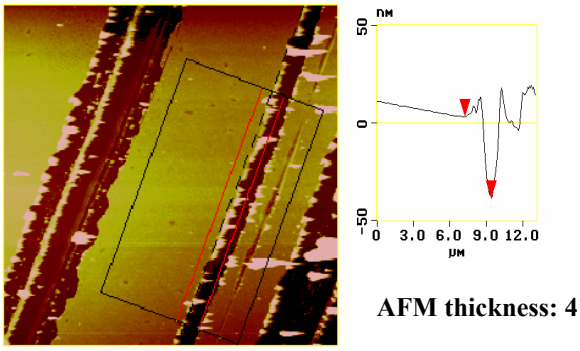

Figure 7. *AFM brush height measurements for POEGMA brush prepared in water for 1 h of polymerization time.*

The composition of the polymerization medium has a great influence on the growth rate of the polymer chains. Fast polymerization rates have been reported in the literature for ATRP performed in water. Perrier et. al. observed an enhancement of the polymerization rate for poly(ethylene glycol) methyl ether methacrylate in water while, the prepared polymers had relatively high polydispersities indicating a loss of control.[53] These observations were attributed to the coordination of water to the metal centre of the copper(II) complex which leads to inefficient deactivation and to faster polymerizations. Moreover, Tsarevsky et. al. showed that the stability of the higher oxidation state complex depends on the solvent composition.[46] As the amount of water in the solvent system decreases the stability of the copper(II)-halide complex increases. As a consequence, polymerizations performed in less polar media exhibit slower kinetics due the presence of a larger quantity of deactivator in the reaction mixture. These findings are in agreement with our results discussed above. A relatively thick POEGMA film was

after only 15 min of reaction time in water, due to a fast initial polymerization rate. Further more the rate of polymerization decreases as the amount of water in the reaction media is diminished. A slower polymerization rate and lower film thicknesses have been observed for the polymerization of OEGMA in less polar reaction media (methanol/water mixture). A similar trend can be observed for the polymerization of DMAEMA monomer. From Table 1 it can be seen that the polymerization performed in a 4/1 methanol/water mixture has faster kinetics than the polymerization in pure methanol. As a result, PDMAEMA films of higher thicknesses were obtained in the 4/1 methanol/water mixture as compared to the films prepared in pure methanol. The polarity of the solvent has a strong influence on the polymerization kinetics. In polar solvents a significant part of the initially added copper(II) deactivator is dissociated in the solvent mixture, while in a non polar organic solvent the ATRP deactivator is more stable and become less dissociated. As a consequence, the rate of polymerization slows down considerably as the polarity of the solvent decreases. These finding are in agreement with our results above. The polymerization of DMAEMA in organic solvents has slowed down the polymerization rate significantly leading to thinner layers. Moreover, the polymerization of THPMA in organic solvents was performed without the addition of copper(II) deactivator to obtain a sufficiently thick film. The film thickness in MeOH which is a polar solvent was higher compared to that obtained in o-dichlorobenzene which has a lower polarity.

From the obtain results it can be concluded that polymer films of different thicknesses can be prepared by varying the reaction medium and the polymerization time. For the synthesis of uniform polymer layers in aqueous media the addition of copper(II) deactivator at the beginning of the polymerization proved to be crucial. The rate of polymerization is very important in controlling the growth of polymer films. As the amount of water in the reaction media decreased and as the solvent became less polar, a lower rate of polymerization was observed, leading to a better control of the polymerization and to the preparation of uniform polymer layers with control over the film thickness.

The successful grafting of the polymers on the initiator modified gold substrates was verified by ATR-FTIR spectroscopy. The vibrational assignments and the peak frequencies of the major groups present in the grafted polymer layers are listed in Table 6.

The ATR-FTIR spectra of PDMAEMA, PDEAEMA, PTHPMA and POEGMA homopolymer brushes are presented in Figure 8. The appearance of the characteristic polymer peaks verifies the successful grafting of the polymers on the modified gold substrates.

Table 6. Peak assignments and wavenumbers (in cm^{-1}) for the ATR-FTIR spectra of the homopolymer brushes

Vibration	Sample			
	PDMAEMA	**PDEAEMA**	**PTHPMA**	**POEGMA**
υ(C=O)	1736	1731	1732	1732
υ_s(C-H)	2957	-	-	2967
υ_{as}(C-H)	2930	2935	2940	2930
υ(C-O)	1255	1260	1254	1266
υ(ring deformation)	-	-	900-1000	-
υ(C-O-C)	-	-	-	1144

The ATR-FTIR spectrum of a 20 nm thick PDMAEMA film is presented in Figure 8a. The carbonyl peak at 1736 cm^{-1}, the peaks at 2957 and 2930 cm^{-1} assigned to the C-H symmetric and asymmetric vibration modes of the $-CH_2-$ groups and the peak at 1255 cm^{-1} due to C-O stretching are characteristic of the PDMAEMA polymer. Figure 8b shows the ATR-FTIR spectrum of the 23 nm PDEAEMA film on a modified gold substrate. The peak at 1731 cm^{-1} assigned to the C=O stretching vibration, the peak at 2935 cm^{-1} due to the C-H asymmetric vibration modes of the $-CH_2-$ groups and the peak at 1260 cm^{-1} assigned to the C-O group were attributed to the grafted PDEAEMA chains. The ATR-FTIR spectrum of the 30 nm PTHPMA film is shown in Figure 8c. The grafted PTHPMA chains present the carboxyl group at 1732 cm^{-1}, the C-H asymmetric vibration mode of the $-CH_2-$ groups at 2940 cm^{-1}, the C-O stretching vibration at 1254 and 1158 cm^{-1} and the ring deformation of the tetrahydropyranyl group between 900-1000 cm^{-1}. The grafted POEGMA film shows the carboxyl group at 1732 cm^{-1}, the C-H symmetric and asymmetric vibration modes of the $-CH_2-$ groups at 2967 and 2930 cm^{-1}, the C-O stretching vibration at 1266 $cm^{-1}$and the C-O-C vibration at 1144 cm^{-1} as seen in Figure 8d.

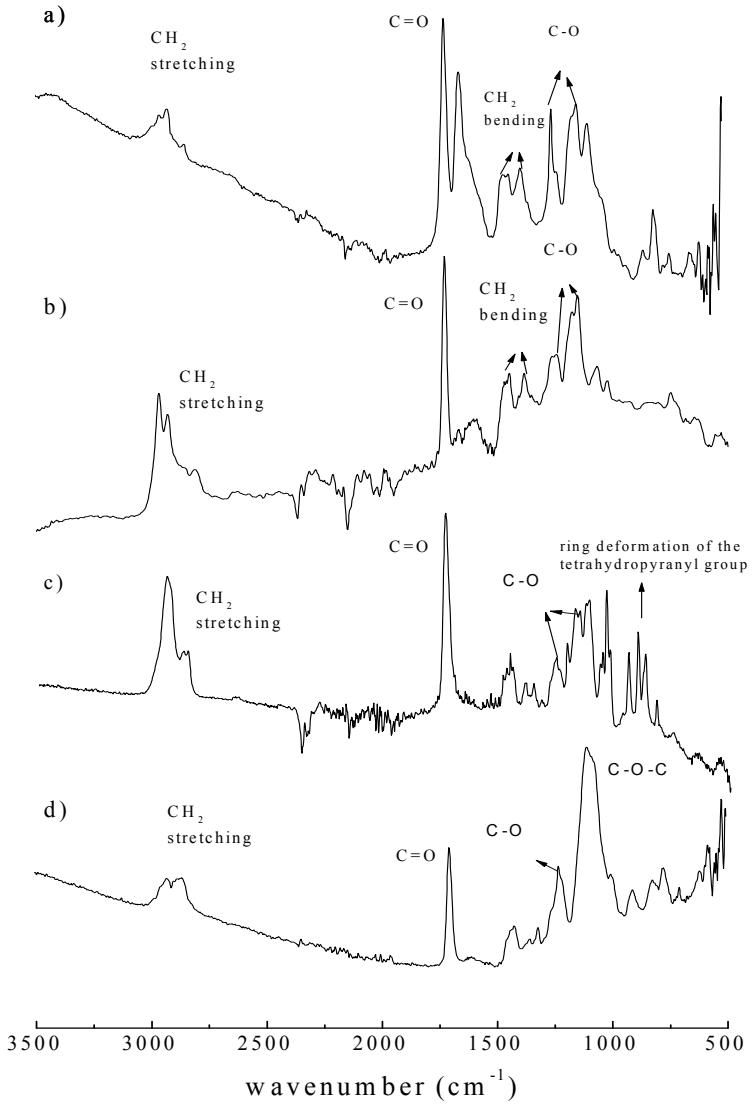

Figure 8. *ATR-FTIR spectra of grafted PDMAEMA (a), PDEAEMA (b), PTHPMA (c) and POEGMA film (d) on initiator modified gold substrates.*

The surface morphology of the dry grafted homopolymer films was probed by AFM operating in tapping mode. Figure 9 presents AFM images of the PDMAEMA grafted films prepared in a 3/2 methanol/water mixture (Figure 9a and Figure 9b) and a 4/1 methanol/water mixture (Figure 9c and Figure 9d). The PDMAEMA brushes prepared in the 3/2 methanol/water mixture without the addition of the deactivator in the beginning of the polymerization present a "patch" like morphology (Figure 9a and Figure 9b). In contrast the PDMAEMA brushes prepared in the 4/1 methanol/water mixture in the

presence of deactivator show a more uniform morphology, suggesting that the polymerization proceeds on the substrates in a controlled manner. Typical AFM images of PDEAEMA, PTHPMA and POEGMA grafted films are presented in Figure 10. For all the samples the surface anchored film covered the substrate surface completely and homogeneously. The root-mean-square (rms) roughness of the grafted polymer films was bellow 1 nm in most of the samples, verifying that the polymerization proceeded uniformly on the substrate.

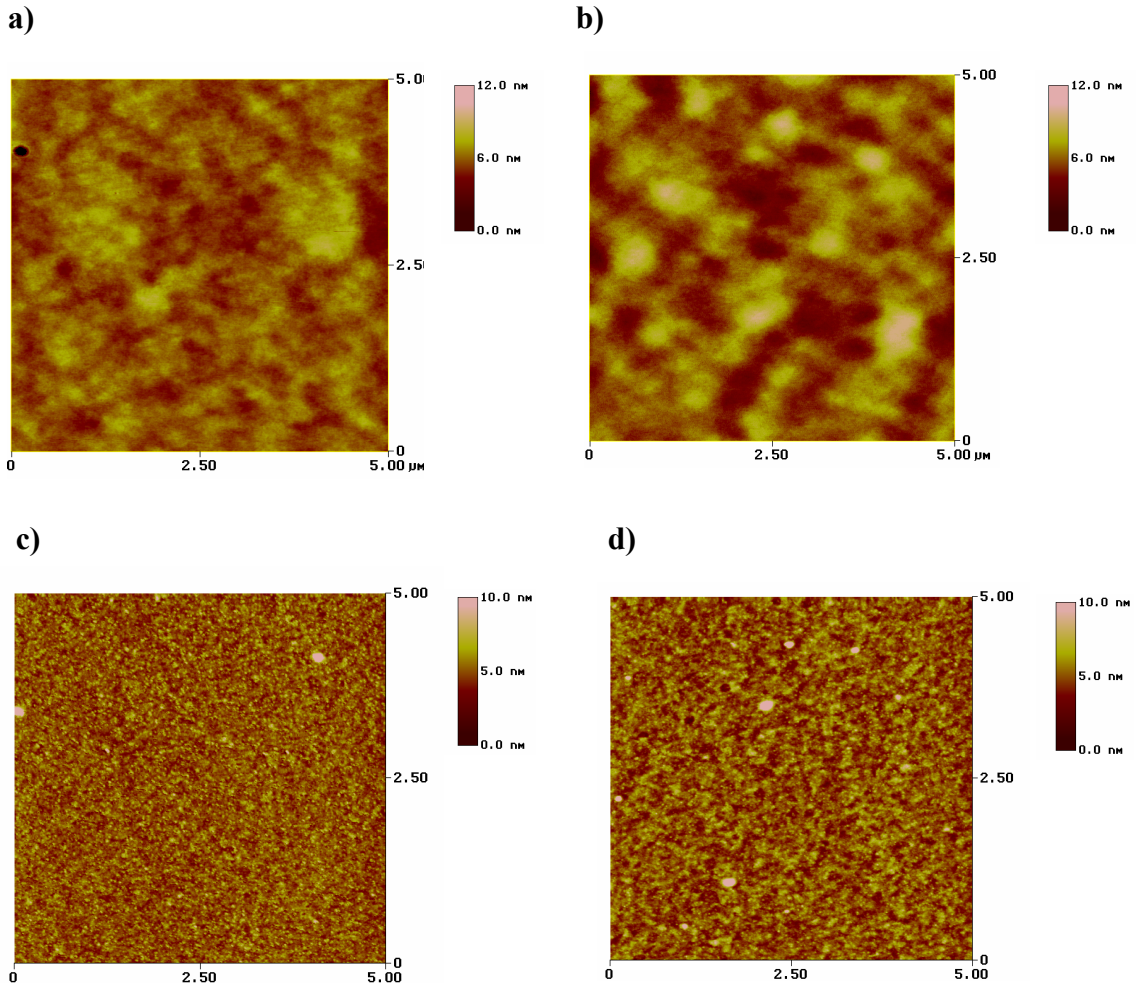

Figure 9. *AFM tapping mode images of PDMAEMA films prepared in methanol/water = 3/2, 15 min polymerization time (a) and 30 min polymerization time (b) without copper(II) deactivator and PDMAEMA films prepared in methanol/water = 4/1, 60 min polymerization time (c) and 120 min polymerization time (d) in the presence of copper(II) deactivator.*

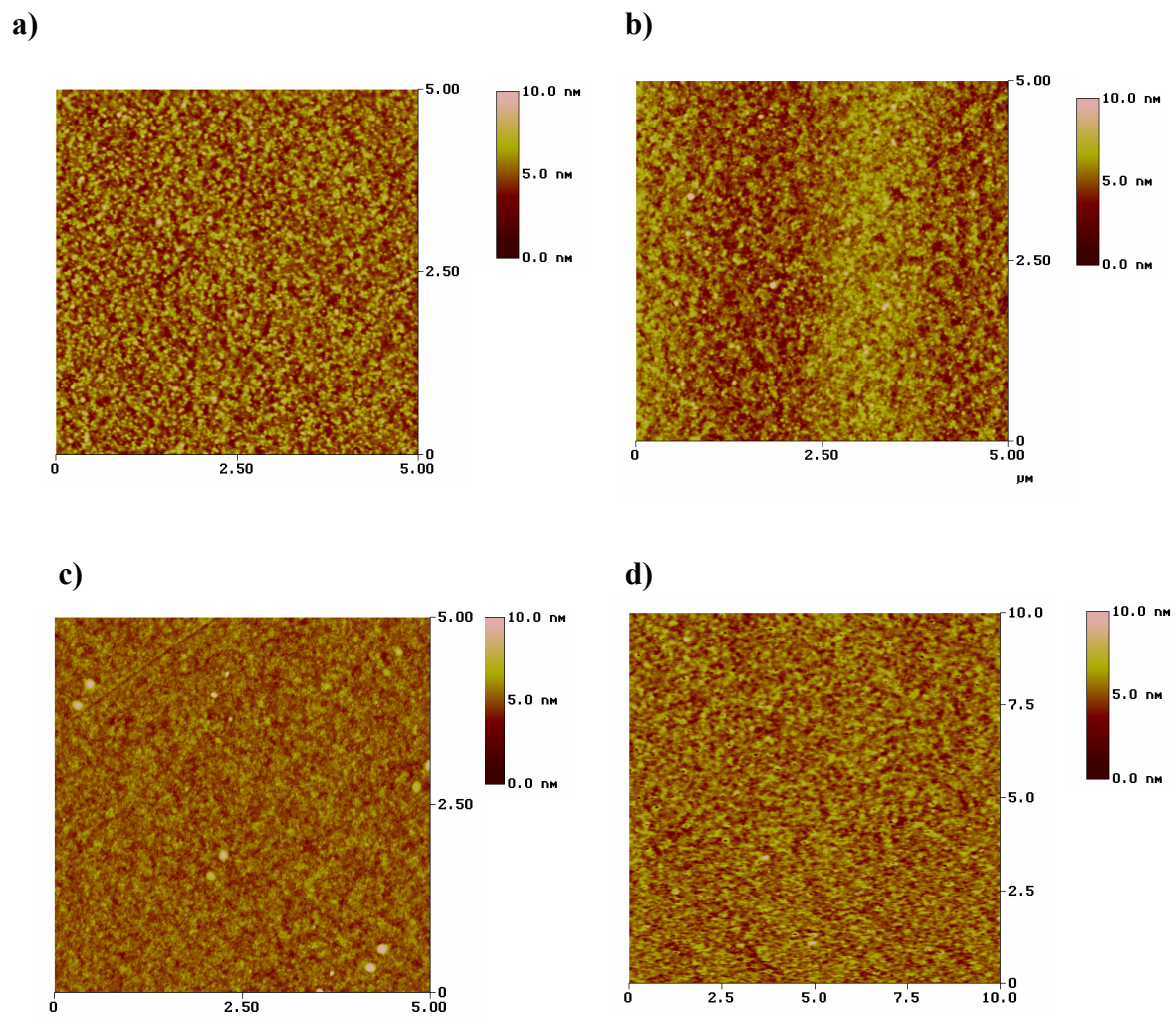

Figure 10. *AFM tapping mode images of PDEAEMA films prepared in methanol, 30 min polymerization time (a) and 3 h polymerization time (b). PTHPMA films prepared in o-dichlorobenzene, 24 h polymerization time (c) and POEGMA films prepared in water, 1 h polymerization time (d).*

An AFM liquid cell was used to image the wet PDMAEMA, PDEAEMA and PMAA grafted films. The polymer brushes were exposed to good solvents and typical images are presented in Figure 11. Upon exposure to a good solvent, the polymer chains swell and the AFM images show featureless and smooth surfaces. The roughness of the grafted polymer films was found bellow 1.2 nm, suggesting a uniform growth of the polymer layers on the gold substrate.

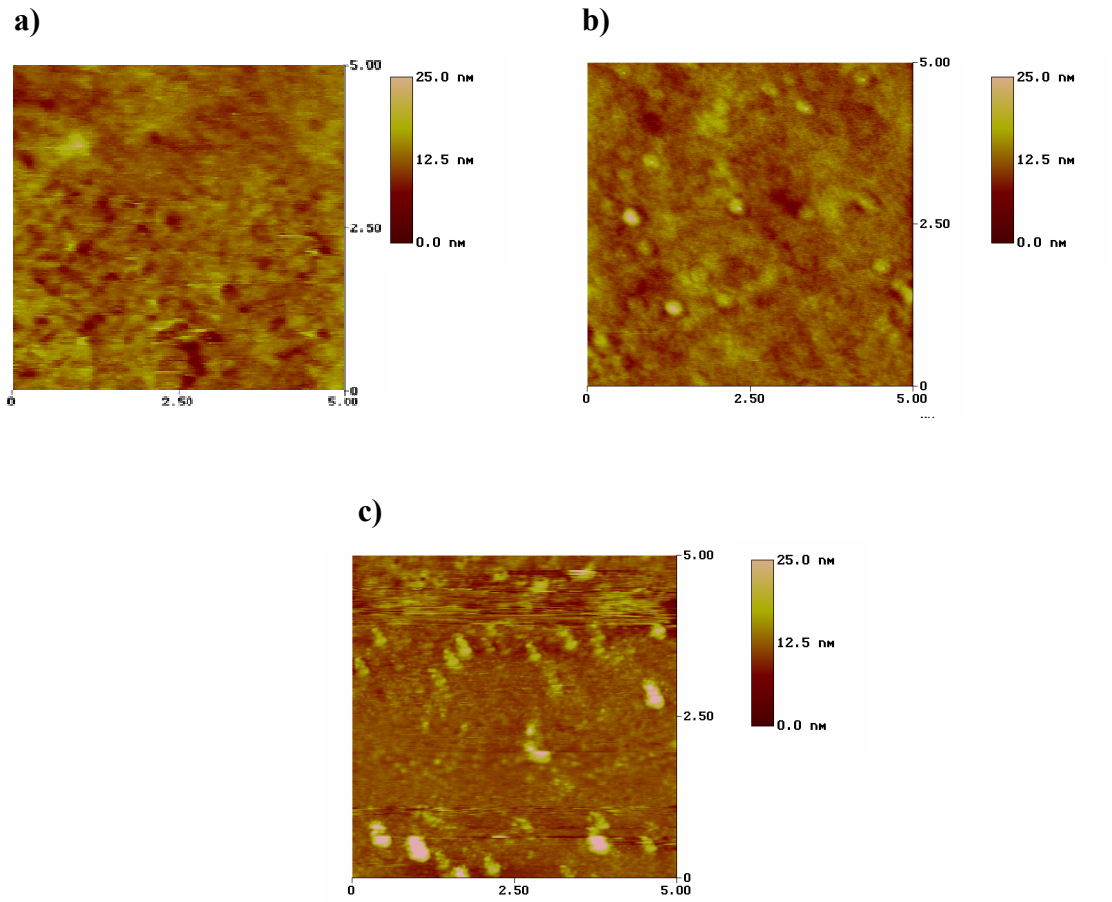

Figure 11. *Liquid AFM tapping mode images of a PDMAEMA brush in water (a), PDEAEMA brush in methanol (b) and PMAA in water (c).*

Determining the molecular weight of a polymer grafted onto a flat substrate can be problematic due to the small amount of brush material. An area of 1 cm^2 contains approximately 2.5 µg of polymeric material for a 25 nm thick polymer brush. The obtained polymer amount is too small to be detected using standard analytical methods. Therefore, the addition of free initiator in to the reaction mixture is one of the most used methods for determining the molecular weights of the grafted polymer films. There are reports in the literature that the polymer synthesized in solution by ATRP in the presence of free initiator and the grafted polymer chains have almost the same molecular weight and molecular weight distribution.[43, 54, 55] Therefore, the molecular weight of the polymer synthesized in solution can be a good approximation of the length of the grafted polymer chains which when combined with the dry film thickness allow the calculation of the polymer grafting density. We have performed a series of polymerizations of the

methacrylate monomers discussed above in the absence of copper(II) but upon addition of EBIB free initiator. The free polymer was isolated and purified and the number average molecular weights and the molecular weight distributions were determined by GPC. Table 7 lists the $M_{n,}$ and M_w/M_n of the free polymers prepared simultaneously from the free initiator in solution. Molecular weights varied between 19,300 and 65,500 for the synthesized polymers. The M_w/M_n was between 1.15-1.39, indicating a controlled polymerization. A very low polydispersity of 1.15 was obtained when the polymerization was carried out in bulk, indicating a very good control of the polymerization under these conditions. However, a value of M_w/M_n = 1.58 was obtained for the PDMAEMA homopolymer prepared in 4/1 methanol/water suggesting that the polymerization was not too well controlled under these reaction conditions in agreement with to discussion above that an aqueous reaction medium decreases the control of the polymerization. The grafting density σ, which is the number of macromolecules/nm^2 of the polymer chains on the gold substrates, was calculated according to Equation 3. 1:[56]

$$\sigma = h \rho N_A/M_n \qquad 3.\ 1$$

where, h is the polymer layer thickness (nm), ρ is the bulk density of the attached polymer assumed to be 1 g/cm^3, N_A is Avogadro's number and M_n is the number-average molecular weight of the polymer chains on the surface, assumed to be the same as that of the polymers synthesized in solution. Grafting densities between 0.1-0.37 were calculated, verifying the successful synthesis of methacrylate based homopolymers brushes of high grafting density on the gold substrates (Table 7).[8, 57]

Table 7. Reaction conditions and molecular characteristics of the free polymers prepared in the presence of free initiator. Brush thickness and calculated grafting densities of the grafted polymer chains.

Sample	Reaction conditions	M_n (g/mol)	M_w/M_n	h (nm)	σ (chains/nm^2)
PDMAEMA	Cu(I)/EBIB = 9 MeOH/H_2O = 4/1 18 h	26,866	1.59	11	0.25
	Cu(I)/EBIB = 2 Bulk 20 h	19,324	1.15	12	0.37
PDEAEMA	Cu(I)/EBIB = 9 MeOH 24 h	33,495	1.39	16	0.28
PTHPMA	Cu(I)/EBIB = 9 MeOH 5 h	55,106	1.28	11	0.12
POEGMA	Cu(I)/EBIB = 9 MeOH/H_2O = 4/1 3 h	65,473	1.26	10	0.1

3. 4. Wetting Behaviour of the Homopolymer Brushes

The wettability of all the prepared homopolymer brushes was investigated by contact angle measurements. The dependence of static contact angle on the pH of the solution in which the polymer film was previously immersed was studied for the ionisable PDMAEMA, PDEAEMA and PMAA homopolymer grafted films. Water contact angle measurements were performed after immersion at pH 3 and 8 and the measured values are listed in Table 8.

A contact angle of 65 ^{o} was measured on the initiator modified substrate. The contact angle of a water droplet on the POEGMA grafted film was found 41 ^{o} indicating the increase in the hydrophilicity of the surface. A contact angle of 68 ° was found for the 19 nm thick PDMAEMA film after immersion at pH 8, which decreased to 61° after immersion at pH 3. A similar trend was observed for the 29 nm thick PDEAEMA film. The contact angle at pH 8 was found to be 83°, which decreased to 56° upon immersion at the low pH (Figure 12a). These changes in the contact angle can be correlated with the chemical nature of the brush. PDMAEMA and PDEAEMA are protonated at pH < 8 and pH < 7 respectively. The charge density and the degree of protonation increase with the

decrease of pH. The lower contact angles measured at pH 3 for both PDMAEMA and PDEAEMA brushes compared to those obtained at pH 8 indicate that the polymer surfaces became more hydrophilic upon the protonation of the amine groups as expected.

On the other hand, the PMAA brush showed an inverse behaviour. The contact angle decreased from 46° after immersion at pH 3 to 35° upon immersion at pH 8, and then it remained almost constant upon further increase of the solution pH (Figure 12b). PMAA becomes dissociated at pH > 5.5 and its degree of ionization increases with the increase of the solution pH. The low contact angle determined for the PMAA grafted film at pH 8 is attributed to the ionization of the carboxylic acid groups which results in an increase in the hydrophilicity of the polymer layer.

Table 8. Contact angle measurements on homopolymer brushes

Polymer	Film thickness (nm)	Static contact angle pH 8 (°)	Static contact angle pH 3 (°)
POEGMA	43	41	-
PDMAEMA	19	68	61
PDEAEMA	29	83	56
PMAA	8	35	46

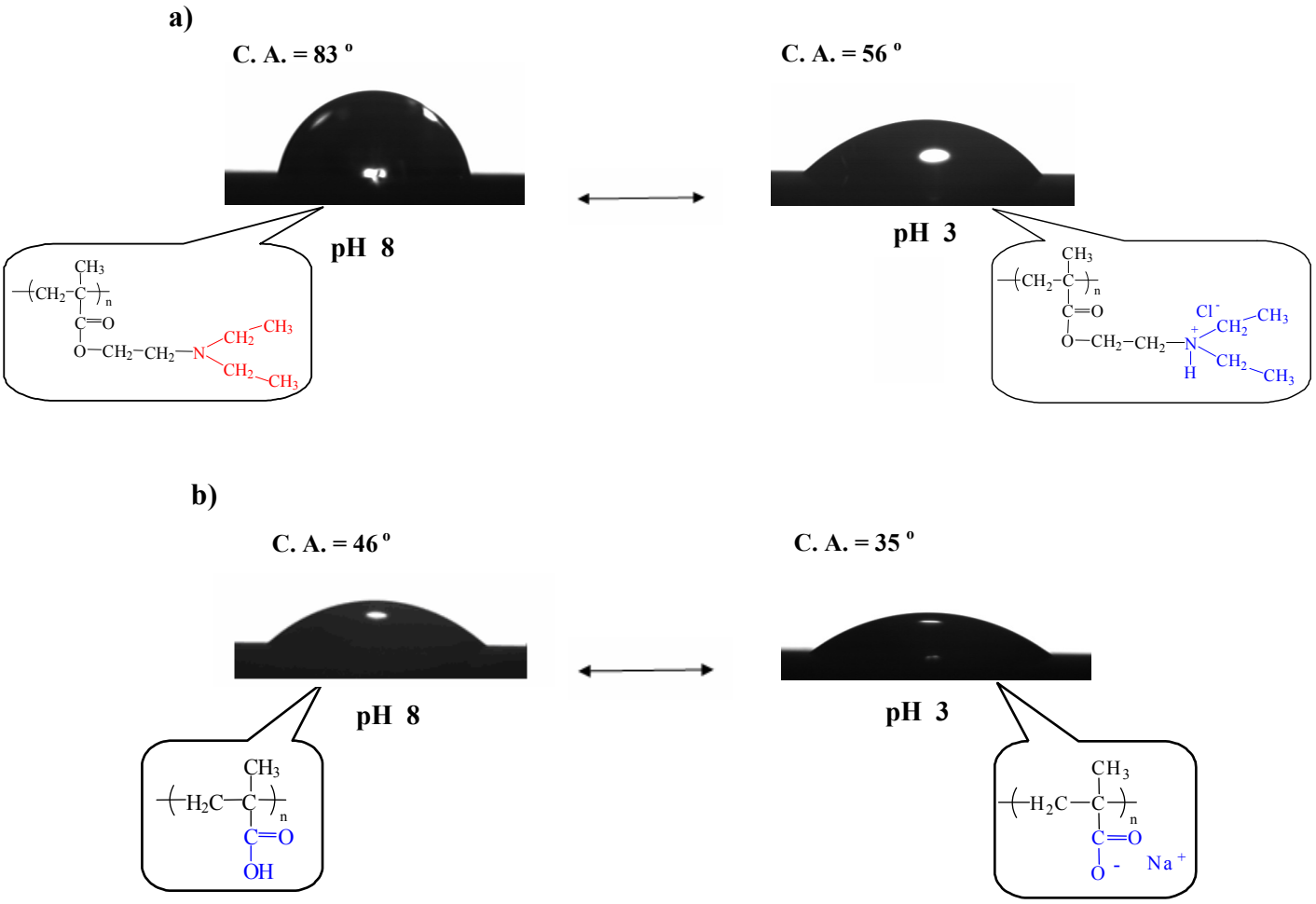

Figure 12. *Images of water droplets on the PDEAEMA (a) and PMAA (b) grafted films at pH 3 and 8.*

3. 5. pH Dependent Swelling Behavior of the of PDMAEMA Brush

The stimuli-responsive nature of the prepared PDMAEMA films was further investigated by ellipsomerty and AFM. The change in the dry polymer film thickness with pH was studied. First the dry thickness of the PDMAEMA brush after immersion in solutions of pH 8 and pH 3 was determined by ellipsometry. We found that the polymer film thickness increased from 19 nm to 24 nm when decreasing the pH from 8 to 3. This expansion of the PDMAEMA brush at low pH is due to the polyelectrolyte effect. As the amine groups along the polymer chains become protonated the similarly charged monomer repeat units experience electrostatic repulsions, forcing the polymer to adopt a

more extended conformation, reflected by the measured increase in brush thickness. However, because the measurements were carried out in the dry state the swelling of the brush was limited. In order to evaluate the real increase of the thickness of the polymer brush in solution at low and high pH, AFM measurements in the respective liquids were employed. To this end, a micropatterned gold-coated silicon wafer (the gold layer was 40 nm) was used to grow the PDMAEMA brushes. The monomer was polymerized in a 4/1 methanol/water solution for 2 h reaction time. The dry film thickness determined by AFM was 19 nm as shown in Figure 13.

Next, the polymer brush was placed in the liquid cell and a pH 3 solution was injected in the cell. The system was allowed to equilibrate for 20 min before the measurement. A thickness of 49 nm was found for the swollen polymer film (Figure 14a). Next, a pH 8 solution was injected over the polymer brush and after equilibration a thickness of 23 nm was found indicating the collapse of that the brush (Figure 14b). The 30 nm increase in film thickness at pH 3 is attributed to the stretched conformation adopted by the polymer chains due to the electrostatic repulsions between the protonated amine group and the osmotic pressure due to the presence of the counter ions inside the polymer brush. The equilibrium chain conformation at this pH is a balance between the electrostatic interactions of the charged monomer repeat units which favor stretching of the chain and the conformational entropy of the polymer chains, which opposes the extension of the chain.

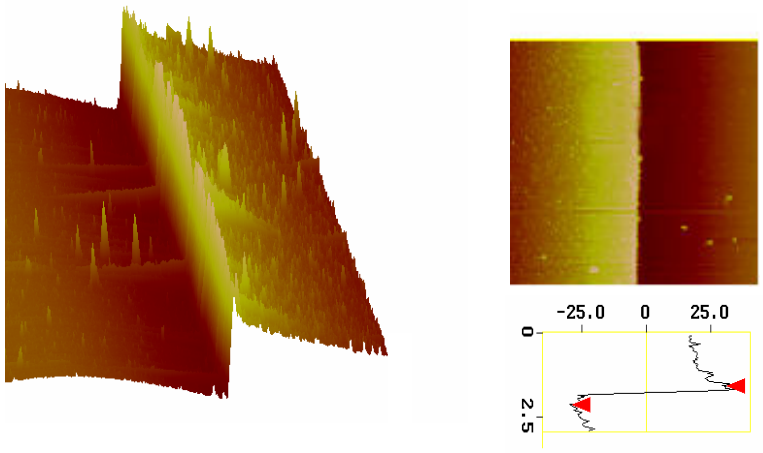

Figure 13. *3D and 2D AFM images of a 19 nm PDMAEMA brush on a patterned gold substrate.*

The small increase in film thickness from the dry state (19 nm) to the wet state at pH 8 (23 nm) is in agreement with the high grafting density of the polymer chains. The prepared PDMAEMA brushes were grown on a highly functional initiator coated substrate. Polymer brushes of such high grafting densities are already extended prior to exposure to solution, and as a consequence their swelling is relatively limited. The percent of swelling of the PDMAEMA brush at pH 8 was found to be 21%. This percentage corresponds to an amount of 0.4 μg/cm^2 of water uptake by the brush. At pH 3 a percent of swelling of 158% was calculated which is induced by the electrostatic repulsion between the protonated amine anions as discussed above. In this case the brush water uptake was calculated to be 3 μg/cm^2. Such an increase in the film thickness of 30 nm and present of brush swelling upon ionization is in accordance with the literature where the swelling of polyelectrolyte brushes of high grafting densities was reported.[50]

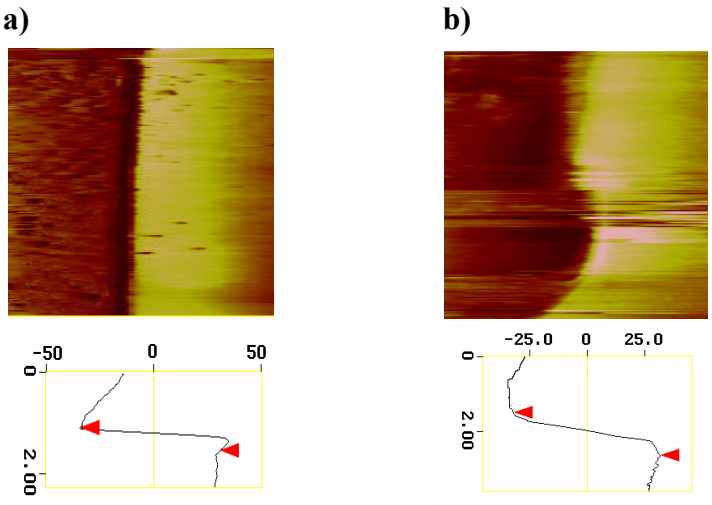

Figure 14. *AFM images of a PDMAEMA brush on a pattern gold surface at pH 3 (a) and pH 8 (b).*

3. 6. Synthesis of Diblock Copolymer Brushes

A method to verify the end functionality of a polymer prepared by ATRP is to use it as a macroinitiator for the ATRP of the same or another monomer. This results in the synthesis of block copolymer brushes. The behavior of tethered diblock copolymer brushes is interesting because the bottom block is constrained by covalent attachment to the substrate leading to vertical phase separation. Furthermore, the morphology and

properties of the surface onto which they are tethered can be reversely changed through the treatment with selective solvents.

Grafted diblock copolymers of PDMAEMA-*b*-POEGMA, PMeOEGMA-*b*-PDMAEMA, PDMAEMA-*b*-PDEAEMA, PDMAEMA-*b*-PTHPMA, and PTHPMA-*b*-PDMAEMA were synthesized on gold substrates. Table 9 summarizes the ATRP reaction conditions used for the synthesis of the grafted homopolymer and block copolymer films and their characteristics. The formation of the homopolymer followed by the diblock copolymer brush was verified by ellipsometry and contact angle measurements. In order to synthesize the PDMAEMA-*b*-POEGMA diblock copolymer film, the initiator modified substrate was first placed in a DMAEMA solution for 30 min, and the film thickness increased by 5 nm. Subsequent polymerization of OEGMA for 30 min increased the film thickness to 23 nm due to the formation of a 18 nm POEGMA layer. A similar procedure was followed for the synthesis of PDMAEMA-*b*-PDEAEMA and PDMAEMA-*b*-PTHPMA block copolymer brushes. A 19 nm thick PDMAEMA film was obtained after 2 h of polymerization, which further increased to a total thickness of 32 nm after the polymerization of the DEAEMA monomer, while a 24 nm thick PDMAEMA film was used as a macroinitiator for the synthesis of PDMAEMA-*b*-PTHPMA block copolymer brush. The successive polymerization of THPMA for 2h resulted in a 23 nm increase of the total film thickness. POEGMA was prepared under different reaction conditions (Chapter 2, Table 3) as the first block for the synthesis of the reverse POEGMA-*b*-PDMAEMA film. Unfortunately, no increase in the film thickness was found by ellipsometry after the polymerization of DMAEMA, suggesting that the synthesis of the block copolymer brush was unsuccessful. We thus concluded that the mono-hydroxy terminated OEGMA could not be polymerized under "living" conditions by ATRP. This was attributed to the hydroxyl group present at the end of the side group of the monomer which can replace the bromine group found at the end of the polymer chain and thus rendering the polymerization nonliving. To overcome this problem, a mono-methoxy terminated oligo(ethylene glycol) methacrylate (MeOEGMA) was chosen instead and polymerized as the first block. A film thickness of 9 nm was obtained after 90 min of polymerization which increased further to a total thickness of 18 nm after the polymerization of DMAEMA for 2 h suggesting the formation of a 9 nm PDMAEMA

layer. The PDEAEMA was used as a first block for the synthesis of the reverse PDEAEMA-*b*-PDMAEMA brushes, however no increase in the film thickness was observed upon the polymerization of DMAEMA, indicating that the PDEAEMA chains did not retained the end functionality and could not act as a macroinitiator. For the synthesis of the reverse PTHPMA-*b*-PDMAEMA film, THPMA was first polymerized in methanol for 5 h and a film thickness of 7 nm was obtained. An increase of the film thickness to 11 nm was observed after the subsequent polymerization of DMAEMA for 2 h suggesting the formation of a thin (4nm) PDMAEMA layer. PTHPMA was also synthesized in o-dichlorobenzene and after 24 h of polymerization a 26 nm thick film was obtained which further increased to 30 nm after 2 h of polymerization of DMAEMA. The increase in the film thickness observed by ellipsometry, after the polymerization of a second monomer verifies that the homopolymer chains remained active and capable of reinitiation. Other polymerization were carried out for the synthesis of PTHPMA-*b*-PDMAEMA films (Chapter 2, Table 5), but proved to be unsuccessful, suggesting that THPMA was not polymerized under living conditions.

Typical AFM images of the first block layer and the block copolymer films in the dry state are shown in Figure 15. The surface topography was imaged by tapping mode AFM, which revealed the synthesis of smooth and uniform homopolymer layers which grow to similarly smooth block copolymer films with a roughness below 1 nm (Table 9). No significant increase in the roughness of the film was observed after the formation of the block copolymer layer suggesting good control of the polymerization reaction. Contact angle experiments were also employed to verify the successful synthesis of the block copolymer brushes (Table 9). A contact angle of 68° was found for the PDMAEMA grafted surface which decreased to 49° after the synthesis of the POEGMA block (41° for the POEGMA homopolymer) verifying the formation of the second hydrophilic layer. However, when PDEAEMA was gown as a second block, the contact angle increased to 83° due to the hydrophobicity of the second layer. The PMeOEGMA film showed a contact angle of 65°, which is higher then that found for the mono-hydroxy terminated OEGMA grafted layers due to a more hydrophobic nature of PMeOEGMA chains. After the consecutive synthesis of the PDMAEMA block, the contact angle further increased to 70° which is in agreement with the previously measured PDMAEMA

contact angle. For the PTHPMA grafted layers the contact angle was between 70°-72° while successive polymerization of DMAEMA changed slightly the contact angle to ~ 67°. Finally, for the PDMAEMA-*b*-PTHPMA copolymer brushes a contact angle of 68° was found for the PDMAEMA first block which increased to 76° for the PTHPMA layer, higher then the value found for the PTHPMA above. This higher contact angle was attributed to a higher roughness of the polymer film which is known to affect the surface wetting properties.

Table 9. Reaction conditions and characteristics of grafted block copolymer films

Sample		Reaction conditions	Reaction time (h)	Film thickness (nm)	Film roughness (nm)	C.A. (°)
PDMAEMA-*b*-POEGMA	Tethered block	Cu(I)/Cu(II)/Bpy MeOH:H_2O = 4/1	0.5	5	0.6	68
	Outer block	Cu(I)/Cu(II)/Bpy H_2O	0.5	18	0.8	49
PDMAEMA-*b*-PDEAEMA	Tethered block	Cu(I)/Cu(II)/Bpy MeOH/H_2O = 4/1	2	19	0.6	68
	Outer block	Cu(I)/HMTETA MeOH	1	13	0.4	83
PMeOEGMA-*b*-PDMAEMA	Tethered block	Cu(I)/Cu(II)/Bpy MeOH/H_2O = 4/1	1.5	9	0.4	65
	Outer block	Cu(I)/Cu(II)/Bpy MeOH/H_2O = 4/1	2	9	0.5	70
PDMAEMA-*b*-PTHPMA	Tethered block	Cu(I)/Cu(II)/Bpy MeOH/H_2O = 4/1	3	24	0.5	68
	Outer block	Cu(I)/HMTETA o-dichlorobenzene	24	23	2.2	76
PTHPMA-*b*-PDMAEMA	Tethered block	Cu(I)/Cu(II)/Bpy MeOH	5	7	0.9	72
	Outer block	Cu(I)/Cu(II)/Bpy MeOH/H_2O = 4/1	2	4	0.5	67
PTHPMA-*b*-PDMAEMA	Tethered block	Cu(I)/HMTETA o-robenzene	24	26	0.7	70
	Outer block	Cu(I)/Cu(II)/Bpy MeOH/H_2O = 4/1	2	4	0.6	67

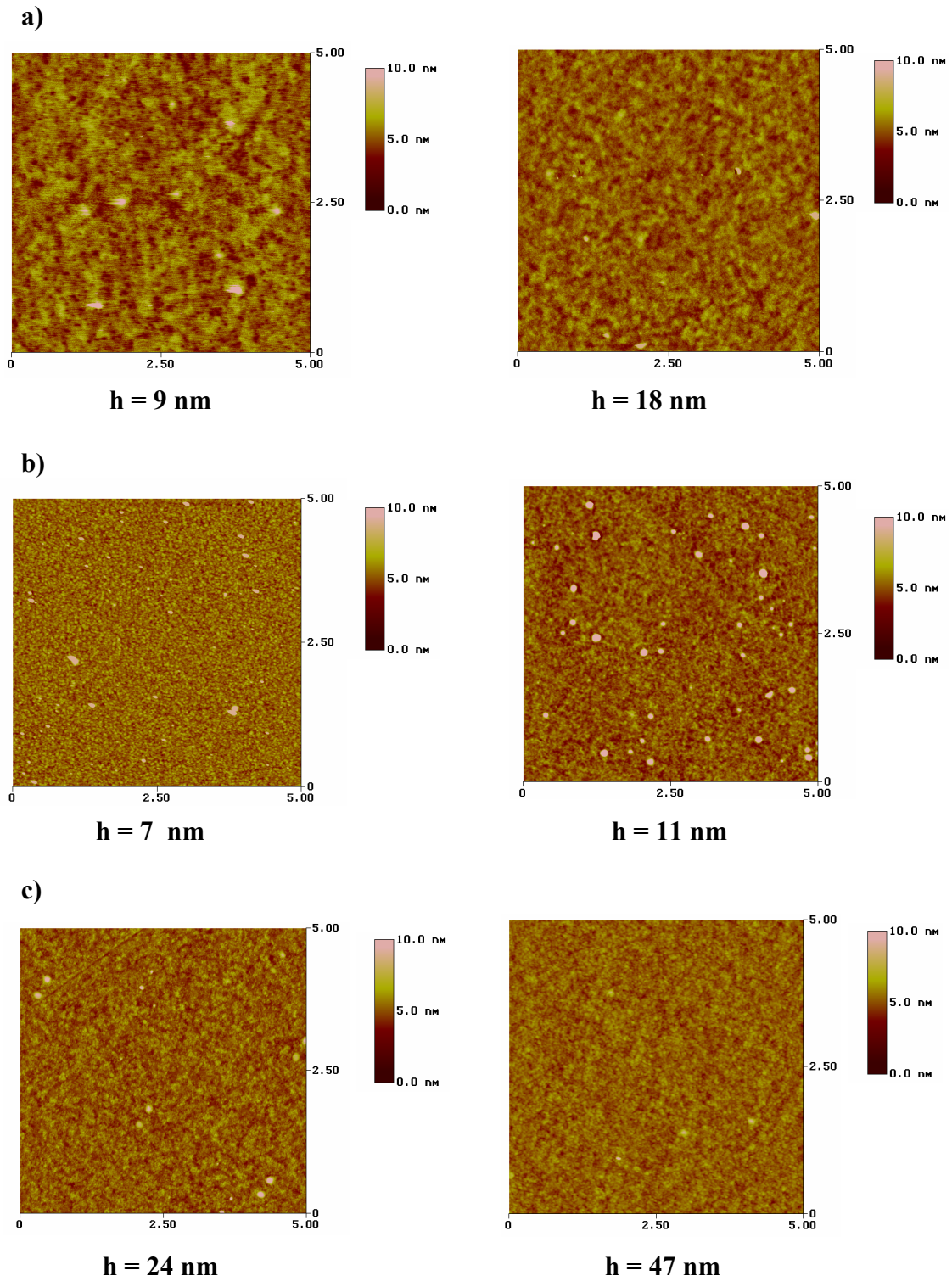

Figure 15. *AFM tapping mode images of PMeOEGMA and PMeOEGMA-b-PDMAEMA (a), PTHPMA and PTHPMA-b-PDMAEMA (b), PDMAEMA and PDMAEMA-b-PTHPMA (c) polymer films on gold substrates (5 × 5 μm).*

3. 7. Reversible Wetting Behavior of the Block Copolymer Brushes

Diblock copolymers brushes are known to be stimuli-responsive with respect to solvent quality. The reversible wettability upon treatment with different solvents was studied for the amphiphilic PDMAEMA-*b*-PDEAEMA and PTHPMA-*b*-PDMAEMA diblock copolymer brushes. The samples were treated with different solvents at room temperature and then dried under a stream of nitrogen followed by characterization by contact angle measurements and AFM. The PDMAEMA-*b*-PDEAEMA diblock copolymer brushes were first treated with n-hexane which is a good solvent for the outer PDEAEMA block and a bad solvent for the inner PDMAEMA block. A contact angle of 81° corresponding to the PDEAEMA block was measured suggesting that the hydrophobic block is at the air-solid interface. Subsequently, the diblock copolymer brushes were treated with water, a good solvent for PDMAEMA block but a bad solvent for PDEAEMA block. After treatment with water the contact angle was measured to be 67° (Figure 16a) which corresponds to the PDMAEMA layer as discussed above, suggesting the rearrangement of the polymer chains on the surface to expose the solvent soluble block at the surface of the film. Next, the two PTHPMA-*b*-PDMAEMA brushes (Table 9) were subject to the solvent treatment. The PTHPMA segment of the block copolymer brushes had a thickness of 7 nm and 26 nm, respectively, while the PDMAEMA layer was kept constant at 4 nm. Since the contact angles measured on the PTHPMA and the PDMAEMA films were very similar (Table 9), the PDMAEMA segment of the diblock brush was modified by quaternization which converted the tertiary amine groups to their quaternary ammonium salt (Scheme 3) (quaternized PDMAEMA will be abbreviated as $PDMAEMA_q$). The quaternization of PDMAEMA was carried out in THF using methyl iodine at RM for 20 h. After quaternization a contact angle of ~48° was measured suggesting the increase in the hydrophilicity of the polymer layer due to the permanent charge formed on the polymer side groups. This value of the contact angle remained constant after treating both the samples with water, indicating the presence of the $PDMAEMA_q$ segment at the top of the brush at the air-solid interface. The contact angle increased to 60° after the exposure of the $PTHPMA_{(7nm)}$-*b*-$PDMAEMA_{q(4nm)}$ film to o-dichlorobenzene, a good solvent for PTHPMA but a bad solvent for the quaternized PDMAEMA (Figure 16b). Moreover, after exposing the $PTHPMA_{(26nm)}$-*b*-

PDMAEMA$_{q(4nm)}$ brush to o-dichlorobenzene a contact angle of 65° was measured (Figure 16c), suggesting a partial rearrangement of the polymer chains on the surface. This result is very important in particular given the glassy nature of the PDMAEMA$_q$ layer and verifies the strong responsiveness of the polymer brushes to solvent quality.

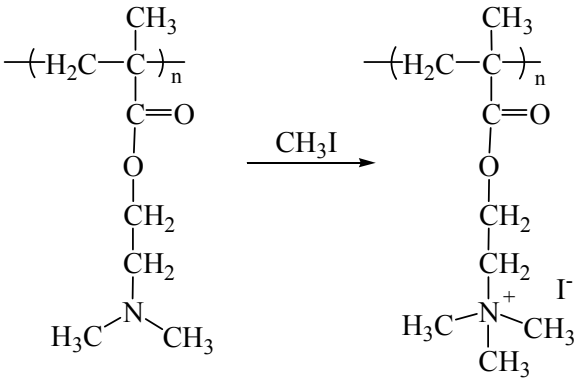

PDMAEMA PDMAEMA$_q$

Scheme 3. *Quaternization of PDMAEMA brushes.*

The surface rearrangements not only brought reversible changing of the water contact angle but also affected the surface roughness. After treating the PTHPMA$_{(26nm)}$-*b*-PDMAEMA$_{q(4nm)}$ with water a smooth surface with a roughness of 0.6 nm was imaged by AFM, similar to the value found for the originally prepared PTHPMA-*b*-PDMAEMA film. However, upon treatment with o-dichlorobenzene the surface roughness increased to 2.6 nm indicating a reorganization of the polymer chains.

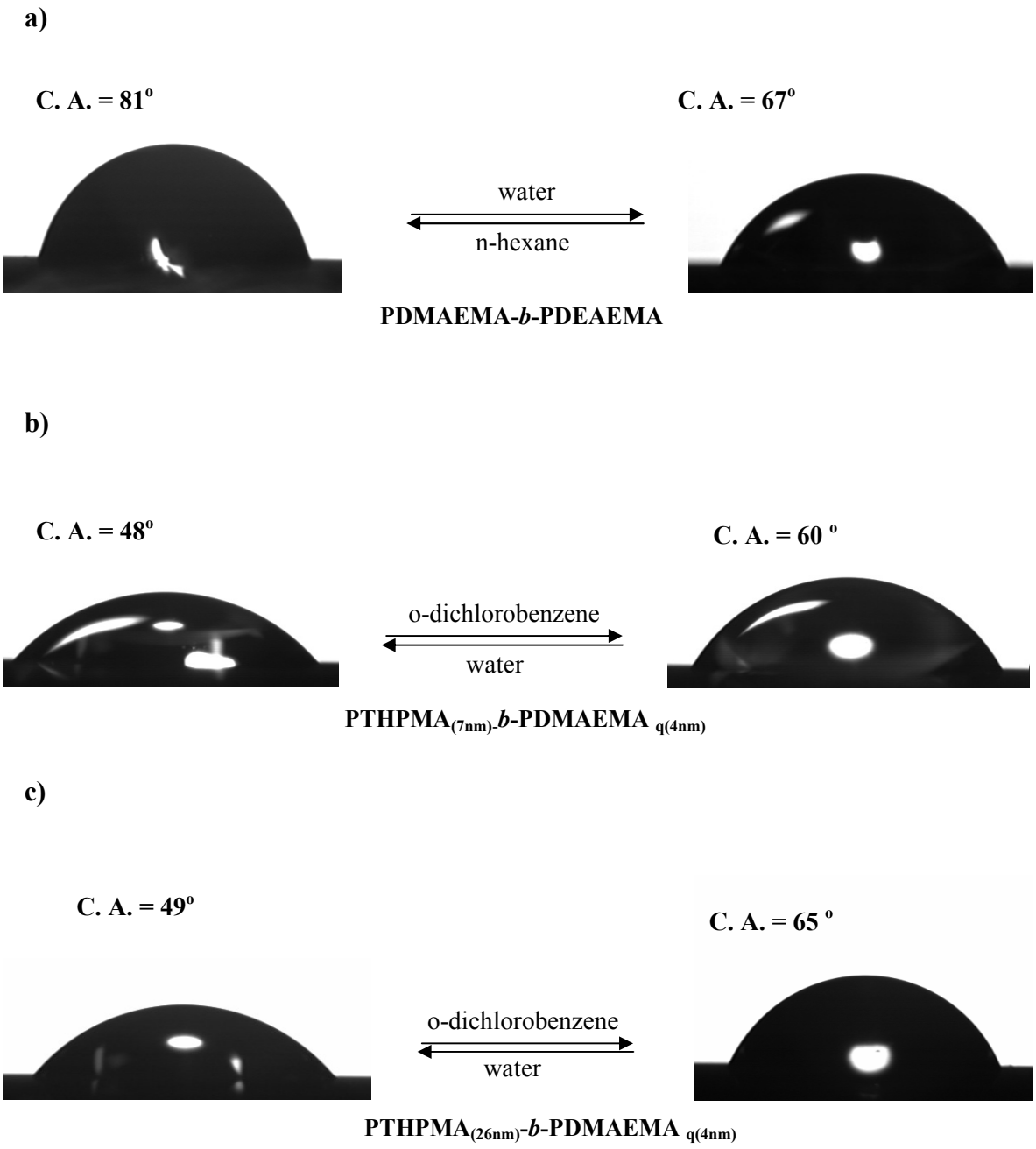

Figure 16. *Images of water droplets on PDMAEMA-b-PDEAEMA (a), PTHPMA$_{(7nm)}$-b-PDMAEMA$_{q(4nm)}$ brushes (b) and PTHPMA$_{(26nm)}$-b-PDMAEMA$_{q(4nm)}$ (c) upon different solvent treatment.*

These reversible changes in the chemical composition at the polymer–air interface are also apparent from the surface fluctuating amplitude (Figure 17a). However, no notable changes appeared in the surface roughness or the fluctuating amplitude for the

PDMAEMA-*b*-PDEAEMA block copolymer brushes upon solvent treatment as seen in Figure 17b.

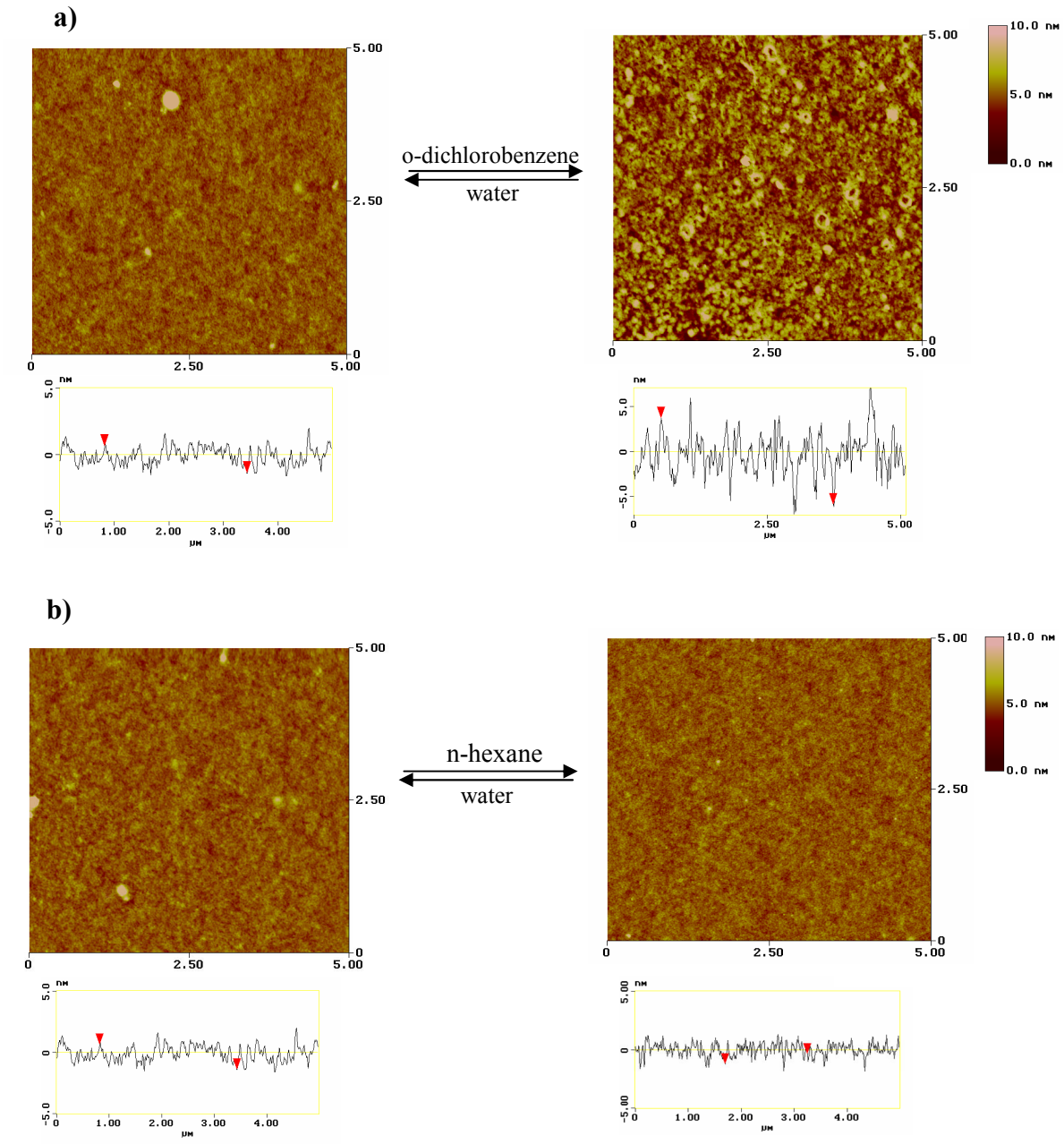

Figure 17. *AFM images of the PTHPMA-b-PDMAEMA$_q$ (a) and the PDMAEMA-b-PDEAEMA (b) block copolymer brushes after solvent treatment.*

The contact angle and the AFM measurements discussed above suggest that the block copolymer brushes are capable of internal rearrangements upon solvent treatment.

In the case of PDMAEMA-*b*-PDEAEMA copolymer brushes, the PDEAEMA segments are found at the top of the brush upon treatment of the sample with hexane according to the contact angle measurements. Since hexane is a bad solvent for the inner block, it can be envisioned that the PDMAEMA chains are in a collapsed sate near the substrate. After the immersion of the sample in water, the PDMAEMA segment is found at the top of the diblock copolymer brush to form a protective shield around the PDEAEMA block (Scheme 4a). The reason that no changes were seen in the AFM images upon solvent treatment is that a total internal rearrangement of the polymer chains took place and the fact that there is no distinguishable difference between the PDMAEMA and the PDEAEMA films in the AFM images. When PTHPMA-*b*-PDMAEMA$_q$ block copolymer brushes were immersed in water, the PDMAEMA$_q$ block was found at the top of the brush. However, upon treatment of the block copolymer film with o-dichlorobenzene only a partial internal rearrangement took place with both segments being present at the solvent interface, as indicated by both the contact angle measurements and AFM due to the glassy nature of both PTHPMA and PDMAEMA$_q$ layer (Scheme 4b). Contact angle measurements suggest that the longer PTHPMA block formed a better shield around the quaternized PDMAEMA segment than the shorter block upon exposure to o-dichlorobenzene.

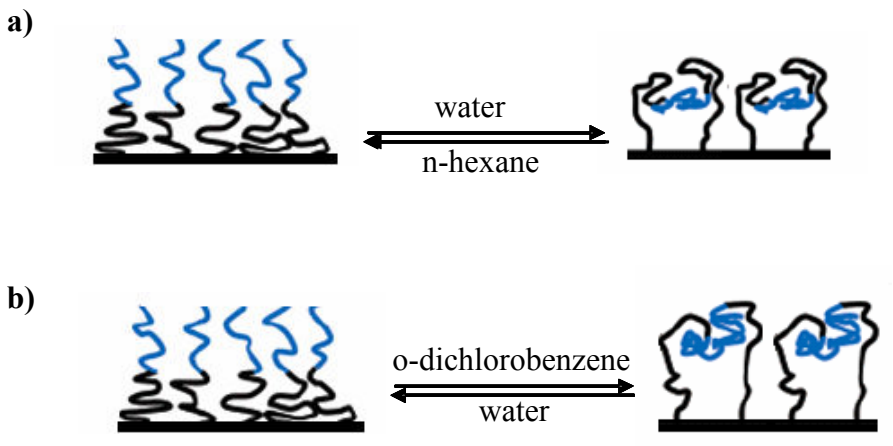

Scheme 4. *Speculative schematic illustration of PDMAEMA-b-PDEAEMA (a) and PTHPMA-b PDMAEMA$_q$ (b) block copolymer after different solvent treatment.*

3. 8. Protein Interactions with the PDMAEMA Homopolymer Brushes

Nonspecific adsorption of proteins and other charged molecules to interfaces bearing positively or negatively charges is the basis for ion exchange chromatography. Due to its mild elution conditions, ion-exchange chromatography has the advantage of preserving the protein biological activity.[58]

Bovine serum albumin (BSA) was employed as a model protein for the adsorption experiments on PDMAEMA brushes. Grafted PDMAEMA layers with a polymer molecular weight of 23,640 and a film thickness of 19 nm were used and protein adsorption was measured by SPR. Figure 18 shows representative SPR curves of grafted PDMAEMA chains and BSA uptake onto the PDMAEMA layer from a 0.1 mg/mL solution containing 1mM NaCl at pH 5.8. The BSA solution was in contact with the PDMAEMA brush for ~10 min, which was enough time for the system to equilibrate. The large change of the resonance angle to a higher value after the protein injection was attributed to the binding of BSA onto the polymer film. An adsorbed amount Γ_{BSA} = 20,24 mg/m^2 was calculated from the SPR sensogram. When the surface was rinsed with a solution of 1 mM NaCl no detectable BSA loss occurred suggesting strong binding of the protein on the polymer layer.

In a previous study Kusumo et. al. measured the BSA adsorption onto a hydrophobic SAM of hexadecanthiol on gold.[26] The adsorbed BSA corresponded to a concentration of 3 mg/m^2 after 115 h. The authors concluded that the adsorbed amount of BSA due to hydrophobic interactions was consistent to a monolayer of the protein. Therefore, in our case we calculated that the uptake of BSA by the PDMAEMA brush is equivalent to ~7 monolayers of BSA. At the working pH of 5.8 the PDMAEMA chains are positively charged, while the BSA molecules are negatively charged (BSA has an isoelectric point of 4.7). Thus, we concluded that the large BSA uptake is most likely due to electrostatic attraction, which allows the penetration of the negatively charged protein molecules into the positively charged PDMAEMA grafted layer.

The BSA distribution within the PDMAEMA brush cannot be found by SPR, therefore a theoretical model was used in order to estimate the three-dimensional BSA concentration $C_{3D,}$ which represents the binding capacity of the brush and can be calculated using Equation 3. 2:

$$C_{3D} = \Gamma_{BSA}/h \qquad 3.\ 2$$

where, h is the thickness of the polyelectrolyte brush in solution. The swelling of the polyelectrolyte brush in a low electrolyte concentration can be calculated according to Zhulina (Equation 3. 3):[59]

$$h \sim N a \alpha^{1/2} \qquad 3.\ 3$$

where, Na is the contour length and α is the degree of protonation of the polymer brush. The contour length was calculated using Equation 3. 4:

$$Na = 0.25\ n_{DMAEMA} \qquad 3.\ 4$$

where, n_{DMAEMA} is degree of polymerization, obtained by dividing the number-average molecular weight M_n by the molecular weight of the DMAEMA monomer. At pH 5.8, using a p*K*a of 7.5, a degree of protonation of 0.98 was calculated for PDMAEMA brushes according to Equation 3. 5:

$$\alpha = ([H^+]/K_a)/(1+ [H^+]/K_a) \qquad 3.\ 5$$

Introducing the calculated values in Equation 3. 3, a value of 37 nm was determined corresponding to the swelling of the polyelectrolyte brush. The concentration of BSA within the brush was calculated using Equation 3. 2. and a value of C_{3D} = 362 mg/mL was calculated, indicating that a relatively large amount of protein was adsorbed by the PDMAEMA brushes.

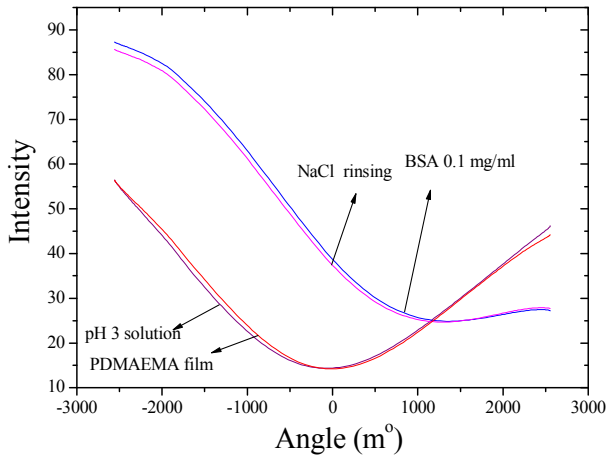

Figure 18. *SPR curves of a grafted PDMAEMA film on a gold sensor chip, the same film after BSA adsorption, after rinsing with a NaCl solution and after rinsing with a solution of pH 3.*

The above results indicate that the prepared PDMAEMA brushes have a high protein binding capacity. However, in order to use these brushes as ion exchange media, it must also be possible to remove the bound protein. Previous work suggested that both the pH and the ionic strength must be adjusted for the removal of proteins from a polymer brush.[26] The BSA desorption was investigated at pH 3, below the isoelectric point of BSA, where the protein and the polymer should repeal each other being both positively charged. A solution of 1 mM NaCl was adjusted to pH 3 by adding HCl and was injected into the SPR cuvette over the surface of the sample. Following rinsing, the SPR dip returned its initial value found for the PDMAEMA film proving that the PDMAEMA/BSA interactions are electrostatic in nature and suggesting that the prepared PDMAEMA brushes can be used as efficient ion exchange media for protein binding.

3. 9. References

1. E. J. Clayfield; E. C. Lumb, *J. Colloid Interface Sci.* **1966,** *22*, 269-284.
2. E. J. Clayfield; E. C. Lumb, *J. Colloid Interface Sci.* **1966,** *22*, 285-293.
3. L. Andruzzi; W. Senaratne; A. Hexemer; E. D. Sheets; B. Ilic; E. J. Kramer; B. Baird; C. K. Ober, *Langmuir* **2005,** *21*, 2495-2504.
4. H. Ma; D. Li; X. Sheng; B. Zhao; A. Chilkoti, *Langmuir* **2006,** *22*, 3751-3756.
5. S. Tugulu; H. A. Klok, *Biomacromolecules* **2008,** *9*, 906-912.
6. R. E. Holmlin; X. Chen; R. G. Chapman; S. Takayama; G. M. Whitesides, *Langmuir* **2001,** *17*, 2841-2850.
7. Z. Zhang; S. Chen; S. Jiang, *Biomacromolecules* **2006,** *7*, 3311-3315.
8. C. Yoshikawa; A. Goto; Y. Tsujii; T. Fukuda; T. Kimura; K. Yamamoto; A. Kishida, *Macromolecules* **2006,** *39*, 2284-2290.
9. I. Cringus-Fundeanu; J. Luijten; H. C. Van Der Mei; H. J. Busscher; A. J. Schouten, *Langmuir* **2007,** *23*, 5120-5126.
10. W. Feng; S. Zhu; K. Ishihara; J. L. Brash, *Langmuir* **2005,** *21*, 5980-5987.
11. A. B. Lowe; M. Vamvakaki; M. A. Wassall; L. Wong; N. C. Billingham; S. P. Armes; A. W. Lloyd, *J. Biomed. Mater. Res.* **2000,** *52*, 88-94.
12. D. E. Bergbreiter; M. L. Liu, *J. Polym. Sci., Part A: Polym. Chem.* **2001,** *39*, 4119-4128.

13. N. Chanunpanich; A. Ulman; Y. M. Strzhemechny; S. A. Schwarz; J. Dormicik; A. Janke; H. G. Braun; T. Kratzmüler, *Polym. Int.* **2003,** *52*, 172-178.
14. K. L. Mulfort; J. Ryu; Q. Zhou, *Polymer* **2003,** *44*, 3185-3192.
15. P. J. Hamelinck; W. T. S. Huck, *J. Mater. Chem.* **2005,** *15*, 381-385.
16. T. Sun; L. Feng; X. Gao; L. Jiang, *Acc. Chem. Res.* **2005,** *38*, 644-652.
17. F. J. Xu; S. P. Zhong; L. Y. L. Yung; E. T. Kang; K. G. Neoh, *Biomacromolecules* **2004,** *5*, 2392-2403.
18. A. Mizutani; A. Kikuchi; M. Yamato; H. Kanazawa; T. Okano, *Biomaterials* **2008,** *29*, 2073-2081.
19. B. Chen; F. J. Xu; N. Fang; K. G. Neoh; E. T. Kang; W. N. Chen; V. Chan, *Acta Biomater.* **2008,** *4*, 218-229.
20. N. Ayres; S. G. Boyes; W. J. Brittain, *Langmuir* **2007,** *23*, 182-189.
21. S. Tugulu; R. Barbey; M. Harms; M. Fricke; D. Volkmer; A. Rossi; H. A. Klok, *Macromolecules* **2007,** *40*, 168-177.
22. R. Dong; S. Krishnan; B. A. Baird; M. Lindau; C. K. Ober, *Biomacromolecules* **2007,** *8*, 3082-3092.
23. S. B. Lee; R. R. Koepsel; S. W. Morley; K. Matyjaszewski; Y. Sun; A. J. Russell, *Biomacromolecules* **2004,** *5*, 877-882.
24. F. J. Xu; S. J. Yuan; S. O. Pehkonen; E. T. Kang; K. G. Neoh, *Nanobiotechnol.* **2006,** *2*, 123-134.
25. G. Zhai; Z. L. Shi; E. T. Kang; K. G. Neoh, *Macromol. Biosci.* **2005,** *5*, 974-982.
26. A. Kusumo; L. Bombalski; Q. Lin; K. Matyjaszewski; J. W. Schneider; R. D. Tilton, *Langmuir* **2007,** *23*, 4448-4454.
27. K. Na; J. Jung; O. Kim; J. Lee; T. G. Lee; Y. H. Park; J. Hyun, *Langmuir* **2008,** *24*, 4917-4923.
28. O. Hollmann; C. Czeslik, *Langmuir* **2006,** *22* 3300-3305.
29. N. Singh; J. Wang; M. Ulbricht; S. R. Wickramasinghe; S. M. Husson, *J. Membr. Sci.* **2008,** *309*, 64-72.
30. F. Zhou; W. Shu; M. E. Welland; W. T. S. Huck, *J. Am. Chem. Soc.* **2006,** *128*, 5326-5327.

31. Y. Ito; Y. S. Park; Y. Imanishi, *Journal of the American Chemical Society* **1997,** *119*, 2739-2740.
32. A. M. Granville; W. J. Brittain, *Macromol. Rapid Commun.* **2004,** *25*, 1298-1302.
33. M. R. Tomlinson; J. Genzer, *Polymer* **2008,** *49*, 4837-4845.
34. B. Zhao; W. J. Brittain, *Macromolecules* **2000,** *33*, 8813-8820.
35. F. J. Xu; Q. J. Cai; E. T. Kang; K. G. Neoh, *Langmuir* **2005,** *21*, 3221-3225.
36. X. Gao; W. Feng; S. Zhu; H. Sheardown; J. L. Brash, *Langmuir* **2008,** *24*, 8303-8308.
37. S. A. Prokhorova; A. Kopyshev; A. Ramakrishnan; H. Zhang; J. Rühe, *Nanotechnology* **2003,** *14*, 1098-1108.
38. R. A. Sedjo; B. K. Mirous; W. J. Brittain, *Macromolecules* **2000,** *33*, 1492-1493.
39. B. Zhao; W. J. Brittain, *J. Am. Chem. Soc.* **1999,** *121*, 3557-3558.
40. M. R. Tomlinson; J. Genzer, *Langmuir* **2005,** *21*, 11552-11555.
41. J. Pyun; T. Kowalewski; K. Matyjaszewski, *Macromol. Rapid Commun.* **2003,** *24*, 1043-1059.
42. M. Ejaz; S. Yamamoto; K. Ohno; Y. Tsujii; T. Fukuda, *Macromolecules* **1998,** *31,* , 5934-5936.
43. M. Husseman; E. E. Malmström; M. McNamara; M. Mate; D. Mecerreyes; D. G. Benoit; J. L. Hedrick; P. Mansky; E. Huang; T. P. Russell; C. J. Hawker, *Macromolecules* **1999,** *32*, 1424-1431.
44. Q. Yang; J. Tian; M. X. Hu; Z. K. Xu, *Langmuir* **2007,** *23*, 6684-6690.
45. K. Matyjaszewski; P. J. Miller; N. Shukla; B. Immaraporn; A. Gelman; B. B. Luokala; T. M. Siclovan; G. Kickelbick; T. Valiant; H. Hoffmann; T. Pakula, *Macromolecules* **1999,** *32*, 8716-8724.
46. N. V. Tsarevsky; T. Pintauer; K. Matyjaszewski, *Macromolecules* **2004,** *37*, 9768-9778.
47. A. Y. Sankhe; S. M. Husson; S. M. Kilbey Ii, *Macromolecules* **2006,** *39*, 1376-1383.
48. S. G. Boyes; B. Akgun; W. J. Brittain; M. D. Foster, *Macromolecules* **2003,** *36*, 9539-9548.

49. N. D. Treat; N. Ayres; S. G. Boyes; W. J. Brittain, *Macromolecules* **2006,** *39*, 26-29.
50. A. J. Parnell; S. J. Martin; C. C. Dang; M. Geoghegan; R. A. L. Jones; C. J. Crook; J. R. Howse; A. J. Ryan, *Polymer* **2009,** *50*, 1005-1014.
51. S. Tugulu; R. Barbey; M. Harms; M. Fricke; D. Volkmer; A. Rossi; H. A. Klok, *Macromolecules* **2007,** *40*, 168-177.
52. N. Singh; X. Cui; T. Boland; S. M. Husson, *Biomaterials* **2007,** *28*, 763-771.
53. S. Perrier; D. M. Haddleton, *Macromolecular Symposia* **2002,** *182*, 261-272.
54. M. Ejaz; S. Yamamoto; K. Ohno; Y. Tsujii; T. Fukuda, *Macromolecules* **1998,** *31*, 5934-5936.
55. M. Ejaz; Y. Tsujii; T. Fukuda, *Polymer* **2001,** *42*, 6811-6815.
56. G. Henn; D. G. Bucknall; M. Stamm; P. Vanhoorne; R. Jérôme, *Macromolecules* **1996,** *29*, 4305-4313.
57. D. M. Jones; A. A. Brown; W. T. S. Huck, *Langmuir* **2002,** *18*, 1265-1269.
58. K. A. Davis; B. Charleux; K. Matyjaszewski, *Journal of Polymer Science, Part A: Polymer Chemistry* **2000,** *38*, 2274-2283.
59. E. B. Zhulina; T. M. Birshtein; O. V. Borisov, *Macromolecules* **1995,** *28*, 1491-1499.

CHAPTER 4

Wettability Switching From Superhydrophobic and Water Repellent Surfaces to Superhydrophilic Surfaces

Chapter 4 presents the preparation of functionalized pH-responsive surfaces that exhibit hierarchical micro- and nano-structured roughness, which can reversibly switch between superhydrophilicity at low pH and superhydrophobicity at high pH. To this end, PDEAEMA and poly(2-(diisopropylamino)ethyl methacrylate) (PDPAEMA) brushes were synthesized onto dual-length-scale roughened silicon substrates by surface-initiated ATRP. The water repellency of the polymer grafted surface in the superhydrophobic state was quantified by investigating the restitution coefficient of water droplets bouncing off the surface as a function of their impact velocity. Moreover, the contact angle hystereses along with the static contact angle data for the responsive surfaces were characterized.

4. 1. Introduction

The understanding and fabrication of functional and responsive materials with controllable wettability has attracted a lot of attention due to their wide range of potential applications. These types of surfaces are able to reversibly switch their wettability in response to external stimuli such as temperature, pH, electric or magnetic fields, chemical treatments, etc.

The effect of surface roughness on the wettability of the surfaces has received increasing interest during the last decade. The wettability of a solid surface is controlled by the chemical composition and the geometric microstructure of the surface. The wetting characteristics of a surface can be significantly enhanced by introducing roughness at two different length scales, micrometer scale and nonometer scale. Depending on the surface chemistry, rough surfaces will become either superhydrophilic or superhydrophobic. A superhydrophilic surface is one with a contact angle lower than 5^{o}, while superhydrophobic water repellent surfaces are characterized by contact angles higher than 150^{o} and small advancing–receding contact angle hysteresis (<5°). Artificial superhydrophilic surfaces are generated by creating micro/nanostructred on hydrophilic substrates or by chemically modifying a micro/nanostructred substrate with high surface

energy materials (500 -5,000 mN/m) such as metal oxides.[1] The strategy of developing artificial superhydrophobic surfaces consists in mimicking superhydrophobic biosurfaces by creating micro/nanostructures on hydrophobic substrates or by chemically modifying a micro/nanostructred surface with low surface energy materials (10 -50 mN/m). Examples of such materials include crystalline substrates and polymers.[2, 3] In the case of the most famous water repellent plant leaves, *Nelumbo nucifera* (the sacred Lotus), it is the dual scale roughness created by papillose epidermal cells and an additional layer of epicuticular waxes on their surfaces that is considered to lead to water repellence and to the so-called "Lotus effect".[4, 5] Attempts to develop surfaces with dual-scale roughness were successful in creating surfaces with high contact angles (~150-160°) and small contact angle hysteresis of only 2.5-5°.[6-9]

Stimuli-responsive materials make it possible to control the wettability of a surface in a reverse maner. Various stimuli have been used to alter the surface chemical properties. However, the responsive wettability is usually limited on a flat surface. The responsive wettability can be enhanced by introducing surface roughness and as a consequence reversible or "smart" switching between superhydrophobicity and superhydrophilicity can be accomplished (Figure 1).

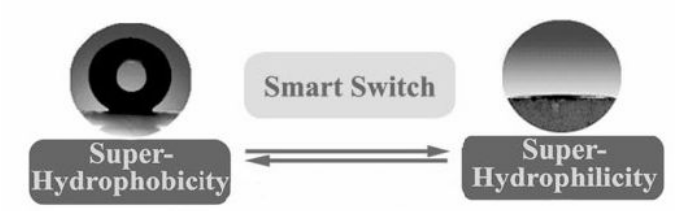

Figure 1. *Water drop profile for a reversible superhydrophobic/superhydrophilic switch.*

Polymer brushes prepared by end-grafting stimuli-sensitive polymers onto surfaces with hierarchical micro/nano roughness have been utilized for the development of such smart surfaces that can respond to changes in pH,[10, 11] temperature[12, 13] and solvent quality.[14, 15] These type of responsive surfaces with wetting properties that can be controllably altered on demand have attracted a lot of attention due to a wide variety of potential applications including controllable drug delivery,[16] enzyme immobilization[17] and separation,[18] adaptive microfluidic devices[19] antifouling[20] and self-cleaning surfaces.[21]

4. 2. Preparation of Stimuli-Responsive Brushes on Flat and Roughened Silicon Substrates

The artificially structured silicon surface was prepared in the presence of sulfur hexafluoride (SF_6) reactive gas at a laser fluence of 2.47 J cm^{-2} with an average of 500 pulses.[9, 22, 23] The roughened silicon substrates were next thermally oxidized at 1000 °C for 20 min to obtain a ~20 nm silicon oxide coating. The scanning electron microscopy (SEM) images of the structured silicon surface are shown in Figure 2a. The morphology of the prepared silicon surface is very similar to that of the Lotus leaf and it consists of micro-scale conical features decorated with nano-scale protrusions. The protrusions (spikes) have conical or pyramidal asperities with average sizes of ~10 μm and aspect ratio of ~ 4, whereas nanostructures with sizes up to a few hundred nanometers can be seen on the walls of the spikes (inset). Next the polymer chains were grown form the structured silicon surfaces using surface initiated ATRP (Scheme 1). Flat and roughened thermally oxidized silicon substrates were first immersed overnight in a vial containing a solution of 3-(2-bromoisobutyramido)propyl (trimethoxy)silane initiator. The surface-initiated ATRP of two different pH sensitive monomers DEAEMA and DPAEMA (Scheme 1) was carried out next form the initiator-modified substrates. The polymerizations were performed at room temperature using CuBr/HMTETA as the catalyst system. The DEAEMA monomer was polymerized in methanol at RT, while the DPAEMA monomer was polymerized in DMF at 70 °C. The EBIB free initiator was added in the reaction mixture to control the polymerization. A flat and a roughened silicon substrate were placed in the same reaction flask, therefore it is expected that the polymer brush growth proceed under identical conditions on the two substrates. The dry polymer film thickness was determined by ellipsometry on the flat modified silicon substrate. After 24 h of polymerization a dry PDEAEMA film of 16 nm was obtained, whereas a thickness of 19 nm was measure for the PDPAEMA grafted film.

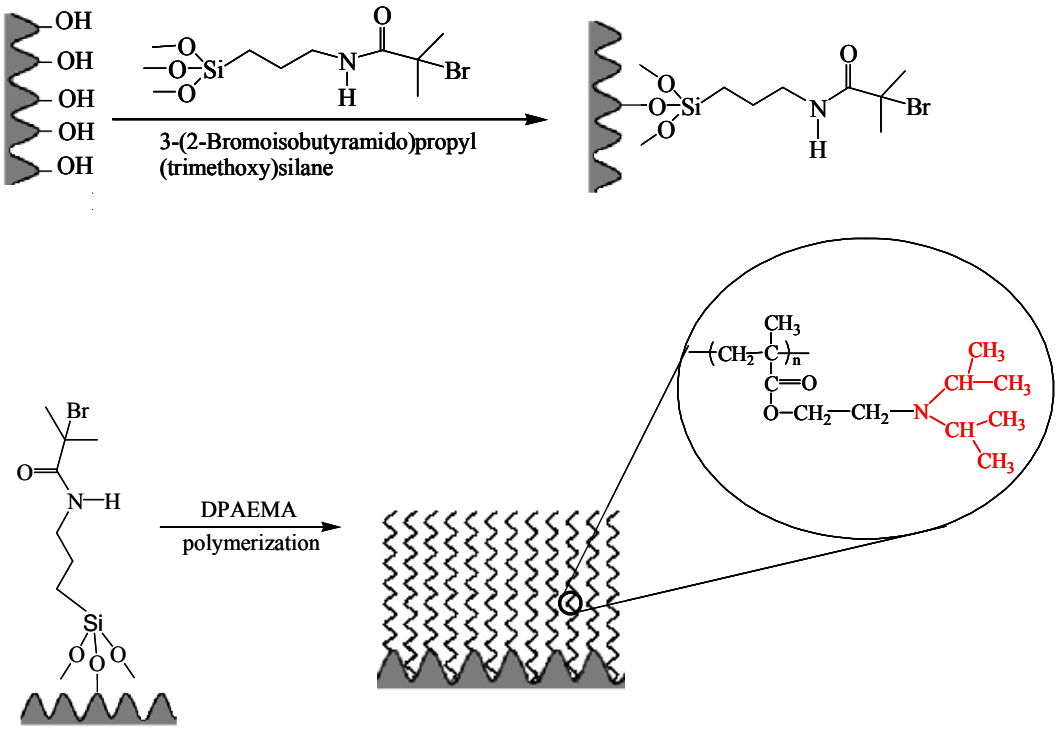

Scheme 1. *Schematic representation of the initiator immobilization and the surface-initiated ATRP of DPAEMA monomer form the roughened silicone substrate.*

The number average molecular weights of the polymers synthesized by the free initiator in solution were determined by GPC. The number average molecular weight of PDEAEMA was M_n = 33,000 g mol^{-1} while, a value of M_n = 15,000 g mol^{-1}, was found for PDPAEMA. The grafting density σ (macromolecule/nm^2) of the polymer chains on the silicon substrate was calculated using Equation 3. 1. A grafting density of 0.29 chains/nm^2 was determined for the PDEAEMA grafted chains and a value of 0.78 chains/nm^2 was calculated for the PDPAEMA brushes.

After the functionalization of the artificially structured silicon with PDPAEMA brushes, SEM images were taken. As it can be seen in Figure 2b that both the micro-scale and the nano-scale protrusions (inset) are evident, verifying that the polymerization did not perturb the hierarchical micro- and nanoscale roughness of the surface.

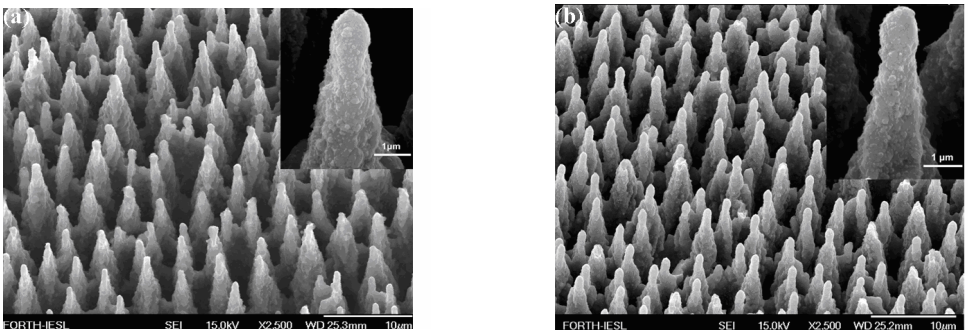

Figure 2. *SEM image of the artificially structured silicon (scale bar 10 μm). Inset: high magnification SEM image of a single protrusion depicting nanostructures of sizes up to few hundred nanometers (scale bar 1 μm) (a); SEM image of a PDPAEMA brush functionalized artificially structured substrate after ten pH cycles, where the protrusions remain unperturbed (scale bar 10 μm). Inset: high magnification SEM image of a single protrusion depicting that the nanostructures on the slopes of the protrusions remain unperturbed (scale bar 1 μm) (b).*

4. 3. Reversible Control of the Surface Wettability via pH Treatment

To date polymers that become superhydrophobic at low pH and anionic and superhydrophilic at high pH have been reported.[24] However, this property imposes some limitations to certain applications. Anionic surfaces cannot interact with DNA, enzymes or polyanion drugs by attractive electrostatic interactions at low pH. In this respect, surfaces functionalized with pH-responsive polymers, which become cationic and superhydrophilic at low pH, are especially desirable. PDEAEMA and PDPAEMA homopolymers are weak polybases with pK_α values of 7.3 and 6.3,[25, 26] respectively which undergo a reversible protonation/deprotonation process upon changing the solution pH and, thus, can interact with anionic substances at low pH when they become cationic.

The PDEAEMA and PDPAEMA functionalized structured silicon was immersed in solutions of high and low pHs and the static contact angle were measured. After the immersion of the PDEAEMA modified substrate at pH 3 a complete wetting was observed indicating that the surface became superhydrophilic. However the behavior after immersion at pH 8 was far from superhydrophobic with the contact angle reaching only ~126º (Figure 3 (top panel)). The behavior of the PDPAEMA brushes was studied next as

a function of pH. After the immersion of the PDPAEMA functionalized roughened surface of at pH 2.5 a complete wetting of the surface (superhydrophilicity) was observed, whereas following immersion at pH 8.5, a contact angle of 154º was measured, indicating the preparation of a superhydrophobic surface (Figure 3 (bottom panel)). The change in the surface wettability with pH is due to the reversible protonation/deprotonation of the tertiary amine groups of the PDEAEMA and DPAEMA brushes, which alter the degree of ionization of the monomer repeat units, thus modifying the hydrophilicity/hydrophobicity of the polymer brush. Measurements of the static contact angle performed on flat silicon substrates grafted with polymer brushes gave a value of ~83º for a PDEAEMA coated surface and ~88º for a PDPAEMA modified substrate. Both measurements were taken in the deprotonated state of the homopolymer brush. From the above results it can be concluded that in order to prepare a superhydrophobic surface the combined effect of the dual-scale roughness together with a sufficient hydrophobicity of the material is necessary. The incorporation of only two extra methyl groups per monomer unit (Figure 3, chemical structure) can lead to a "hydrophobic enough" material and thus to a superhydrophobic surface.

a)

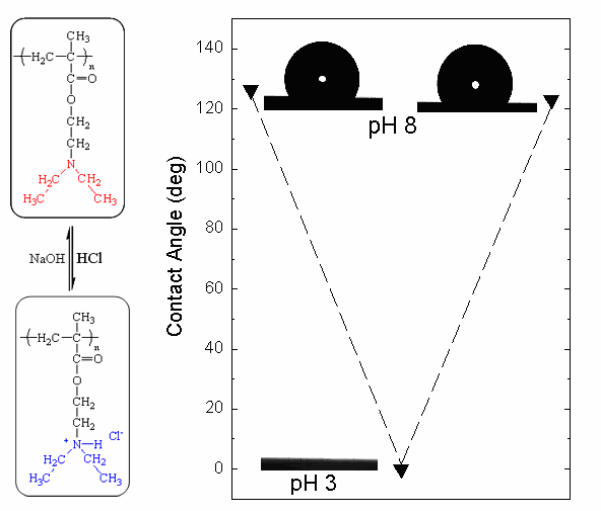

b)

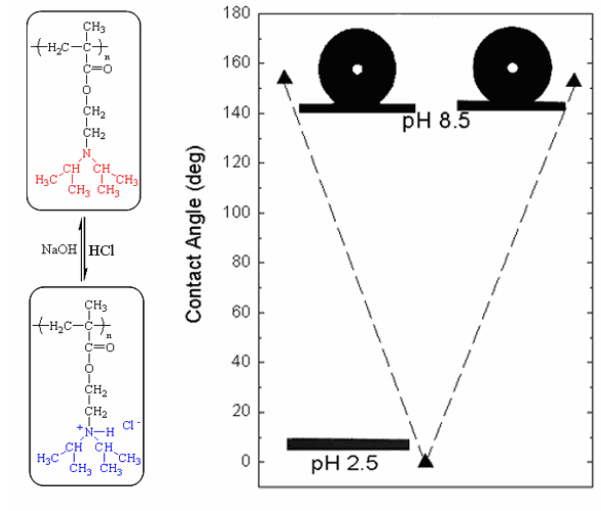

Figure 3. *Characteristic images of water droplets on the PDEAEMA functionalized structured surface following immersion at pH 8 (contact angle: 126°), pH 3 (complete wetting) and again at pH 8 (contact angle: 123°) (a). The scheme shows the protonation/deprotonation process of PDEAEMA. Characteristic images of water droplets residing on the PDPAEMA functionalized structured surface following immersion at pH 8.5 (contact angle: 151°), pH 2.5 (complete wetting) and again at pH 8.5 (contact angle: 154°) (b). The scheme shows the protonation/deprotonation process of PDPAEMA.*

Successive immersions of the PDEAEMA and PDPAEMA functionalized roughened surfaces at high and low pH were carried out next. The PDEAEMA modified substrate was immersed in solutions of pH 8 and 3 while the PDPAEMA functionalized substrate was immersed in solutions of pH 8.5 and 2.5. The variation in the contact angle upon repeated cycles of pH was recorded and is presented in Figure 4a and Figure 5a for the PDEAEMA and the PDPAEMA functionalized roughened surface, respectively. The results show excellent reversibility for at least ten cycles, whereas the values of the contact angles of both the hydrophobic (PDEAEMA functionalized substrate)/ superhydrophobic (PDPAEMA functionalized substrate) and the superhydrophilic state are very stable. A quick transformation between hydrophobicity/superhydrophilicity and superhydrophobicity/superhydrophilicity was observed, as a single cycle lasted only several seconds. The above results verify that the polymer brushes grafted on the dually-roughened surfaces are resistant to successive pH variations, which is especially important since the brushes were immersed in basic and strongly acidic solutions. Compared with the large change of the contact angles on the PDEAEMA and PDPAEMA modified rough substrates (~120° and ~150°), a small change in the contact angle was seen for the PDEAEMA and the PDPAEMA flat functionalized substrates (~20° and ~30°) (Figure 4b and Figure 5b), verifying that the surface wettability is enhanced by the surface roughness.

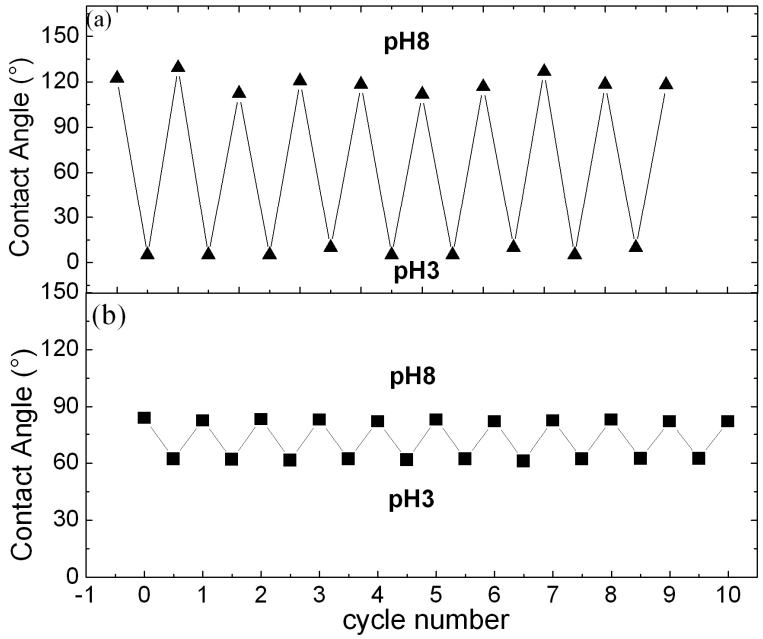

Figure 4. *Average contact angle values of water drops residing on the PDEAEMA functionalized hierarchically structured surface (a) and the PDEAEMA functionalized flat surface (b) following successive immersions at pH 8 and pH 3.*

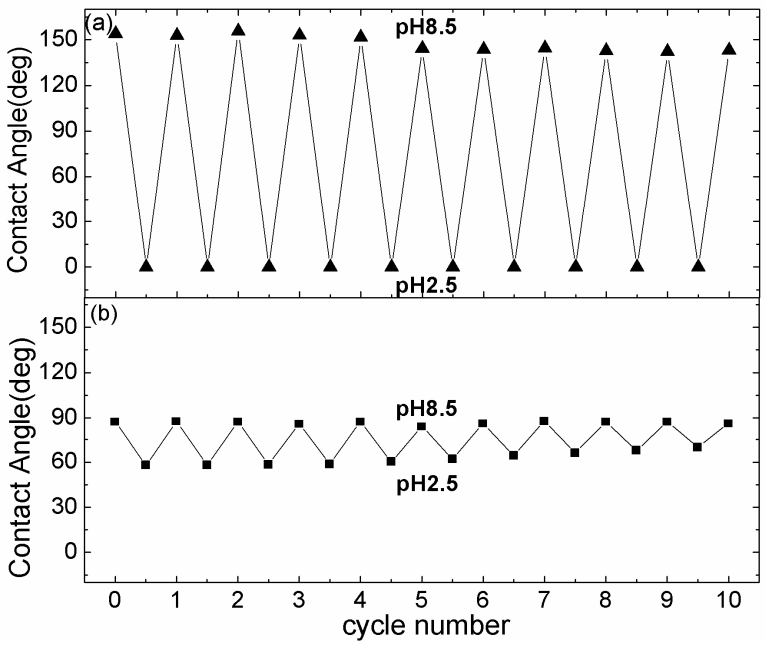

Figure 5. *Average contact angle values of water drops residing on the PDPAEMA functionalized hierarchically structured surface (a) and the PDPAEMA functionalized flat surface (b) following successive immersions at pH 8.5 and pH 2.5.*

A superhydrophobic and hence water repellent behavior can only be achieved for contact angles of 150-160°. A water repellent surface must also be characterized by low values of the contact angle hysteresis (less than 5°),[6-8, 27] which is defined as the difference between the advanced (θ_A) and the receding (θ_R) angle. The smaller the hysteresis is, the easier will be to move the liquid droplet. Figure 6 shows the average contact angles of water droplets on the PDPAEMA functionalized dually-roughened surface following immersions in a solution of pH 8.5 together with the respective sliding angles (α) as a function of immersion time. The sliding angle is defined as the critical angle above which a water droplet of a certain weight begins to slide down the inclined plate. For this surface at high pH a sliding angle of 5° was found experimentally. The equilibrium value of the contact angle of ~154° was reached after only about 10s, however the equilibrium value of the sliding angle of about 5° was only reached after longer times of about 40-50s. Most probably, although the incomplete deprotonation of the polymer brush can be sufficient to result to an apparent hydrophobicity of the surface (larger than 150° contact angle), the presence of even a few charged monomer units can lead to chemical heterogeneities[28] which may cause contact line pinning and, thus, contact angle hysteresis.[3]

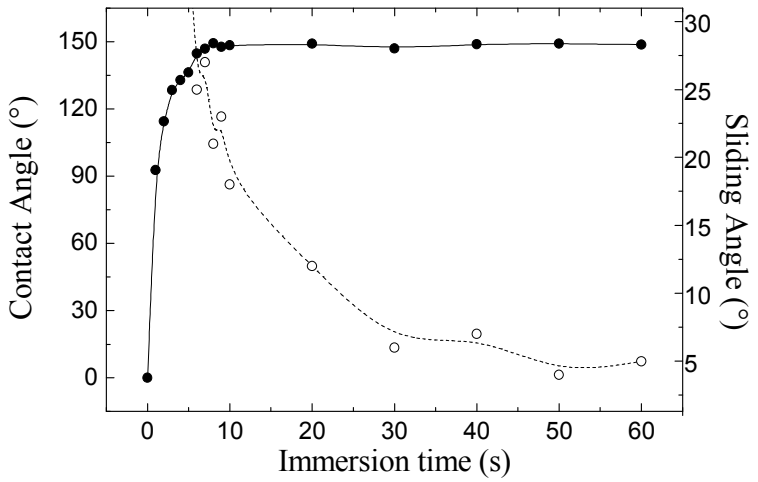

Figure 6. *Average contact angle (filled symbols) and sliding angle (open symbols) values for a PDPAEMA functionalized hierarchically structured surface following immersions in a solution of pH 8.5.*

The inset of Figure 7 presents selected snapshots of a water droplet with a radius of 1.35 mm impinging on the PDPAEMA functionalized artificial surface following its immersion in a solution of pH 8.5. Selected maxima of its trajectory are shown as a function of time. The water drop impacts the surface with a velocity that corresponds to a dimensionless Weber number of We = 3.5. The Weber number was calculated using Equation 4.1:

$$We = \rho V^2 R / \gamma_{LV} \qquad 4.1$$

where ρ is the liquid density, R the liquid drop radius, V is impact velocity and γ_{LV} is the liquid surface tension taken as 72 dynes/cm at 25 ^{o}C. The drop bounced back numerous times from the polymer coated substrate, indicating that the prepared surface is water repellent. The drop came to rest on the surface after ~ 250 ms. Part of the initial kinetic energy of the drop was transferred into vibrational energy after the impact, and, subsequently, damping of the bouncing motion occurred due to viscous dissipation.[29, 30]

The elasticity of the collisions on the PDPAEMA functionalized structured surface indicates a high degree of repellency. A direct measure of this elasticity is the restitution coefficient (ε) described by Equation 4. 2:

$$\varepsilon = V'/V \qquad 4.2$$

where, V' is the center of mass velocity of a droplet just after impact and V is the centre of mass velocity just before impact. This coefficient was deduced from the recorded video images shown in Figure 7 as a function of the impact velocity V in comparison with the behavior of droplets impinging on top of the natural Lotus leaf.[9] The highest elasticity is observed at intermediate velocities, from ~0.17 m/sec to ~0.30 m/sec, where the restitution coefficient is found to exceed 0.90. This value matches that of the Lotus leaf and it is among the highest ever reported.[3, 29, 30] For small velocities, ε decreases abruptly with decreasing V and reaches zero at some velocity that depends on the droplet volume. This is the threshold that quantifies the water repellency of the surface. The smaller this velocity, the more water repellent the surface is. The threshold velocity necessary to avoid the sticking of the drops for the PDPAEMA functionalized artificially structured surface is comparable to that of the Lotus leaf (Figure 7).

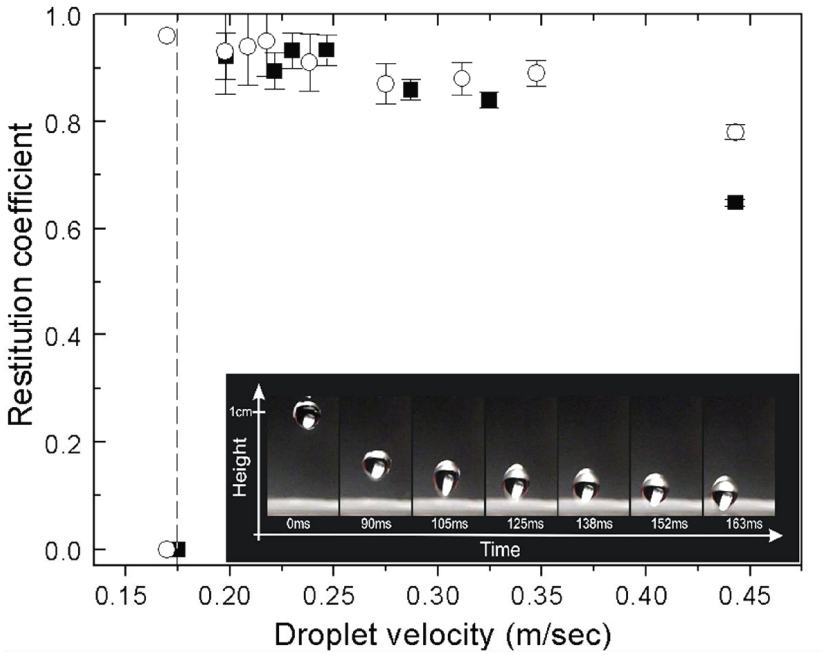

Figure 7. *Restitution coefficient (ε) for the PDPAEMA functionalized hierarchically structured surface after immersion at pH 8.5 (filled squares) and for a natural Lotus leaf surface (open circles), for falling water droplets with radii R of 1.35 mm. The dashed line signifies the threshold velocity of 0.175 m/s for the functionalized artificial surface. Inset: Selected snapshots of a water drop (radius 1.35 mm) hitting the surface. The maxima of the drop trajectory are shown here as a function of time.*

It is considered that the bouncing to non-bouncing transition arises from the presence of surface defects; the contact line pins on such defects resulting in a difference between the advancing and receding contact angles, θ_a and θ_r. The pinning force per unit length is given by Equation 4. 3: [31, 32]

$$F = \gamma_{LV}(\cos\theta_r - \cos\theta_a) \qquad 4.\ 3$$

And the energy dissipated will scale according to Equation 4. 4:

$$E = \gamma_{LV}R^2(\cos\theta_r - \cos\theta_a) \qquad 4.\ 4$$

The drop will bounce provided that its kinetic energy, which scales as ρR^3V^2, can overcome this dissipation. An estimate of the threshold velocity for water repellency can be obtained by equating the two energies (Equation 4. 5):

$$V = \sqrt{\frac{\gamma_{LV}\left((\cos\theta_r - \cos\theta_a\right)}{\rho R}} \qquad 4.5$$

The relative contact angles were measured as θ_a = 154º and θ_r = 149º for the PDPAEMA superhydrophobic surface. For a drop with radius R~1.35mm, the estimated threshold velocity was calculated from Equation 4.5 to be ~0.07 m/sec, a value close to the one observed experimentally.

Tethering stimuli-responsive polymer brushes onto special topographic structured surfaces results in a remarkably amplified wettability responsive and gives an opportunity to realize responsive switching between superhydrophilicity and superhydrophobicity. Such surfaces with tunable ionization and wetting properties in response to certain chemical stimuli are very important and may find applications in different area of science including microfluidic devices, chemical and biochemical gates, programmed adsorption of proteins or controlled cell adhesion.

4. 4. References

1. X. Feng; L. Jiang, *Adv. Mater.* **2006,** *18*, 3063-3078.
2. T. Sun; L. Feng; X. Gao; L. Jiang, *Acc. Chem. Res.* **2005,** *38*, 644-652.
3. M. Callies; D. Quéré, *Soft Matter* **2005,** *1*, 55-61.
4. W. Barthlott; C. Neinhuis, *Planta* **1997,** *202*, 1-8.
5. P. Wagner; R. FuÌˆrstner; W. Barthlott; C. Neinhuis, *J. Exp. Bot.* **2003,** *54*, 1295-1303.
6. R. Fürstner; W. Barthlott; C. Neinhuis; P. Walzel, *Langmuir* **2005,** *21*, 956-961.
7. M. Miwa; A. Nakajima; A. Fujishima; K. Hashimoto; T. Watanabe, *Langmuir* **2000,** *16*, 5754-5760.
8. N. J. Shirtcliffe; G. McHale; M. I. Newton; G. Chabrol; C. C. Perry, *Adv. Mater.* **2004,** *16*, 1929-1932.
9. V. Zorba; E. Stratakis; M. Barberoglou; E. Spanakis; P. Tzanetakis; S. H. Anastasiadis; C. Fotakis, *Adv. Mater.* **2008,** *20*, 4049-4054.
10. Y. Zhu; L. Feng; F. Xia; J. Zhai; M. Wan; L.Jiang, *Macromol. Rapid Commun.* **2007,** *28*, 1135–1141.

11. F. Xia; H. Ge; Y. Hou; T. Sun; L. Chen; G. Zhang; L. Jiang, *Adv. Mater.* **2007,** *19*, 2520–2524.
12. F. Xia; L. Feng; S. Wang; T. Sun; W. Song; W. Jiang; L. Jiang, *Adv. Matter.* **2006,** *18*, 432-436.
13. T. Sun; G. Wang; L. Feng; B. Liu; Y. Ma; L. Jiang; D. Zhu, *Angew. Chem. Int. Ed.* **2004,** *43*, 357-360.
14. P. Uhlmann; L. Ionov; N. Houbenov; M. Nitschke; K. Grundke; M. Motornov; S. Minko; M. Stamm, *Prog. Org. Coat.* **2006,** *55*, 168-174.
15. S. Minko; M. Müller; M. Motornov; M. Nitschke; K. Grundke; M. Stamm, *J. Am. Chem. Soc.* **2003,** *125*, 3896-3900.
16. Y. Qiu; K. Park, *Adv. Drug Delivery Rev.* **2001,** *53*, 321-339.
17. K. Christian; H. Andreas; S. Wolfgang, *Anal. Chem.* **2002,** *74*, 355–361.
18. E. Vasheghani-Farahani; D. G. Cooper; J. H. Vera; M. E. Weber, *Chem. Eng. Sci.* **1992,** *47*, 31-40.
19. L. Ionov; N. Houbenov; A. Sidorenko; M. Stamm; S. Minko, *Adv. Funct. Mater.* **2006,** *16*, 1153-1160.
20. J. Genzer; K. Efimenko, *Biofouling* **2006,** *22*, 339-360.
21. R. Blossey, *Nat. Mater.* **2003,** *2*, 301-306.
22. V. Zorba; L. Persano; D. Pisignano; A. Athanassiou; E. Stratakis; R. Cingolani; P. Tzanetakis; C. Fotakis, *Nanotechnology* **2006,** *17*, 3234-3238.
23. V. Zorba; P. Tzanetakis; C. Fotakis; E. Spanakis; E. Stratakis; D. G. Papazoglou; I. Zergioti, *Appl. Phys. Lett.* **2006,** *88*.
24. F. Xia; L. Feng; S. Wang; T. Sun; W. Song; W. Jiang; L. Jiang, *Adv. Mater.* **2006,** *18*, 432-436.
25. X. Bories-Azeau; S. P. Armes; H. J. W. Van Den Haak, *Macromolecules* **2004,** *37*, 2348-2352.
26. S. Edmondson; C. D. Vo; S. P. Armes; G. F. Unali, *Macromolecules* **2007,** *40*, 5271-5278.
27. W. Chen; A. Y. Fadeev; M. C. Hsieh; D. Öner; J. Youngblood; T. J. McCarthy, *Langmuir* **1999,** *15*, 3395-3399.
28. R. E. Johnson Jr; R. H. Dettre, *J. Phys. Chem.* **1964,** *68*, 1744-1750.

29. D. Richard; D. Quéré, *Europhys. Lett.* **2000,** *50*, 769-775.
30. A. L. Biance; F. Chevy; C. Clanet; G. Lagubeau; D. Quéré, *J. Fluid Mech.* **2006,** *554*, 47-66.
31. R. Blossey, *Nat. Mater.* **2003,** *2*, 301-306.
32. C. G. L. Furmidge, *J. Colloid Sci.* **1962,** *17*, 309-324.

CHAPTER 5

Synthesis and Characterization of Novel Glycopolymer Brushes

Chapter 5 reports the direct synthesis of well defined glycopolymer brushes of high grafting densities from gold, glass and silicon substrates by surface-initated ATRP. Two sugar-based monomers D-gluconamidoethyl methacrylate (GAMA) carrying a glucose functionality and 2-lactobionamidoethyl methacrylate (LAMA) possessing a lactose moiety were used for the synthesis of the glycopolymer brushes. The prepared films were characterized by attenuated total reflectance (ATR)-FTIR spectroscopy, AFM, ellipsometry and contact angle measurements. Both the molecular structure of the sugar moieties and the glycopolymer film thickness, which are expected to influence the interaction kinetics with biological systems, were varied.

The specific binding interactions of the glycopolymer films with two different lectins were investigated by SPR. Hepatocyte and fibroblast cell lines were cultured on the glycopolymer layers and their adhesion and spreading properties on the glycosurfaces were studied. The influence of the glycopolymer molecular structure and film thickness on the cell deposition was examined.

5. 1. Introduction

Natural saccharides or carbohydrates have been recognized to play a key role in many important biological processes. Inflammation, fertilization, immune defense, cell growth and cellular recognition are some of the biological functions in which carbohydrates participate through the interaction of their corresponding saccharide protein recognition receptors.[1] Synthetic polymers containing sugar moieties, also known as glycopolymers, have attracted great attention lately as they exhibit similar functionalities with the natural occurring polysaccharides and are expected to mimic their biorecognition capabilities. Such carbohydrate based polymers have been increasingly proposed for use in many promising applications. The participation of saccharides in biological recognition phenomena has led to the development of glycosylated based drug and gene delivery systems, in which the carbohydrate receptors are used to direct drugs to

organs or cell targets.[2-5] Based on such phenomena are also the developed glucose-sensitive biosensors to monitor saccharide molecular recognition processes.[6,7] The highly hydrophilic nature of glycopolymers makes them also suitable for use in surfactants. Their combination with various hydrophobic monomers results in amphiphilic copolymers possessing a hydrophilic block with a stable chemical C-C backbone and hydrophilic sacharide side chains.[8,9] Recently, cell-recognizable glycopolymers have been extensively studied for use in biomedical applications.[10-13] Due to their excellent biocompatibility and hydrophilicity, glycopolymers have been proposed for use as scaffold materials in tissue engineering to enhance the selective interactions between the scaffold and the cells.[14,15] Moreover, sugar based hydrogels have been prepared by the copolymerization of a glyco – monomer with a cross-linking reagent, and were proposed for use as water absorbent and biocompatible materials.[16-18]

Synthetic glycopolymers are also employed to help elucidate the molecular recognition functions of saccharides.[19-23] The mechanism of carbohydrate-protein interactions is still not well understood due to the weak attractive forces which are involved in the binding events. In the past decade it has been acknowledged that the strength of binding in biological systems is enhanced by multivalent interactions which occur between clustered carbohydrates and the protein receptors which contain multiple saccharide recognition sites.[24] These multivalent interactions lead to a stronger affinity and a greater specificity than the sum of successive monovalent interactions. The ability and ease in controlling the molecular structure of synthetic glycopolymers have made them emerge as important tools for investigating the multivalent interaction mechanism in biosystems. However, the entanglement of the glycopolymeric chains in solution lower their protein recognition properties.[25] Attaching the glycopolymer chains on a surface, in close proximity to one another forces the polymers to adopt a stretched conformation and to avoid overlapping (Figure 1). Therefore, surface-anchored glycopolymers are interesting model systems to study and understand the carbohydrate – protein interactions. It has been suggested that the polymer chain length and the molecular structure of the glycopolymer saccharide residues as well as the distribution of the sugar recognition groups can greatly influence the binding events in solution. On the other hand, the surface coverage of active carbohydrates attached onto a surface has been also

shown to play an important role in protein binding.[26-31] As a consequence, in order to understand the multivalent interaction mechanism, the synthesis of glycopolymer chains with well – defined macromolecular architectures and high surface grafting densities is required.

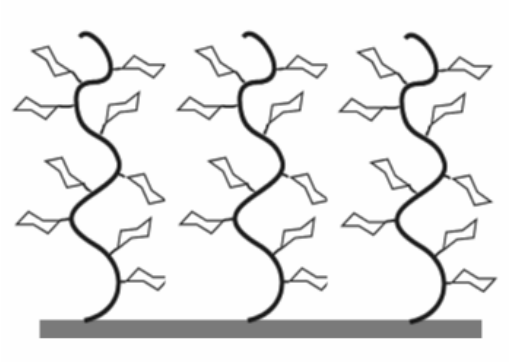

Figure 1. *Glycopolymer brushes thread on a flat substrate.*

The non-specific adsorption of biological cells and bacteria onto various surfaces is driven by interactions between cell proteins and the surface, lacking specific receptor-recognition binding events. This results in biological contamination, which reduces the sensitivity of biosensors and chip-based diagnostic assays and also limits the use of certain materials in implants, food processing equipments and industrial cooling water devices. To overcome these problems efforts have been made to identify materials that resist non-specific adsorption of biological molecules. Functional self assembled monolayers (SAMs),[32] polymers based on poly(ethylene glycol) (PEG) and its derivatives[33,34] and zwitterionic materials[35,36] have been investigated as potential candidates for the minimization of non-specific protein adsorption.

On the other hand, specific cellular adhesion to artificial matrices has lately attracted great interest in biomaterial research. The adhesion of cells to extracellular surfaces is an important phenomenon required for cell growth and proliferation and depends on the surface energy, hydrophilicity and the presence of cell recognition groups on the surface. These characteristics are of utmost importance for the design of biomaterials to be used in sensors, chips and implants. Several studies have been attempted to identify suitable materials for cell adhesion and proliferation. Biocompatible SAMs and polymeric surfaces were shown to enable the integration of living cells.[37,38]

Recently, polymer brushes have received great attention as versatile platforms for the immobilization of cells. Different methods have been used to control protein adsorption and cell adhesion on polymer brushes. One approach employs an inert polymer layer as a platform, which is further functionalized with specific peptides or proteins to induce cell adhesion.[39,40] Another strategy involves the use of stimuli responsive polymer brushes. The control of cell adhesion is accomplished by the reversible hydration/dehydration of the polymer layer induced by the external stimulus.[41]

The interactions of glycopolymers with different cell lines have been reported in the literature.[42] Hepatocyte cells adhere strongly to surfaces coated with galactose-based polymers, due to the specific recognition between the ASGPR receptors on the surface of the cells and the terminal galactose moieties of the polymer.[43] They were also shown to interact specifically with glycopolymers bearing terminal glucose moieties modified at the C-6 position.[43] In a recent study, the adhesion of hepatocytes to a poly(2-lactobionamidoethyl methacrylate)-based tri-block copolymer film spin-coated on ethylene terephthalate plates was investigated and was found to increase with the 2-lactobionamidoethyl methacrylate (LAMA) content of the copolymer.[44] Heparin based glycopolymers were also shown to selectively bind fibroblast cells through the recognition of the heparin bound basic fibroblast growth factor, bFGF, by the growth factor receptors of the fibroblasts.[45] Mono and disaccharide glycopolymers containing heparin and heparan sulfate glycomimetics were found to activate the fibroblast growth factor.[46] However, although the synthesis of well-defined glycopolymer brushes covalently tethered to a substrate has been reported in the literature,[47-50] their interactions with cell lines were only recently investigated.[51] Surface-anchored polymer chains prepared by a controlled/"living" polymerization technique have the advantage of possessing well-defined macromolecular architectures and high grafting densities. Moreover, their flexible nature allows the reorganization of the chains upon adhesion of cells and makes them an interesting model for studying the adhesion, spreading and differentiation behavior of specific cells.

In most cases, the synthesis of glycopolymers by ATRP involved the use of a protected monomer and was followed by deprotection to obtain the sugar moieties.[52-57] However, recently the direct synthesis of glycopolymers without the requirement of using

the protection/deprotection strategy has been also reported. Narain et al. was the first to successfully synthesize sugar methacrylate – based homopolymers and block copolymers by ATRP without the requirement of protecting group chemistry.[58-60] In a latter study Vázquez–Dorbatt and Maynard prepared glycopolymers from biotinylated initiators by direct polymerization of the unprotected monosaccharide[61], while recently, Dai and Dong synthesized star-shaped block copolymers by direct ATRP of an unprotected methacrylate - glycomonomer using a star-shaped macroinitiator.[62]

So far there are very few reports in the literature on the synthesis of glycopolymer chains from surface-bound initiators by ATRP. Fukada and co-workers prepared glycopolymer brushes on silicon substrates, modified with a silane attached-initiator, using a protected methacrylate monomer, followed by a second deprotection step to obtain the sugar functionalities.[47] In a latter work, Müller and coworkers reported the synthesis and characterization of glycocylindrical polymer brushes from a polymeric polyinitiator using the same protected sugar-carrying methacrylate monomer followed by deprotection.[48] Recently Xu and co-workers synthesized glycopolymer chains on polypropylene microporous membranes by a combination of UV-induced graft polymerization and ATRP without the use of deprotection chemistry.[49]

5. 2. Synthesis and Characterization of Glycopolymer Brushes on Gold Substrates

5. 2. 1. Self-Assembly of the Initiator

First the ATRP initiator ω-mercaptoundecyl bromoisobutyrate was immobilized onto a gold-coated silicon substrate. The successful immobilization of the initiator was verified by ATR-FTIR spectroscopy (Figure 2a). The appearance of a characteristic peak at 1739 cm^{-1} corresponding to the C=O stretching vibration of the ester carbonyl group, the peaks at 2967 and 2930 cm^{-1} assigned to the C-H symmetric and asymmetric vibration modes of the $-CH_2-$ and $-CH_3$ groups and the peaks at 1266 and 1167 cm^{-1} due to the C-O stretching in the ATR-FTIR spectrum were attributed to the grafted initiator.

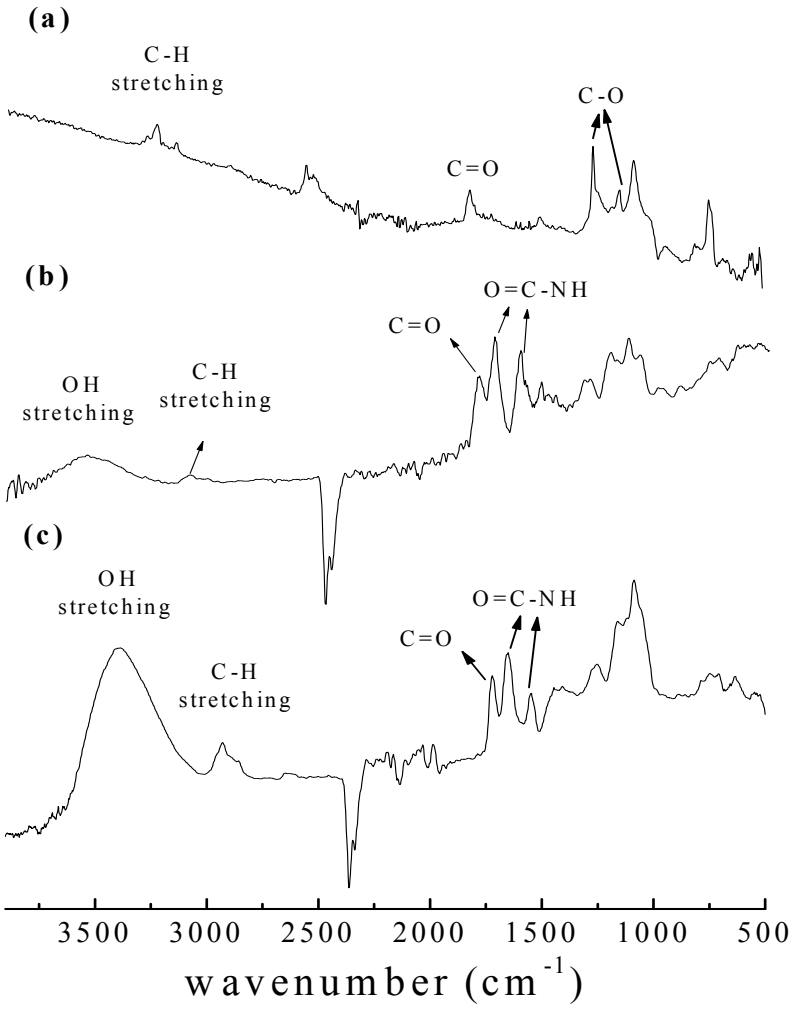

Figure 2. *ATR-FTIR spectra of the immobilized ω-mercaptoundecyl bromoisobutyrate ATRP initiator (a), the grafted PGAMA film (b) and the grafted PLAMA layer (c) on a gold substrate.*

5. 2. 2. Preparation of Glycopolymer Brushes

The ATRP of GAMA and LAMA was carried out from the initiator modified gold substrates at 20 °C. The polymerizations were performed using CuBr/2,2′-bipyridyl as the catalyst system in either water or a methanol/water mixture (Scheme 1).

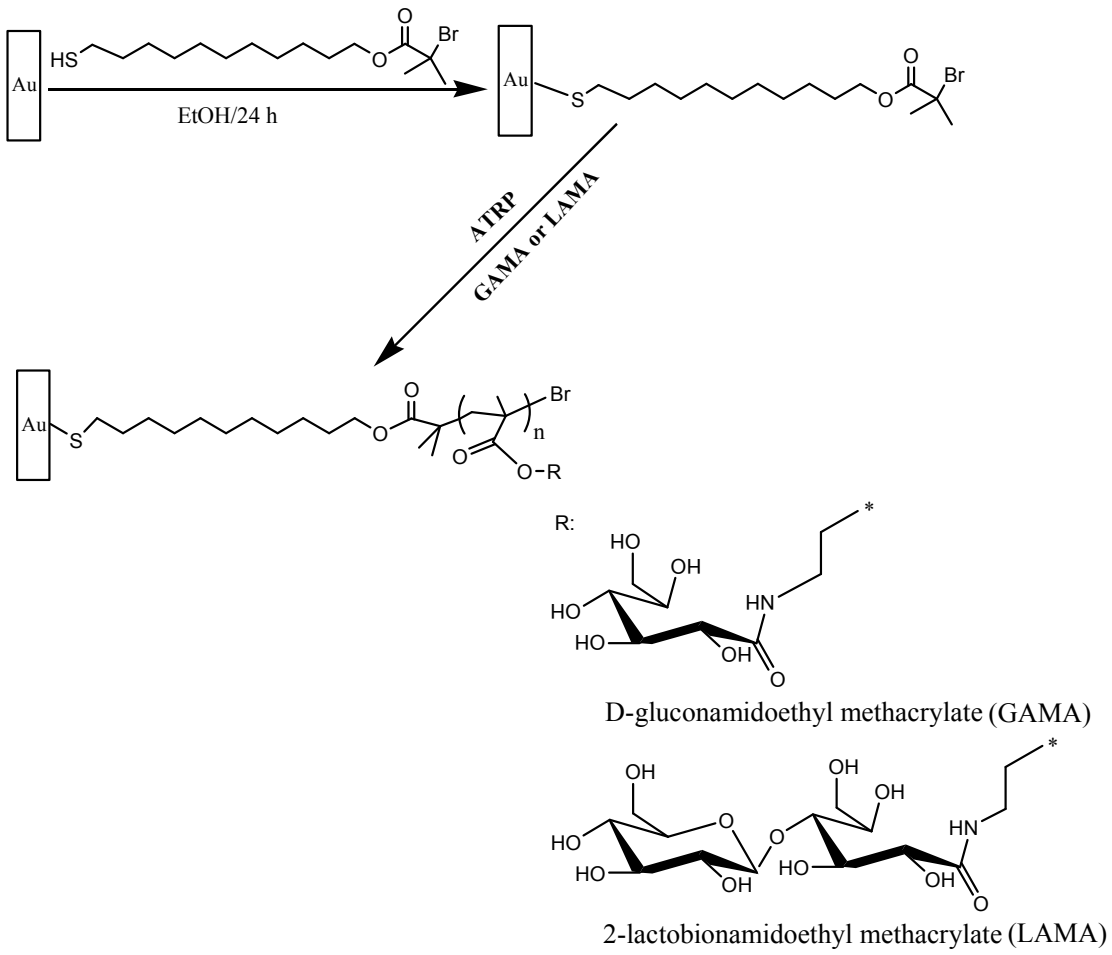

Scheme 1. *Schematic representation of the immobilization process of the ω-mercaptoundecyl bromoisobutyrate initiator onto the gold substrate and of the surface-initiated ATRP of the GAMA and LAMA monomers.*

As mentioned earlier, a sufficient amount of deactivator (Cu (II)) must be present in the ATRP process to provide a good control of the polymerization. For the controlled synthesis of the glycopolymer chains prepared in this work, the required copper (II) species were provided by the termination of a few percent of the polymer chains formed in solution by the free initiator. When the polymerization was carried out in the absence of free initiator the required amount of Cu(II) deactivator, 0.1 wt% relative to Cu(I), was added at the beginning of the reaction.

Table 1 summarizes the ATRP reaction conditions used for the synthesis of the glycopolymer brushes and the polymer film characteristics. GAMA was polymerized in

1-methyl-2-pyrolidinone, water and in a 3/2 and 4/1 methanol/water mixture. In the 4/1 methanol/water mixture the monomer was dissolved by heating the solution at 70 ^{o} C before the addition of the catalyst system, while no heating was required in the 3/2 methanol/water mixture, in pure water and in 1-methyl-2-pyrolidinone. The reactions were allowed to proceed for the desired period of time after which the substrates were removed from the reaction flask, washed with water and ethanol and the dry film thicknesses were determined by ellipsometry. 1-methyl-2-pyrolidinone is an aprotic solvent and was preferred for the polymerizations conducted in the absence of water. A PGAMA film with a thickness of 3 nm was obtained after 2 h of polymerization in 1-methyl-2-pyrolidinone, while an increase of only 1 nm was observed after 24 h of reaction, suggesting a slow rate of polymerization in this media. In order to obtain glycopolymer brushes of higher thickness, the polymerization of GAMA was carried out in aqueous media. For the aqueous ATRP of GAMA, a dry film thickness of 8 nm was found after 5 h of polymerization, whereas no further increase in the film thickness was observed after 24 h reaction time (Table 1), suggesting that the polymerization was terminated within 5 h and the polymer chains did not grow further. This is in agreement with the literature where a non-living polymerization and a loss of the reaction control was reported for the aqueous ATRP of poly(ethylene glycol) methyl ether methacrylate using Cu(I)Br/*N*-(*n*-alkyl)-2-pyridylmethanimine as the catalyst system.[63]

In order to retain control of the polymerization and to diminish the secondary reactions which take place in aqueous ATRP, methanol, a protic solvent was used as a cosolvent. The ATRP of GAMA in a 3/2 methanol/water mixture resulted in a dry film thickness of 37 nm after 24 h of reaction time, indicating that the presence of methanol in the solvent system prolonged the reaction time and minimized the termination processes. For the polymerization of GAMA in a 4/1 methanol/water mixture a 22 nm dry film thickness was obtained after 5 h of reaction which increased further to 63 nm for 24 h of polymerization. The above results suggest that the dry film thickness of the grafted films increases as the water content of the reaction mixture decreases verifying the suppression of the termination reactions in less polar solvent media.

LAMA is a more hydrophilic monomer and thus was insoluble in the 4/1 methanol/water mixture. The polymerization of LAMA was carried out in 1-methyl-2-

pyrolidinone, pure water and a 3/2 methanol/water mixture. The monomer was dissolved by heating at 80 °C in the 3/2 methanol/water mixture before the addition of the catalyst system. Similarly to PGAMA, PLAMA films of 2 nm and 3 nm were obtained when the polymerization was carried out in 1-methyl-2-pyrolidinone for 2 h and 24 h of polymerization time, respectively. As a consequence, the polymerization of LAMA was carried out in water and a 3/2 methanol/water mixture. For the aqueous ATRP of LAMA, a dry film thickness of 7 nm was measured by ellipsometry after 5 h of polymerization which did not increase further for longer polymerization times. This in agreement with the results discussed above for GAMA and verifies the premature termination of the polymerization in the aqueous medium. For the reaction in the 3/2 methanol/water mixture a dry film thickness of 31 nm was found after 5 h of polymerization, which increased further to 40 nm for 24 h of reaction time and suggests the reduction of the termination processes and the prolonged chain growth in the less polar reaction media.

Table 1. Synthesis parameters and characteristics of the glycopolymer layers

Monomer	**Solvent**	**Reaction time (h)**	**Thickness by Ellipsometry (nm)**	**Roughness by AFM (nm)**	**Static contact angle (^{o})**
GAMA	1-methyl-2-pyrolidinone	2	3	-	-
		24	4		
	H_2O	5	8	0.7	53
		24	8	0.9	53
	MeOH/H_2O = 3/2	24	37	0.5	44
	MeOH/H_2O = 4/1	5	22	0.5	33
		24	63	0.6	37
	MeOH/H_2O = 4/1	24	23	0.7	-
LAMA	1-methyl-2-pyrolidinone	2	2	-	-
		24	3		
	H_2O	5	7	1.0	35
		24	7	1.2	33
	MeOH/H_2O = 3/2	5	31	0.8	25
		24	40	1.2	29
	MeOH/H_2O = 3/2	24	31	0.5	-

The premature termination of the polymerization in water which resulted in glycopolymer films of low ellipsometric thicknesses has been reported in the literature. Yang et. al. observed a short propagation time and a plateau in the degree of polymerization after only 1 h reaction time for the aqueous ATRP of GAMA from UV - modified polypropylene microporous membranes.[49] The most reasonable explanation for this premature termination of the polymerization in copper mediated aqueous ATRP, are the side reactions that can take place, of which the hydrolysis of the deactivator species is the most significant. Water can coordinate to the metal centre of the copper (II) complex, resulting in an irreversible dissociation of the halide ligand, thus lowering the deactivator concentration and rendering the efficiency of the deactivation process very low.[64,65] This leads to an increase in the radical concentration, which promotes radical coupling or disproportionation and hence premature chain termination. It has been shown by Tsarevsky et. al. that the stability of the higher oxidation state complex depends on the solvent composition.[64] As the amount of water in the solvent system decreases the stability of the copper (II)-halide complex increases. As a consequence, polymerizations performed in less polar media exhibited slower kinetics and longer propagation times due the presence of a larger quantity of deactivator in the reaction. In our case, an increase in the film thickness and prolonged polymerization times were found for both monomers when methanol was used as a cosolvent which reduced the secondary reactions that take place in the high water content solvent media. Therefore, a good control of the polymerization of GAMA was achieved in a 4/1 methanol/water mixture, whereas the highly hydrophilic nature of LAMA rendered the monomer insoluble in this medium, and a 3/2 methanol/water mixture was used for the controlled growth of the glycopolymer chains.

After synthesis, the dry glycopolymer films were characterized by FTIR-ATR spectroscopy. Figures 2b and 2c show the ATR spectra of the GAMA and LAMA homopolymer films on the gold substrates. The ATR-FTIR spectrum of the 22 nm thick polyGAMA film prepared in a 4/1 methanol/water mixture is presented in Figure 1b. The presence of the carbonyl group at 1731 cm^{-1}, the C-H asymmetric vibration mode of the -CH_2- groups at 2930 cm^{-1} and the O=C-NH vibration modes at 1655 and 1543 cm^{-1} are characteristic of the sugar moieties suggesting the successful grafting of the GAMA

chains on the gold surface. The broad absorption band at 3300 cm^{-1} is assigned to the OH stretching vibration of PGAMA. Figure 1c shows the ATR-FTIR spectrum of the 31 nm PLAMA film prepared in a 3/2 methanol/water mixture. The peak at 1731 cm^{-1} assigned to the C=O stretching vibration, the peak at 2930 cm^{-1} due the C-H asymmetric vibration mode of the $-CH_2-$ groups and the peaks at 1655 and 1543 cm^{-1} assigned to the O=C-NH amide vibration modes are attributed to the grafted polymer. The characteristic broad absorption band at 3300 cm^{-1} assigned to the OH stretching vibration of PLAMA is also observed and is significantly more pronounced, than that observed in the spectrum of PGAMA. This is expected and is attributed to the presence of a larger number of hydroxyl groups on the PLAMA monomer repeat units.

The surface morphology of the homopolymer brushes in the dry state was imaged by tapping mode AFM. Typical AFM images of the PGAMA and PLAMA films are presented in Figures 3 and 4, respectively. For all the samples the surface-anchored film covered the substrate surface completely and homogeneously, suggesting that the ATRP polymerization proceeded uniformly on the substrates. This was also verified by the AFM phase mode images of the samples. Figure 3e shows a typical phase mode image for a PGAMA film prepared in a methanol/water mixture illustrating that the surface of the substrate is completely and uniformly covered by the polymer phase. A low surface roughness (0.5 - 0.6 nm) was found for the PGAMA films synthesized in a methanol/water mixture (Table 1). A small increase in the film roughness to 0.7 - 0.9 nm was observed for the PGAMA films prepared by aqueous ATRP possibly due to the lower control of the polymerization reaction as discussed above. The PLAMA films prepared in water and a 3/2 methanol/water mixture exhibited similar surface roughness, which are in general slightly higher than those of the PGAMA films (Table 1). Overall, the surface roughness of the polymeric films was below 1 nm, verifying that the prepared polymer surfaces are very smooth.

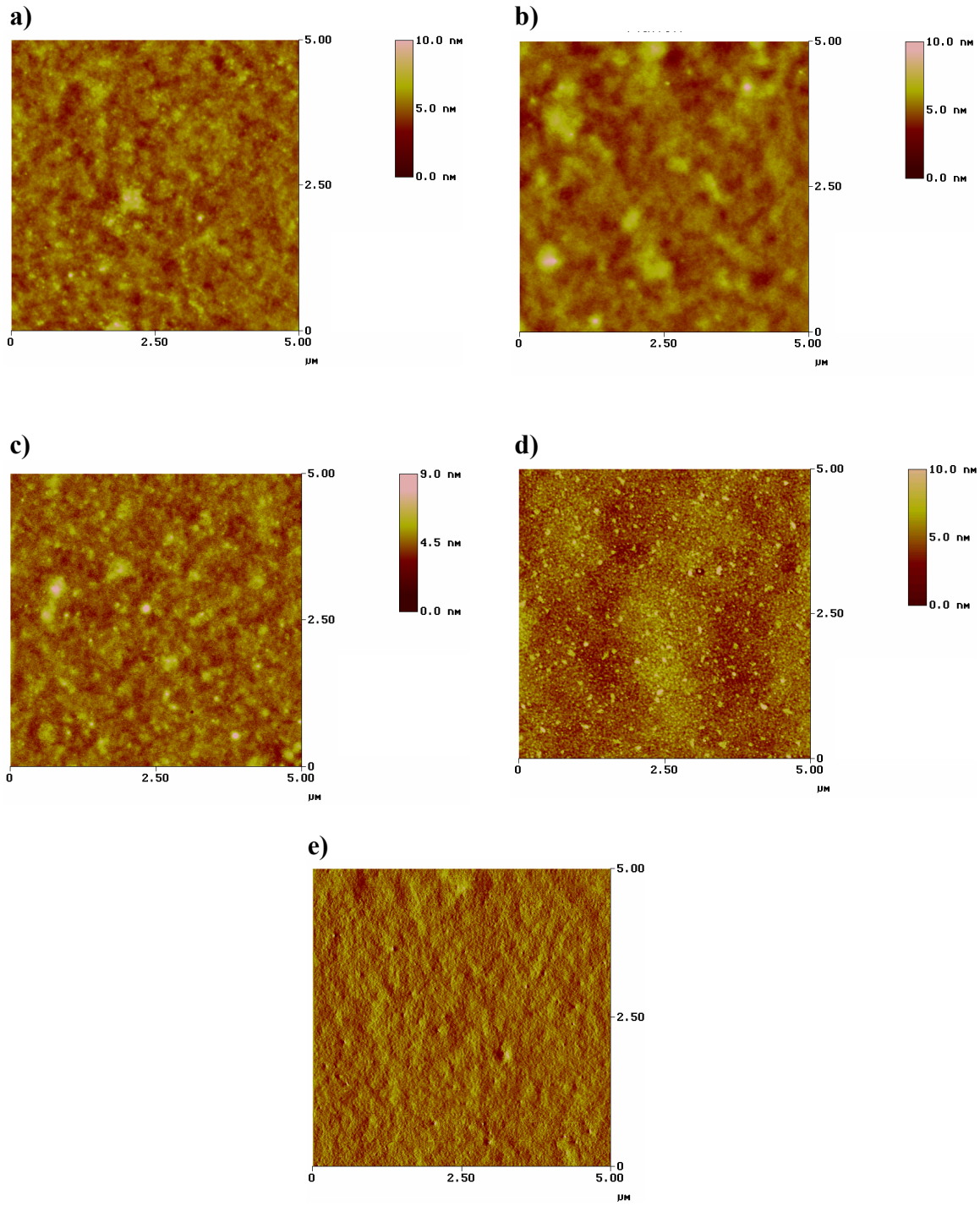

Figure 3. *AFM tapping mode images of PGAMA films prepared in methanol/water = 4/1, 5 h polymerization time (a), methanol/water = 4/1, 24 h polymerization time (b), methanol/water = 3/2, 24 h polymerization time (c), water, 5 h polymerization time (d) and the phase mode image of a PGAMA film prepared in methanol/water = 4/1, 24 h polymerization time (e) (5 × 5 µm).*

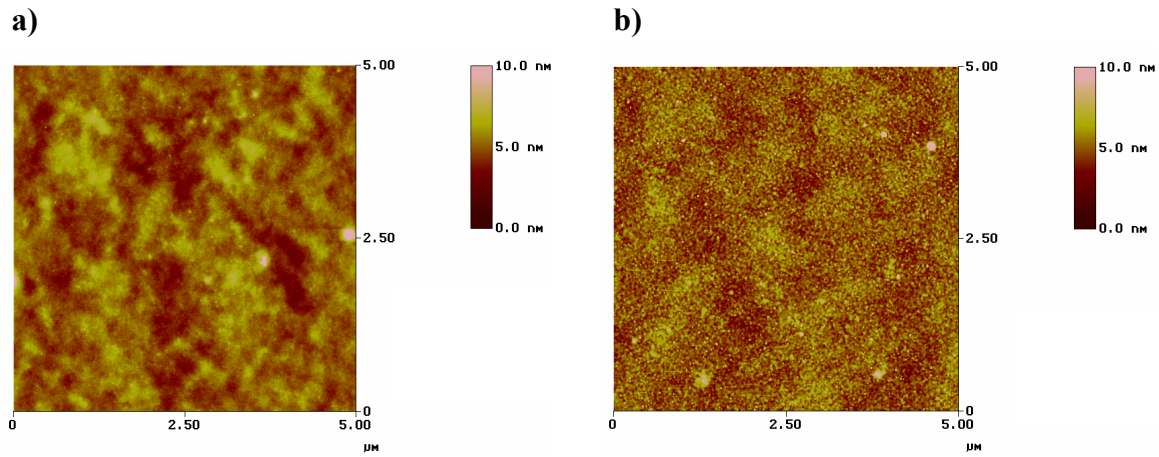

Figure 4. *AFM tapping mode images of PLAMA films prepared in methanol/water = 3/2, 5 h polymerization time (a) and water, 5 h polymerization time (b) (5 × 5 µm).*

The polymeric surfaces were further characterized by contact angle measurements (Table 1). A contact angle of 65 ^{o} was found for an initiator modified gold substrate. For the PGAMA films the contact angle decreased to values between 33^{o} and 53^{o}, while even lower contact angles between 25^{o} and 33^{o} were obtained for the PLAMA surfaces. The hydrophilic character of the prepared films is attributed to the hydroxyl groups present on the monomer moieties. The more hydrophilic nature of the LAMA monomer resulted in the lower contact angles measured for the PLAMA films. In general the contact angle decreases for the films prepared in a methanol/water mixture possibly due to the controlled growth of the grafted polymer chains which also resulted in a lower surface roughness as discussed above.

The grafting density σ (macromolecule/nm^2) of the glycopolymer chains on the gold substrate was calculated from the according to Equation 3. 1. The number average molecular weights of the synthesized glycopolymers in solution by the free initiator were determined by aqueous GPC. The number average molecular weight of PGAMA synthesized in a 4/1 methanol/water mixture was M_n = 19,680 g mol^{-1} and the molecular weight distribution M_w/M_n = 1.6. A value of M_n = 68,000 g mol^{-1} and M_w/M_n = 1.8 was found for PLAMA prepared in the 3/2 methanol/water mixture. A grafting density of 0.70 chains/nm^2 was calculated for the 23 nm PGAMA brush synthesized in a 4/1 methanol/water mixture. The grafting density for the 31 nm PLAMA brush prepared in a 3/2 methanol/water mixture was calculated as 0.27 chains/nm^2. These values are

comparable to those reported in the literature and verify the successful synthesis of glycopolymer brushes of high grafting density on the gold substrates.[66, 67]

5. 3. Synthesis and Characterization of Glycopolymer Brushes on Glass and Silicon Substrates

5. 3. 1. Self-Assembly of the Initiator

Prior to the immobilization of the ATRP initiator, the silicon substrates were treated with Piranha solution in order to remove the organic matter and to hydroxylate the silicon surface. A contact angle close to 0° was measured on the silicon surface after the Piranha treatment. Glass and silicon substrates were functionalized with the ATRP initiator 3-(2-bromoisobutyryl)propyl)triethoxysilane in dry THF. The substrates were left in the initiator solution overnight and were next extensively rinsed with solvent and dried in stream of nitrogen. A contact angle of 74 ° was measured on the initiator modified surface, indicating the successful immobilization of the initiator.

5. 3. 2. Preparation of Glycopolymer Brushes on Modified Glass and Silicon Substrates

The ATRP of GAMA and LAMA monomers was carried out next from the initiator modified silicon and glass substrates at room temperature. The polymerizations were performed using CuBr/2,2'-bipyridyl as the catalyst system in methanol/water mixtures. To control the synthesis of the glycopolymer chains, EBIB free initiator was added in the polymerization solution. Hence, the required amount of the copper (II) deactivator was afforded by the termination in the beginning of the polymerization of a few percent of the polymer chains formed in solution by the free initiator.

Table 2 summarizes the ATRP reaction conditions used for the synthesis of the glycopolymer brushes and the glycopolymer film characteristics. GAMA was polymerized in a 4/1 methanol/water mixture, while LAMA which is more hydrophilic was thus insoluble in the 4/1 methanol/water mixture and was polymerized in a 3/2 methanol/water mixture. Initiator modified glass and silicon substrates were placed in the same reaction flask and therefore the polymer brush growth is expected to proceed under identical conditions on both substrates. The reactions were allowed to proceed for 24 h after which the substrates were removed from the reaction flask and were washed

extensively with water and ethanol. The polymer dry film thickness was determined by ellipsometry on the silicon modified substrates.

Glycopolymer brushes of different thickness were obtained by varying the Cu(I)/EBIB molar ratio while keeping the polymerization time constant. A PGAMA film thickness of 3 nm was obtained when a mole ratio of Cu(I)/EBIB = 2 was employed for the polymerization. The low polymer film thickness obtained under these conditions suggests that the concentration of the copper(II) deactivator in the reaction mixture was relatively high. Therefore, in order to prepare thicker polymer films the amount of free initiator in the reaction mixture was reduced. Using a mole ratio of Cu(I)/EBIB = 9, the PGAMA film thickness increased to 7 nm, while only a small increase in the glycopolymer film thickness of ~1.5 nm was found when a mole ratio of Cu(I)/EBIB = 16 was used. Further experiments showed that we could not grow a PGAMA brush with a thickness higher then 10 nm in the presence of free initiator. Consequently, we polymerized GAMA in the absence of free initiator using copper(II) deactivator in the reaction mixture to control the polymerization and a 13 nm PGAMA brush was obtained. Similar to the GAMA surface-imitated polymerization, a PLAMA film with a thickness of 3 nm was obtained when a large amount of free initiator was used in the polymerization mixture (Cu(I)/EBIB = 2). For a mole ratio of Cu(I)/EBIB = 9 a PLAMA film with a thickness of 8 nm was obtained, whereas the film thickness increased to 15 nm when a mole ratio of Cu(I)/EBIB = 16 was employed in the polymerization.

Table 2. Synthesis parameters and characteristics of glycopolymer brushes

Polymer	Cu(I)/ EBIB	Thickness by ellipsometry (nm)	Roughness by AFM (nm)		Contact angle (°)
			glass	silicon	glass
PGAMA	2	3	0.5	0.8	70
	9	7	0.6	1.2	35
	-	13	1.2	1.4	37
PLAMA	2	3	0.6	0.5	68
	9	8	0.8	1.0	32
	16	15	0.6	1.0	26

The surface morphology of the glycopolymer brushes in the dry state was imaged by tapping mode AFM. Typical AFM images of the PGAMA and PLAMA films grafted on glass substrates are presented in Figure 5. The prepared films were uniform and smooth with a low roughness. Overall, the surface roughness of the glycopolymer films grafted on glass and silicon substrates was ~1 nm (Table 2).

The prepared glycopolymer films were further characterized by contact angle measurements (Table 2). Contact angles of 70 ° and 68 ° were found for the 3 nm thick PGAMA and PLAMA films, whereas the contact angles decreased to 35 ^{o} and 37 ^{o} for the 7 nm and 13 nm PGAMA films, respectively. Lower values of 32 ^{o} and 26 ^{o} were measured for the 8 nm and 15 nm PLAMA films. The hydrophilic character of the thick glycopolymer films was attributed to the hydroxyl groups present on the PGAMA and PLAMA moieties, while the high contact angles found for the thin glycopolymer layers perhaps suggest insufficient surface coverage by the glycopolymer chains.

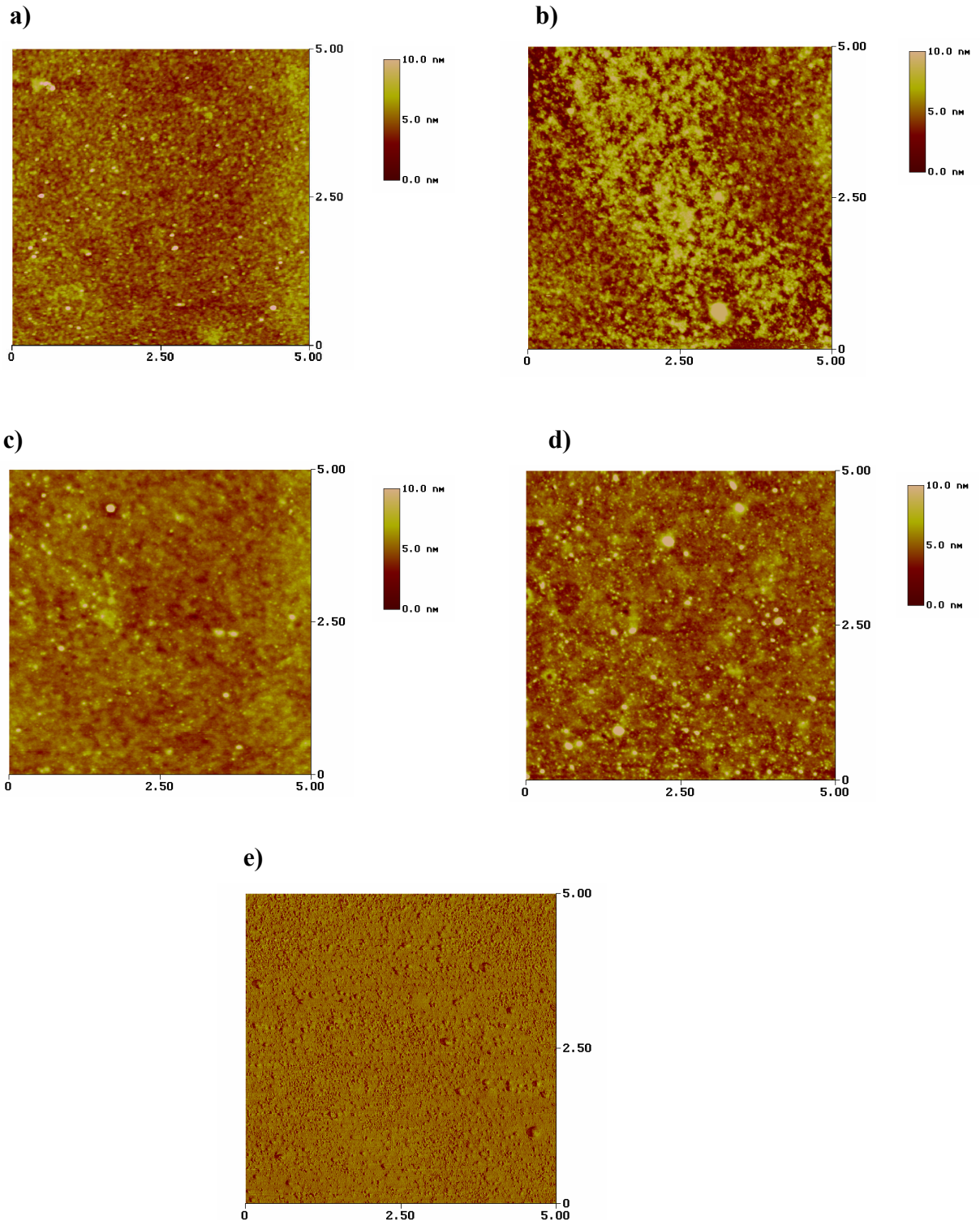

Figure 5. *AFM tapping mode images of PGAMA grafted films of 7 nm (a) and 13 nm (b) thickness, PLAMA grafted films of 8 nm (c) and 15 nm thickness (d) and the phase mode image of the 13 nm PGAMA brush on a glass substrate (5 × 5 μm).*

The number average molecular weights of the glycopolymers synthesized in solution by the free initiator were used as an approximation of the length of the grafted polymer chains. Table 3 lists the M_n and M_w/M_n values of the free glycopolymers simultaneously prepared from the free initiator in solution. A molecular weight of 18,000 g/mol and a polydispersity of 1.5 was obtained for PGAMA for a mole ratio of Cu(I)/EBIB = 2. Reducing the amount of free initiator in the polymerization mixture to Cu(I)/EBIB = 9, gave a polymer with an increased molecular weight of 24,300 g/mol and a polydispersity of 1.73. Similarly, for PLAMA the obtained molecular weights increased with the decrease of the free initiator in the reaction mixture. More specifically, a molecular weight of 6,300 g/mol and a polydispersity of 1.10 was obtained for a Cu(I)/EBIB mole ratio of 2, while increasing the mole ratio of Cu(I)/EBIB to 9,lead to a glycopolymer with a molecular weight of 17,100 g/mol and a polydispersity of 1.10. A further increase of the Cu(I)/EBIB mole ratio to 16 produced a glycopolymer with molecular weight of 19,100 g/mol and a polydispersity of 1.33. The above results suggest that the synthesis of PGAMA in the 4/1 methanol/water mixture is less controlled than the polymerization of PLAMA in the 3/2 methanol/water mixture. This is probably due to the lower solubility of the hydrophilic monomers in the alcoholic media and suggests that the solvent selection is an interplay between the monomer solubility and the activity of the reaction center.

Table 3. Molecular characteristics of the prepared glycopolymers in solution and thickness and grafting density of the prepared glycopolymer films

Polymer	**M_n (g/mol)**	**M_w/M_n**	**h (nm)**	**σ (chains/nm^2)**
PGAMA	18,000	1.5	3	0.1
	24,300	1.73	7	0.17
PLAMA	6360	1.10	3	0.28
	17,100	1,10	8	0.28
	29,100	1,33	15	0.31

Finally, the grafting density of the glycopolymer brushes was calculated according to Equation 3.1. A grafting density of 0.1 chains/nm^2 was determined for the 3 nm PGAMA brush, while a value of 0.17 chains/nm^2 was obtained for the 7 nm PGAMA brush. On the other hand, for the 3 nm and 8 nm PLAMA brushes a constant grafting density of 0.28 cahins/nm^2 was calculated, which increased to 0.31 cahins/nm^2 for the 15 nm PLAMA brush (Table 3). These values suggest the synthesis of glycopolymer brushes of high grafting density on the glass and silicon substrates.

5. 4. Recognition Properties of the PGAMA and PLAMA Films

The interaction of the synthesized glycopolymer brushes with lectins was investigated by surface plasmon resonance (SPR) spectroscopy. SPR occurs when a light beam impinges at the interface between a thin metal layer and a dielectric media at a specific angle of the incident light. At that angle, a sharp minimum in the intensity of the reflected light is observed and is detected as a "dip" in the reflectivity. The SPR detection principle relies on the changes in the refractive index upon binding of analyte molecules to the sensor surface which results in changes in the incident angle at which SPR occurs. Plots of the reflectivity versus angle of incident light show the changes in the resonance angle upon binding of the analyte and can be converted into adsorbed amount of analyte.

The change in the resonance angle due to the binding of the lectin on the grafted glycopolymer brushes was monitored. The lectins used in this study were Con A, a tetrameric lectin at neutral and alkaline pH which specifically recognizes mannose and glucose residues[68,69] and RCA_{120} shown to have a binding affinity for galactose/lactose moieties.[70]A non-regenerative protocol was chosen for the SPR experiments, which did not require regeneration of the polymer-modified substrate between successive lectin injections.[71]

The SPR response at equilibrium is related to the lectin concentration, by the following Equation 5. 1:

$$\frac{1}{R_{eq}} = \frac{1}{R_{\max} K_A} \cdot \frac{1}{C} + \frac{1}{R_{\max}} \qquad 5.1$$

where R_{eq} is the SPR response to the injection of the lectin with concentration C at equilibrium, R_{max} is the equilibrium response when C is infinity and K_A is the apparent

binding affinity. The plot of $1/R_{eq}$ *vs*. $1/C$ is a straight line and the value of K_A can be calculated from the slope of the linear fit to the data.

A typical example of SPR curves for different RCA_{120} concentrations binding on a grafted PLAMA film is shown in Figure 6. After each lectin addition a change in the resonance angle to a higher value was observed and was attributed to the binding of the protein onto the glycopolymeric film.

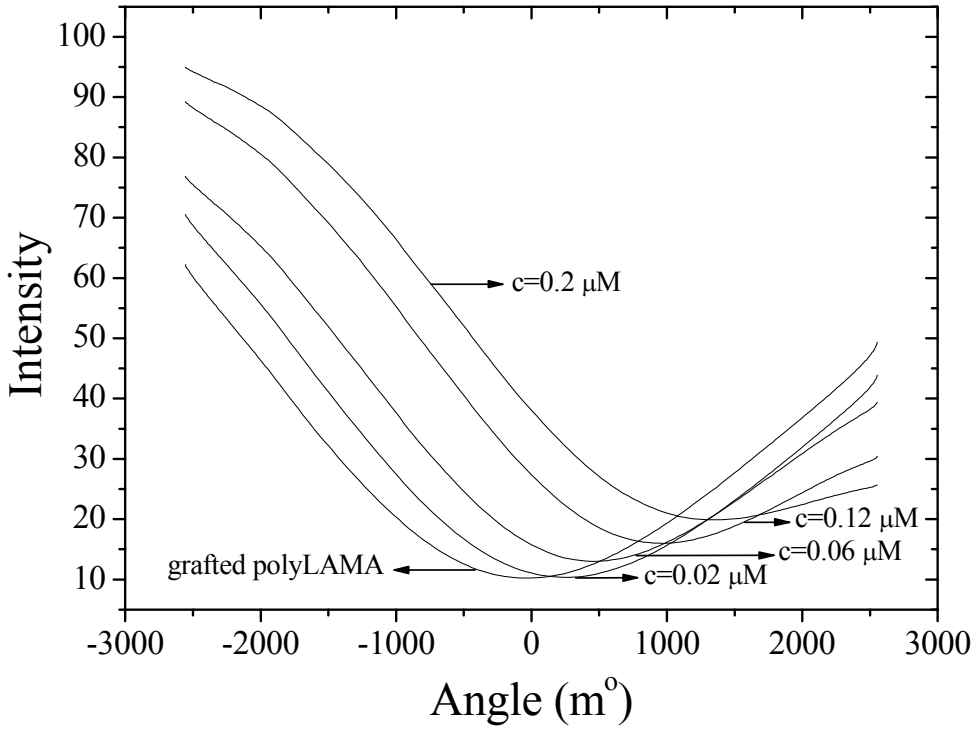

Figure 6. *SPR curves of a grafted PLAMA film on a gold sensor chip and of the RCA_{120} adsorption on the grafted PLAMA layer at different concentrations.*

By using a non-regenerative protocol, R_{eq} was calculated after each injection from the SPR sensograms and the obtained values were plotted against the lectin concentration. The linear relationship between $1/R_{eq}$ and $1/C$ obtained for Con A binding on the PGAMA layer and RCA_{120} binding on the PLAMA film is shown in Figures 7a and 7b. R_{max} and the affinity constant K_A were calculated from the intercept and the slop of the linear fits, respectively. For the Con A binding to the glucose-based film a K_A value of 8.54×10^4 M^{-1} was calculated, while a K_A of 1.86×10^5 M^{-1} was found for RCA_{120} binding to the lactose-based layer. The higher affinity of the RCA_{120} lectin for the

PLAMA film in comparison to that of Con A for the PGAMA layer is due to the specific binding of RCA_{120} to lactose-based sugars, whereas Con A has a higher affinity for mannose rather than the glucose moieties found in PGAMA.[72] When Con A was brought in contact with the grafted PLAMA a negligible increase in the resonance angle was observed, indicating the absence of nonspecific adsorption of the lectin (Figure 8). A similar binding constant for RCA_{120} has been reported in the literature for a PLAMA containing triblock copolymer spin-coated on a gold substrate ($K_A = 2.77 \times 10^5$ M^{-1}).[44] This suggests a high accessibility of the LAMA moieties by the lectin molecules in the grafted glycopolymer film. The high binding affinity values obtained for the glycopolymer surfaces prepared in this work indicate that the lectins bind strongly onto the glycopolymer films by the saccharide "cluster" effect.[73]

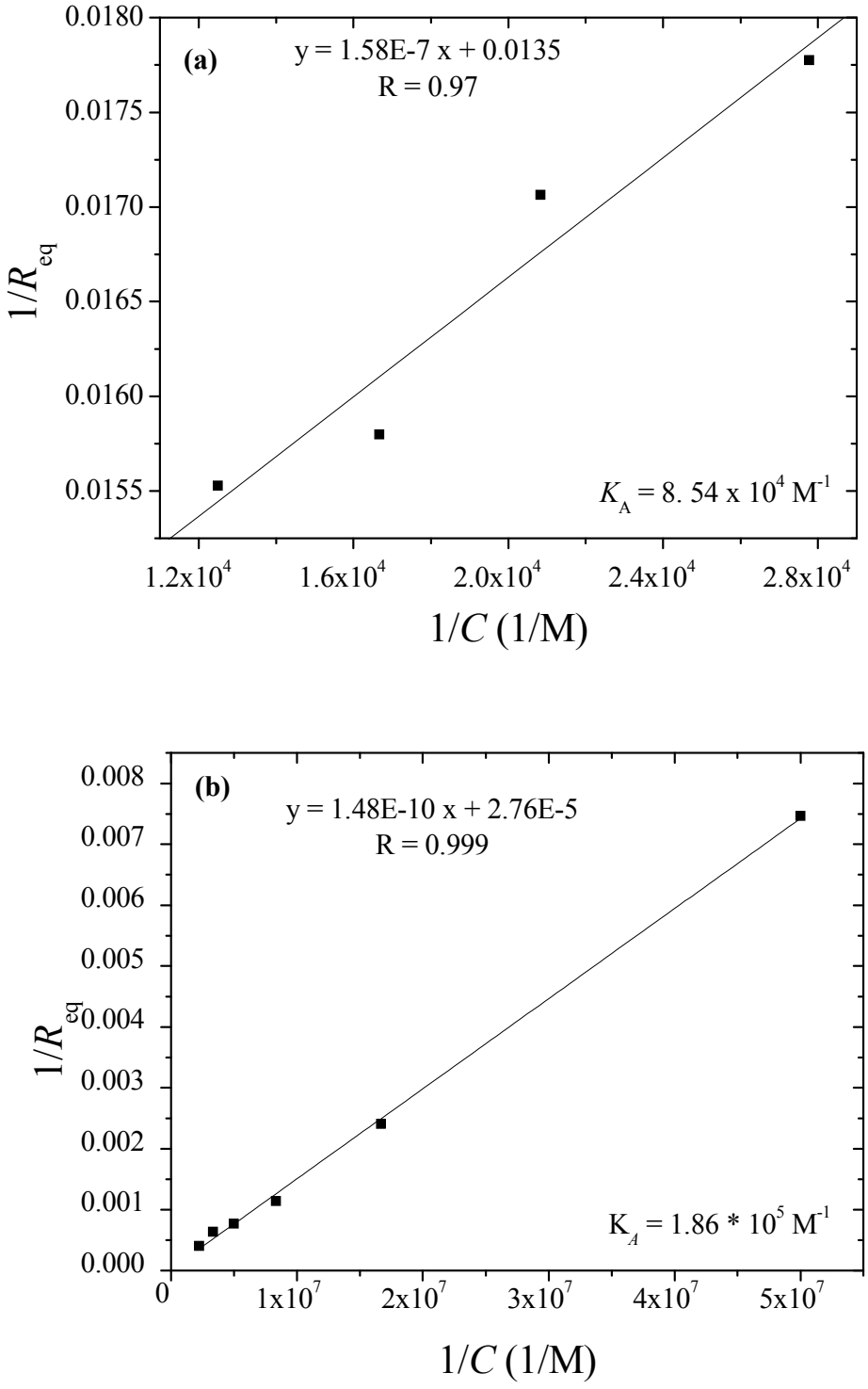

Figure 7.. *Plots of $1/R_{eq}$ vs. 1/C obtained from the SPR data for Con A binding on a grafted PGAMA layer (a) and RCA_{120} binding on a grafted PLAMA film (b).*

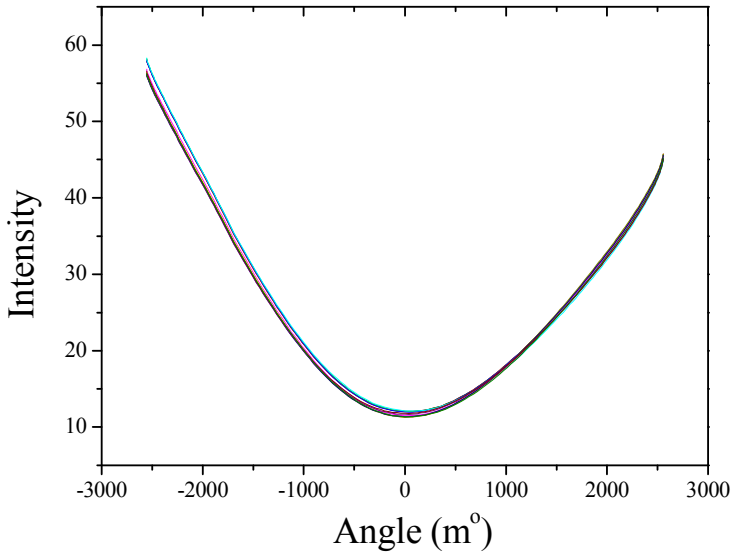

Figure 8. *SPR curves of a grafted PLAMA film on a gold sensor chip and of the ConA adsorption on the grafted PLAMA film at different concentrations.*

5. 5. Cell Adhesion and Spreading Behavior on Glycopolymer Brushes

Hepatocyte and fibroblast cells were incubated onto the prepared glycopolymer brushes (Scheme 2) and their adhesion and spreading behaviour was studied.

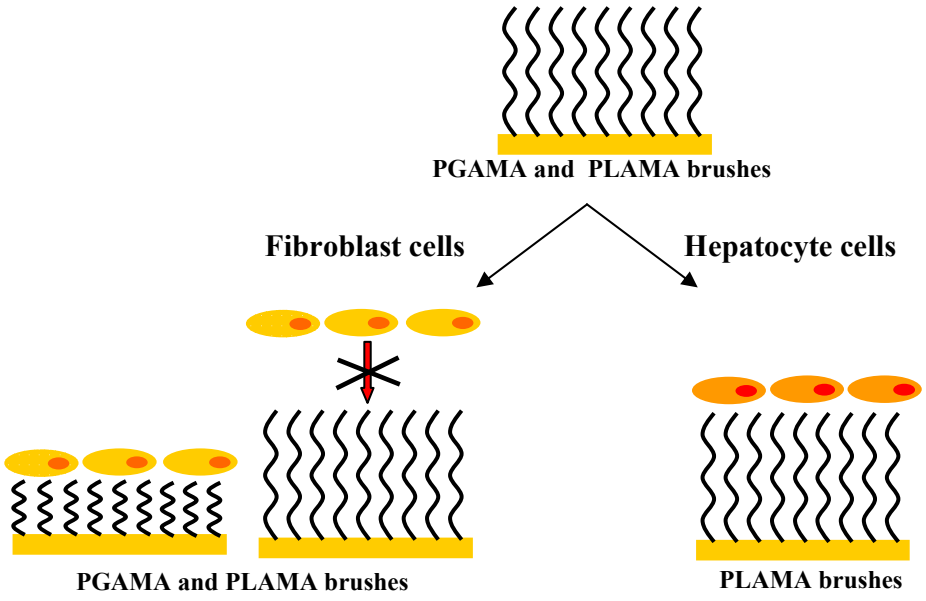

Scheme 2. *Schematic representation of the interactions of glycopolymer brushes with the hepatocyte and fibroblast cell lines.*

Table 4 summarizes the characteristics of the glycopolymer layers used for the cell adhesion and spreading studies.

Table 4. Characteristics of the glycopolymer films

Polymer	Thickness by ellipsometry (nm)	Roughness by AFM (nm)	Static contact angle (^{o})
PGAMA[a]	8	2.3	-
	37	0.5	44
PGAMA[b]	8	0.9	53
	22	0.5	33
	57	0.6	37
PLAMA[a]	4	1.7	39
	31	0.5	-
PLAMA[b]	7	1.0	35
	31	0.8	25

[a] Glycosurfaces used in the hepatocyte cells experiments
[b] Glycosurfaces used in the fibroblast cells experiments

First, human liver cells were incubated on the PLAMA and PGAMA surfaces for 20 hrs in a humidified atmosphere. Eukaryotic cell binding requires the secretion of extracellular matrix that adsorbs onto a surface and facilitates firm cell adhesion and spreading. Different areas of the glycopolymer functionalized gold substrates were examined and the average adherent cell densities are reported in Figure 9. As seen in the figure enhanced human hepatocyte cell adhesion was found to the PLAMA grafted surface compared to the PGAMA functionalized substrates. This is attributed to the specific interactions between the ASGPR receptors which are present on the hepatocyte cell membrane and the galactose moieties of PLAMA, which promote cell adhesion. Moreover, the cell density is higher on the PLAMA surfaces and it remains constant regardless of the film thickness suggesting the tight adhesion of the cells. On the other hand, the thickness of the grafted PGAMA layer had a pronounced influence on cell adhesion. Only a small number of cells adhered on the thick PGAMA film indicating weak cell interactions with the polymer layer. However, when the film thickness of PGAMA decreased to 8 nm a remarkable increase in cell adhesion was observed. Although, some round cells were observed most of the adhered cells were well spread providing evidence that the cells adhere more tightly on the thinner glycopolymer films.[74]

This is consistent with a previous study, in which polymer concentration dependent cell spreading studies showed that cell spreading is enhanced on glycopolymer surfaces of lower coating density.[75] The morphology of the cultured cells is often dependent upon the forces the cells exert on the extracellular surfaces and the elasticity of the substrate.[76,77] The increase in the film thickness is expected to increase the hydration of the polymer brushes and the elasticity of the substrate and hence to decrease the cell adhesion and spreading. Similar resistance to cell adhesion has been reported for thick saccharide polymer brushes grafted on a titanium substrate.[51] In that work control over MC3T3-E1 osteoblast-like cell adhesion was shown by the appropriate functionalization of the surface. Thick unmodified glycopolymer surfaces resisted cell adhesion, whereas brushes with a covalently tethered adhesion peptide sequence promoted the deposition of well-spread cells.

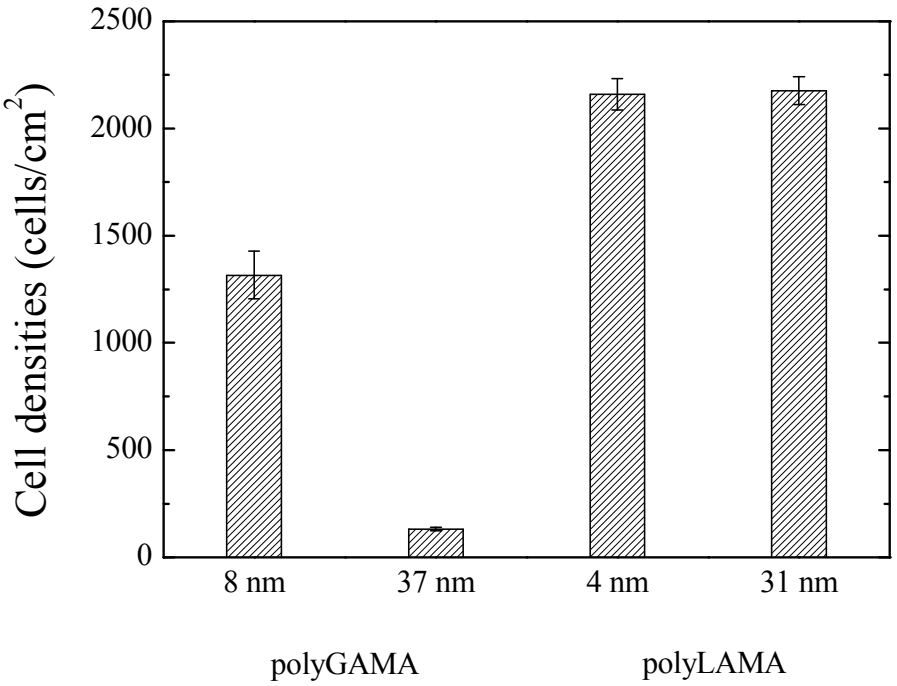

Figure 9. *Cell densities of hepatocyte cells adhered on PGAMA and PLAMA functionalized substrates of different film thicknesses. The Hep G2 cells were incubated at a concentration of 3.0 × 10^5 cell/mL on the glycopolymer substrates for 20 hrs at 37^o C.*

The PGAMA and PLAMA glycopolymer films were investigated as potential coatings for the minimization of non-specific cell adsorption. Fibroblast cells, which do not bind specifically to the glucose and the galactose moieties of the synthesised glycopolymers, were utilized. The cells were incubated on the polysaccharide films at 37 °C in 5% CO_2 for 24 hrs. TCPS and glass surfaces were used in control experiments. Before the morphology observation by SEM adherent cells were fixed with paraformaldehyde solution. The cell morphologies on the PGAMA and PLAMA films are shown in Figure 10.

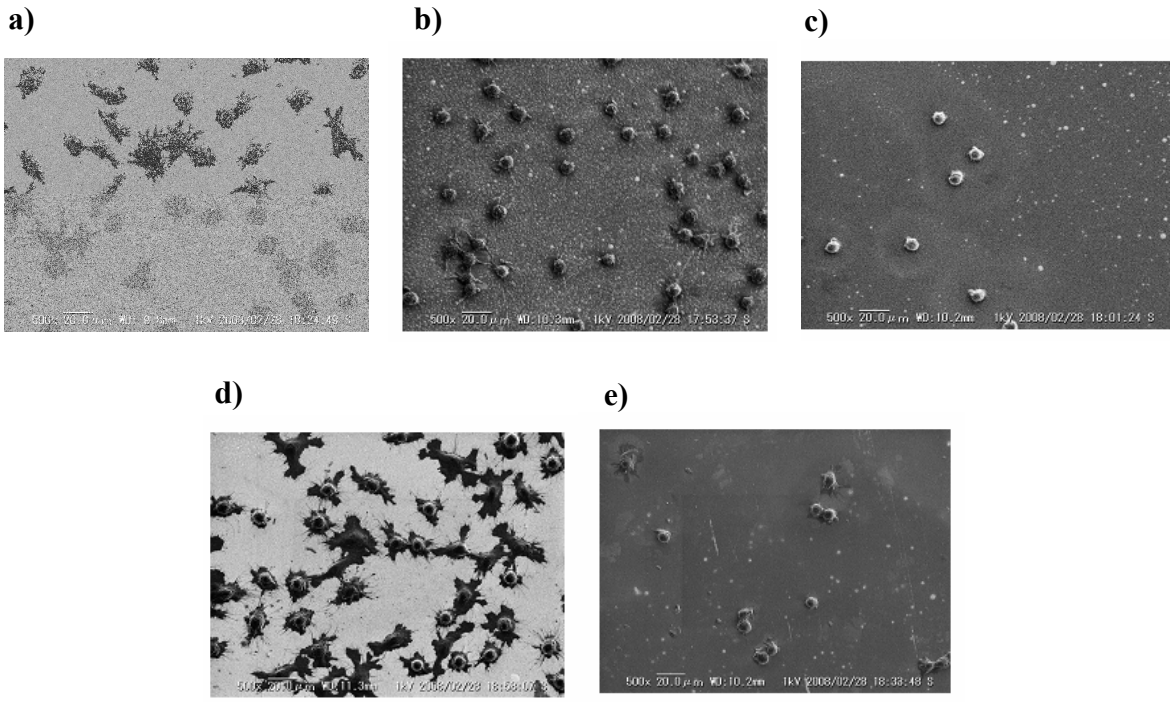

Figure 10. *Fibroblast cell morphologies on the PGAMA films A) 8 nm, B) 22 nm and C) 57 nm and the PLAMA films A) 7 nm and B) 31 nm. The fibroblast cells were incubated on the glycopolymer-functionalized surfaces at a concentration of 2.0 × 10^5 cell/mL for 24 hrs in 10 % FBS DMEM. Adherent cells were fixed with paraformaldehyde solution.*

Both glycopolymer films exhibited similar cell adhesion properties suggesting that the molecular structure of the saccharide did not play a significant role on cell binding. However, cell adhesion and spreading decreased dramatically on the glycopolymer brushes when the polymer film thickness increased and only very few loosely adhered

fibroblast cells were found on the polymer films with thickness higher than 20 nm (Figures 10C and 10E). This finding is quantified in Figure 11, which shows the fibroblast cell densities on the glycopolymer films and the control surfaces. The 31 nm PLAMA and 57 nm PGAMA films exhibited minimum cell adhesion, lower than that found for the control TCPS and glass substrates (Figure 12), while the number of adhered cells increased monotonically as the film thickness increased.

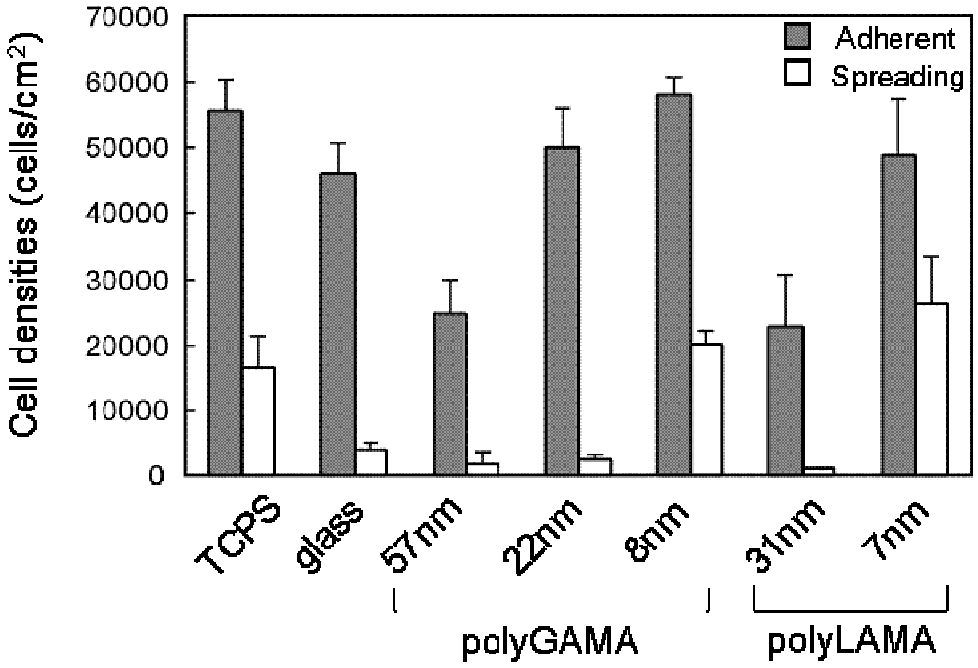

Figure 11. *Adhesion and spreading densities of fibroblast cells on TCPS, glass, PGAMA and PLAMA functionalized substrates.*

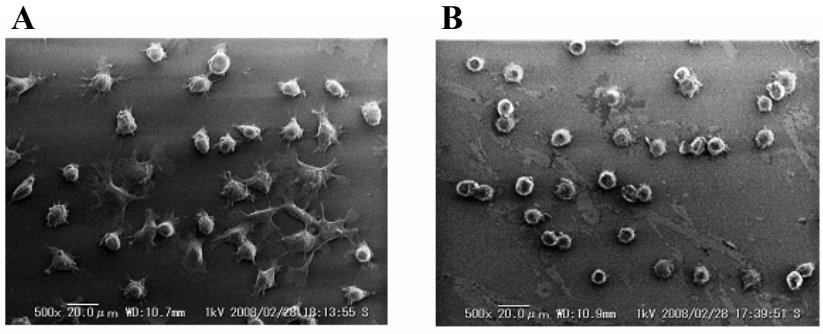

Figure 12. *Fibroblast cell morphologies on TCPS (A) and glass (B) substrates.*

Figure 13 shows the spread cell densities on the PGAMA and PLAMA films as a function of film thickness. Although the PGAMA and PLAMA films exhibited similar cell spreading properties, the spread cells increased with the decrease of the glycopolymer film thickness and only the films with a thickness below 10 nm exhibited well-spread and tightly adhered cells. This is in agreement with previous studies which showed a significant reduction of non-specific adsorption of proteins and cells on polymer brushes of high grafting density and film thickness[51,78] and suggests that the surface carbohydrate groups in the thinner glycopolymer films promoted cell binding. For the polymeric films with a thickness higher than 20 nm cell spreading was minimized indicating that the increase in the film thickness causes a higher hydration and mobility of grafted polymer chains as well as an increase in the elasticity of the substrate, which would likely decrease cell spreading as discussed above for the hepatocyte cells. These results suggest that the variation of the thickness of the glycopolymer brushes can be employed to afford control over cell adhesion and spreading.

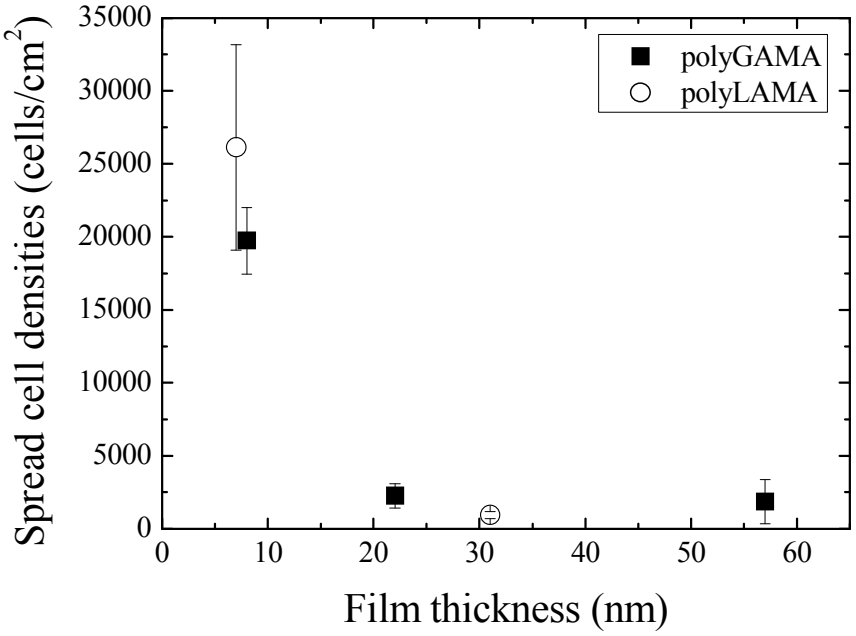

Figure 13. *Ffibroblast spread cell densities as a function of the grafted PGAMA and PLAMA film thickness.*

5. 6. References

1. R. A. Dwek, *Chem. Rev.*, **1996**, *96,* 683-720.
2. R. C. Rathi, P. Kopeckova, B. Rihova, J. Kopecek, *J. Polym. Sci. A: Polym. Chem.* **1991**, *29*, 1895-1902.
3. E. Palomino, *Adv. Drug Delivery Rev.* **1994**, *13,* 311-323.
4. M. G. Garcia-Martin, C. Jimenez-Hidalgo, S. S. J. Al-Kass, I. Caraballo, M. V. de Paz, J. A. Galbis, *Polymer* **2000**, *41*, 821-826.
5. Y. H. Yun, D. J. Goetz, P. Yellen, W. Chen, *Biomaterials* **2004**, *25*, 147-157.
6. H. Uzawa, S. Kamiya, N. Minoura, H. Dohi, Y. Nishida, K. Taguchi, S. Yokoyama, H. Mori, T. Shimizu, K. Kobayashi, *Biomacromolecules* **2002**, *3*, 411-414.
7. T. Hasegawa, T. Yonemura, K. Matsuura, K. Kobayashi, *Bioconj. Chem.* **2003**, *14*, 728-737.
8. V. v. Braunmühl, G. Jonas, R. Stadler, *Macromolecules* **1995**, *28*, 17-24.
9. G. Wulff, L. Zhu, H. Schmidt, *Macromolecules* **1997**, *30*, 4533-4539.
10. G. Maheshwari, G. Brown, D. A. Lauffenburger, A. Wells, L. G. Griffith, *J. Cell Sci.* **2000**, *113*, 1677-1686.
11. S. H. Kim, M. Goto, T. Akaike, *J. Biol. Chem.* **2001**, *276*, 35312-35319.
12. J. S. Lee, S. H. Kim, Y. J. Kim, T. Akaike, S. C. Kim, *Biomacromolecules* **2005**, *6*, 1906-1911.
13. H. Sato, Y. Miura, N. Saito, K. Kobayashi, O. Takai, *Biomacromolecules* **2007**, *8*, 753-756.
14. J. K. F. Suh, H. W. T. Matthew, *Biomaterials* **2000**, *21*, 2589-2598.
15. T. Onodera, K. Niikura, N. Iwasaki, N. Nagahori, H. Shimaoka, R. Kamitani, T. Majima, A. Minami, S. I. Nishimura, *Biomacromolecules* **2006**, *7*, 2949-2955.
16. X. Chen, J. S. Dordick, D. G. Rethwisch, *Macromolecules* **1995,** *28*, 6014-6019.
17. T. Miyata, A. Jikihara, K. Nakamae, *Macromol. Chem. Phys.* **1996**, *197*, 1135-1146.
18. W. J. Zhou, M. E. Wilson, M. J. Kurth, *Macromolecules* **1997**, *30*, 7063-7068.
19. K. Matsuura, H. Kitakouji, N. Sawada, H. Ishida, M. Kiso, K. Kitajima, K. Koboyashi, *J. Am. Chem. Soc.* **2000**, *122,* 7406-7407;

20. M. G. Baek, R. C. Stevens, D. H. Charych, *Bioconj. Chem.* **2000**, *11,* 777-788;
21. Y. Miura, H. Sato, T. Ikeda, H. Sugimura, O. Takai, K. Kobayashi, *Biomacromolecules* **2004**, *5*, 1708-1713;
22. M. Ambrosi, N. R. Cameron, B. G. Davis, S. Stolnik, *Org. Biomol. Chem*. **2005**, *3*, 1476-1480;
23. C. Xue, S. P. Jog, P. Murthy, H. Liu, *Biomacromolecules* **2006**, *7*, 2470-2474.
24. V. Ladmiral, E. Melia, D. M. Haddleton, *Eur. Polym. J.* **2004**, *40*, 431-449.
25. Q. Yang, M. X. Hu, Z. W. Dai, J. Tian, Z. K. Xu, *Langmuir* **2006**, *22*, 9345-9349.
26. L. L. Kiessling, N. L. Pohl, *Chem. Biol.* **1996**, *3*, 71-77;
27. D. A. Mann, M. Kanai, D. J. Maly, L. L. Kiessling, *J. Am. Chem. Soc.* **1998**, *120*, 10575-10582;
28. C. W. Cairo, J. E. Gestwicki, M. Kanai, L. L. Kiessling, *J. Am. Chem. Soc.*, **2002**, *124*, 1615-1619;
29. E. K. Woller, E. D. Walter, J. R. Morgan, D. J. Singel, M. J. Cloninger, *J. Am. Chem. Soc.* **2003**, *125*, 8820-8826;
30. E. A. Smith, W. D. Thomas, L. L. Kiessling, R. M. Corn, *J. Am. Chem. Soc.*, **2003**, *125***,** 6140-6148.
31. S. H. Kim, T. Hoshiba, T. Akaike *Biomaterials*, **2004**, *25,* 1813-1823.
32. K. L. Prime and G. M. Whitesides, *J. Am. Chem. Soc.*, 1993, **115**, 10714-10721.
33. L. Andruzzi, W. Senaratne, A. Hexemer, E. D. Sheets, B. Ilic, E. J. Kramer, B. Baird and C. K. Ober, *Langmuir*, 2005, **21**, 2495-2504.
34. S. Tugulu and H. A. Klok, *Biomacromolecules*, 2008, **9**, 906-912.
35. A. B. Lowe, M. Vamvakaki, M. A. Wassall, L. Wong, N. C. Billingham, S. P. Armes and A. W. Lloyd, *J. Biomed. Mater. Res.*, 2000, **52**, 88-94.
36. R. E. Holmlin, X. Chen, R. G. Chapman, S. Takayama and G. M. Whitesides, *Langmuir*, 2001, **17**, 2841-2850.
37. G. P. López, M. W. Albers, S. L. Schreiber, R. Carroll, E. Peralta, G. M. Whitesides, *J. Am. Chem. Soc.* **1993**, *115*, 5877-5878.
38. B. J. Chang, O. Prucker, E. Groh, A. Wallrath, M. Dahm, J. Rühe, *Colloids Surf., A* **2002**, *198-200*, 519-526.

39. F. J. Xu, S. P. Zhong, L. Y. L. Yung, Y. W. Tong, E. T. Kang, K. G. Neoh, *Tissue Eng.* **2005**, *11*, 1736-1748.
40. S. Tugulu, P. Silacci, N. Stergiopulos, H. A. Klok, *Biomaterials* **2007**, *28*, 2536-2546.
41. A. Mizutani; A. Kikuchi; M. Yamato; H. Kanazawa; T. Okano, *Biomaterials* **2008**, *29*, 2073-2081.
42. A. David, P. Kopečkova, A. Rubinstein, J. Kopeček, *Bioconjugate Chem.* **2001**, *12*, 890-899.
43. S. H. Kim, M. Goto, T. Akaike, *J. Bio. Chem.* **2001**, *276*, 35312-35319.
44. Y. Iwasaki, U. Takami, Y. Shinohara, K. Kurita, K. Akiyoshi, *Biomacromolecules* **2007**, *8*, 2788-2794.
45. H. Sato, Y. Miura, N. Saito, K. Kobayashi, O. Takai, *Biomacromolecules* **2007**, *8*, 753-756.
46. S. Baskaran, D. Grande, X. L. Sun, A. Yayon, E. L. Chaikof, *Bioconjugate Chem.* **2002**, *13*, 1309-1313.
47. M. Ejaz, K. Ohno, Y. Tsujii, T. Fukuda, *Macromolecules* **2000**, *33,* 2870-2874.
48. S. Muthukrishnan, M. Zhang, M. Burkhardt, M. Drechsler, H. Mori, A. H. E. Müller, *Macromolecules* **2005**, *38*, 7926-7934.
49. Q. Yang, J. Tian, M. X. Hu, Z. K. Xu, *Langmuir* **2007**, *23*, 6684-6690.
50. M. H. Stenzel, L. Zhang, W. T. S. Huck, *Macromolecular Rapid Communications* **2006**, *27*, 1121-1126.
51. J. E. Raynor, T. A. Petrie, K. P. Fears, R. A. Latour, A. J. Garcia, D. M. Collard, *Biomacromolecules* **2009**, *10*, 748–755.
52. C. M. Dong, K. M. Faucher, E. L. Chaikof, *J. Polym. Sci. Part A: Polym. Chem.* **2004**, *42*, 5754-5765.
53. S. Muthukrishnan, G. Jutz, X. André, H. Mori, A. H. E. Müller, *Macromolecules* **2005**, *38,* 9-18.
54. S. Muthukrishnan, H. Mori, A. H. E. Müller, *Macromolecules* **2005**, *38*, 3108-3119.
55. Z. C. Li, Y. Z. Liang, G. Q. Chen, F. M. Li, *Macromol. Rapid Commun.* **2000**, *21*, 375-380.

56. K. Ohno, Y. Tsujii, T. Fukuda, *J. Polym. Sci. Part A: Polym. Chem.* **1998**, *36*, 2473-2481.
57. Y. M. Chen, G. Wulff, *Macromol. Rapid Commun.* **2002**, *23*, 59-63.
58. R. Narain, S. P. Armes, *Chem. Commun.* **2002**, 2776-2777.
59. R. Narain, S. P. Armes, *Macromolecules* **2003**, *36*, 4675-4678.
60. R. Narain, S. P. Armes, *Biomacromolecules* **2003**, *4*, 1746-1758.
61. V. Vázquez-Dorbatt, H. D. Maynard, *Biomacromolecules* **2006**, *7*, 2297-2302.
62. X. H. Dai, C. M. Dong, *J. Polym. Sci. Part A: Polym. Chem.*, **2008**, *46*, 817-829.
63. S. Perrier and D. M. Haddleton, *Macromol. Symp.*, **2002**, *182*, 261-272.
64. N. V. Tsarevsky, T. Pintauer and K. Matyjaszewski, *Macromolecules*, **2004**, *37,* 9768-9778.
65. J. K. Oh, K. Min and K. Matyjaszewski, *Macromolecules*, **2006**, *39*, 3161-3167.
66. D. M. Jones, A. A. Brown and W. T. S. Huck, *Langmuir*, **2002**, *18*, 1265-1269.
67. C. Yoshikawa, A. Goto, Y. Tsujii, T. Fukuda, T. Kimura, K. Yamamoto and A. Kishida, *Macromolecules*, **2006**, *39*, 2284-2290.
68. J. Švitel, A. Dzgoev, K. Ramanathan and B. Danielsson, *Biosens. Bioelectron.*, **2000**, *15*, 411-415;
69. S. Morokoshi, K. Ohhori, K. Mizukami and H. Kitano, *Langmuir*, **2004**, *20,* 8897-8902.
70. W. Zhou, X. H. Dai and C. M. Dong, *Macromol. Biosci.*, **2008**, *8*, 268-278.
71. Y. Tang, R. Mernaugh and X. Zeng, *Anal.Chem.*, **2006**, *78*, 1841-1848.
72. R. V. Weatherman, K. H. Mortell, M. Chervenak, L. L. Kiessling and E. J. Toone, *Biochemistry*, **1996**, *35*, 3619-3624.
73. J. J. Lundquist and E. J. Toone, *Chem. Rev.*, **2002**, *102*, 555-578.
74. T. Sordel, F. Kermarec-Marcel, S. Garnier-Raveaud, N. Glade, F. Sauter-Starace, C. Pudda, M. Borella, M. Plissonnier, F. Chatelain, F. Bruckert and N. Picollet-D'hahan, *Biomaterials*, **2007**, *28*, 1572-1584.
75. S. H. Kim, T. Hoshiba and T. Akaike, *Biomaterials*, **2004**, *25*, 1813-1823.
76. N. Q. Balaban, U. S. Schwarz, D. Riveline, P. Goichberg, G. Tzur, I. Sabanay, D. Mahalu, S. Safran, A. Bershadsky, L. Addadi and B. Geiger, *Nature Cell Biology*, **2001**, *3*, 466-472.

77. H. B. Wang, M. Dembo and Y. L. Wang, *Am. J. Physiol. Cell Physiol.*, **2000**, *279*, C1345-C1350.

78. W. Feng, J. L. Brash and S. Zhu, *Biomaterials*, **2006**, *27*, 847-855. N. Singh, X. Cui, T. Boland and S. M. Husson, *Biomaterials*, **2007**, *28*, 763-771.

CHAPTER 6

Conclusions and Outlook

This thesis described the synthesis of polymer brushes on gold, silicon/glass substrates utilizing surface-initiated ATRP. Monomers with different functionalities were used for the development of grafted polymer films with diverse surface properties. The synthesized polymer films were characterized by a variety of experimental techniques such as ellipsometry, AFM, ATR-FTIR spectroscopy and contact angle measurements. The main directions pursued were: (i) the synthesis of responsive surfaces utilizing homopolymer and block copolymer brushes, (ii) the development of artificial surfaces switching form superhydrophobicity to superhydrophilicity and (iii) the preparation of novel glycosurfaces of controllable protein and cell adhesion properties.

6. 1. Synthesis and Characterization of Stimuli Responsive Homopolymer and Block Copolymer Brushes on Gold Substrates

ATRP was employed to prepare a variety of homopolymer and block copolymer brushes from initiator-modified gold substrates. For the synthesis of uniform polymer layers in aqueous media, copper(II) deactivator was added at the beginning of the reaction. The effect of solvent composition on the surface polymerizations was investigated. It was observed that faster kinetics leading to thicker polymer films were obtained as the amount of water in the polymerization medium increased, while the rate of polymerization slowed down significantly in organic solvents. High grafting densities were calculated for the prepared homopolymer layers, indicating that the polymer chains are in the brush regime. ATR-FTIR experiments confirmed the presence of the homopolymer brushes on the gold substrates, while AFM revealed the preparation of very smooth polymer films with a roughness general below 1 nm. The amine-based polymer films (PDMAEMA and PDEAEMA) exhibited a decrease in the contact angle when immersed at low pH compared to that found when immersed at high pH due to the protonation of the amine groups which increased the hydrophilicity of the polymer at low pH, while the acidic PMAA films showed the opposite behaviour. pH dependent swelling studies of the PDMAEMA brushes reveled that the polymer chains are in a stretched

conformation at low pH, due to electrostatic repulsions between the charged amine groups, while they collapse upon deprotonation. The living character of the polymerization was demonstrated by the successful synthesis of block copolymer brushes. After the polymerization of the second monomer an increase in the film thickness was observed by ellipsometry, verifying that the homopolymer chains remained active and capable of reinitiation. The successful synthesis of diblock copolymer brushes was also verified by contact angle measurements. The wetting properties of the surface switched depending on the solvent into which the block copolymer brushes were immersed to expose the solvent soluble block at the air-solid interface. These block copolymer brushes are attractive materials for solvent switchable surfaces. The protein binding studies showed that the PDMAEMA brushes have a high protein binding capacity and can potentially be used as efficient ion exchange media for protein binding. The prepared polymer brushes are attractive due to their ability to tune the surface properties upon application of an external stimulus. In this way surface properties such as adhesion or wetting could be rapidly switch off and on for capillary flow, protein adsorption, cell detachment or drug release.

6. 2. Switching Wettability From Superhydrophobic and Water Repellent Surfaces to Superhydrophilic Surfaces

pH-responsive polymeric surfaces, which can reversibly switch between superhydrophilicity at low pH and superhydrophobicity and water repellent at high pH were developed. The artificial surfaces exhibited controlled hierarchical micro- and nano-structured roughness, which mimics the morphology of natural water repellent surfaces. When the artificial surfaces were functionalized with pH-sensitive polymer brushes, they were able to alter their behavior from superhydrophilic (~0 ^{o}) to hydrophobic (~120 ^{o}) (for PDEAEMA) and from superhydrophilic to superhydrophobic (~150 ^{o}) (for PDPAEMA) upon immersion in a solution of appropriate pH. The superhydrophilic to superhydrophobic transition was due to the combined effect of hierarchical micro- and nano-roughness and the appropriate hydrophobicity of the functionalizing polymer. The water repellency of the prepared surfaces in their superhydrophobic state was quantified by investigating the restitution coefficient of water droplets bouncing off the surface as a

function of their impact velocity. The highest elasticity was observed at intermediate velocities, from ~0.17 m/sec to ~0.30 m/sec, where a value of 0.90 was found for the restitution coefficient, comparable with the Lotus leaf. A value of 5 ^{o} was determined for the contact angle hysteresis, proving that superhydrophobicity and water repellency demand both high values of the static water contact angles and low contact angle hysteresis. Such surfaces with tunable ionization and wetting properties in response to certain chemical stimuli are very important and may find applications in the fields of adaptive microfluidic devices, chemical and biochemical gating, proteins adsorption, controlled cell adhesion.

6. 3. Synthesis and Characterization of Novel Glycosurfaces by ATRP

Surface-initiated ATRP was used to synthesize uniform glycopolymer brushes from a surface-attached initiator on gold and glass substrates. Two different monomers were used for the synthesis of the glycopolymer brushes GAMA carrying a glucose functionality and LAMA possessing a lactose moiety. An early termination of the polymerization was observed in aqueous ATRP due to side reactions which are frequent at high radical concentrations. Longer propagation times and higher film thicknesses were obtained when methanol was used as a cosolvent. The film thickness increased with the methanol content of the solvent mixture and with the decrease of the amount of free initiator in the polymerization mixture. The successful grafting of the glycopolymer brushes on the substrates was confirmed by ATR-FTIR measurements. The surface morphology of the polymer films was imaged by tapping mode AFM. The surface-anchored film covered the substrate surface completely and homogeneously. The roughness of the films was found below 1 nm suggesting the preparation of very smooth glycopolymer surfaces. Contact angle experiments showed that the synthesized glycopolymer brushes increased the hydrophilicity of the surfaces on which they were tethered. The protein recognition properties of the prepared glycopolymer chains were monitored by SPR. The end-grafted glycopolymers exhibited strong interactions with specific lectins by the glycoside “cluster” effect.

Next, the interactions of human hepatocyte and mouse fibroblast cells lines with glycopolymer brushes of various thicknesses were investigated. It was found that

regardless of the film thickness, hepatocyte cells adhered more tightly on the PLAMA grafted films, compared to the PGAMA modified substrates due to the specific interactions between the galactose groups of PLAMA and the ASGPR receptors on the cell membrane. The adhesion of the hepatocyte cells on the PGAMA brushes was dependent on the film thickness and increased for the thinner polymer layers. The latter was attributed to the low hydration of the thin polymer films which resulted in lower polymer chain mobility and film elasticity and exerted stronger forces on the cells causing their tight adhesion. For the fibroblast cells comparable cell adhesion properties were observed for the PGAMA and PLAMA functionalized surfaces, due to the lack of specific carbohydrate-cell interactions. The increased number of adhered cells and the increased number of well-spread cells on the thin glycopolymer films suggested the tight adhesion of the cells. However, fibroblast cell adhesion and spreading exhibited a significant decrease as the polymer film thickness increased rendering these coatings a versatile platform for the development of surfaces with controllable cell adhesion properties.

6. 4. Final Remarks and Outlook

The design and synthesis of functional surfaces has received a lot of attention in modern polymer science. This work hopefully provided a small contribution to a rapidly evolving field that is the study of *polymer brushes*. The use of surface attached polymer chains in commercial applications is still in its early stages, nevertheless the potential of these materials for future applications holds great promise.

A detailed study of the swelling dependency of the prepared polyelectrolyte brushes on the solution pH and ionic strength is worthy of further investigation. However, the swelling abilities of these brushes are relatively limited due to their high grafting density, as found for the PDMAEMA brushes. In a future work, polyelectrolyte brushes of lower grafting densities could also be prepared, as they adopt a less extended conformation prior to exposure to a good solvent which would result in greater swelling/deswelling ratios upon exposure to different stimuli. The response of the prepared polyampholyte, PDMAEMA-*b*-PMAA block copolymer brushes as a function of pH would also be another interesting issue to be addressed. In order to determine the

reversible change of the thickness of the polymer brushes in solution, liquid cell AFM is an appropriate technique, however a nano-patterned surface would be necessary to facilitate the measurements.

The design, synthesis and applications of new structured surfaces functionalized with stimuli responsive materials hold great promise for the near future. The stimuli responsive structured surfaces prepared in this work respond to one kind of external stimuli, namely the pH. However, research in smart materials with a surface wettability that can be tuned by dual or multiple external stimuli such as a combination of pH and temperature, light and temperature, pH and solvent and so on is indispensable. For example considering the complex conditions in human body with variations in temperature, pH, and glucose concentration, multiresponsive surfaces may prove to be suitable candidates as drug carriers.

In order to study the spreading and differentiation of the hepatocyte and fibroblast cell lines to a greater extent the preparation of glycopolymer brushes on transparent substrates is desirable. We have already synthesized PGAMA and PLAMA glycopolymer brushes on glass substrates and future work will involve the study of the interactions of the prepared glycosurfaces with different cell lines. An important issue to be addressed here is the removal of the cultured cells from the glycopolymer functionalized substrates without damaging the cell lines. To this end, mixed homopolymer brushes comprising of PLAMA and a thermo-responsive polymer could be used as tissue culture supports. The most studied thermo-responsive polymer to date is poly(N-isopropylacrylamide) (PNIPAAm) which posses a lower critical temperature (LCST) of 32^{o} C. The hepatocytes cells will adhere and spread above the LCST onto the mixed PLAMA/PNIPAAm homopolymer brush. At this temperature the PNIPAAm chains are collapsed and the cells will interact with the PLAMA chains. By lowering the temperature below the LCST the PNIPAAm chains will become hydrated and swollen resulting in cell desorption (Scheme 1). Such temperature triggered cell detachment will provide a gentler alternative to traditional cell removal methods such as mechanical dissociation and enzymatic digestion.

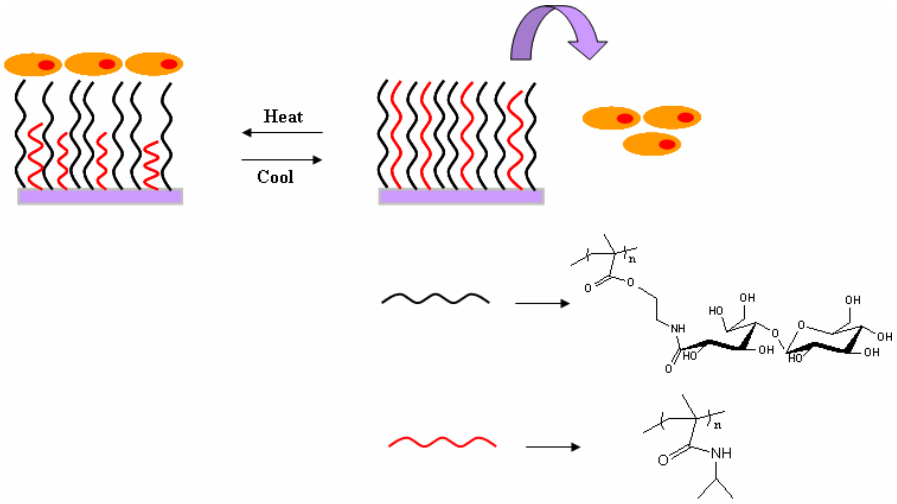

Scheme 1. *Schematic illustration of temperature induced cell detachment from a mixed PLAMA/PNIPAAm homopolymer brush.*

CHAPTER 7

Characterization Techniques

7. 1. Atomic Force Microscopy (AFM)

AFM or scanning force microscope (SFM) is a mechanical imaging instrument that measures the three dimensional topography of a surface. AFM provides a number of advantages over conventional microscopy techniques. It performs measurements in three dimensions, *x, y,* and *z* (normal to the sample surface), thus enabling the presentation of three-dimensional images of the sample. The resolution in the *x*-*y* plane ranges from 0.1 to 1.0 nm and in the *z* direction the resolution is 0.01 nm (atomic resolution). It does not require any special sample preparation and can be used either in ambient or liquid environment. AFM can measure a range of tip-surface interactions, depending on the distance between the tip and the sample. At short distances the tip predominantly experiences interatomic forces: the very short range (~ 0.1 nm) Born repulsive forces and the longer range (up to 10 nm) van der Waals forces. At higher distances from the surface (100-500 nm above the surface) long-range electric, magnetic and capillary forces can be probed.

The AFM consists of a cantilever with a sharp mechanical tip (probe) at its end that is used to scan the surface of a sample. The tips are commonly fabricated from silicon or silicon nitride with a radius of curvature in the order of nanometers. The tip is positioned close enough to the surface such that it can interact with the force fields associated with the surface, which leads to a deflection of the cantilever according to Equation 7. 1:

$$F = -kz \qquad 7.\ 1$$

where, F is the force, k is the stiffness of the lever, and z is the distance the lever is bent. The AFM head comprises an optical detection system in which a diode laser is focused onto the back of the reflective cantilever. As the tip scans the surface of the sample, moving with the contour of the surface, the laser beam is deflected off the cantilever into an array of photodiodes. In most cases a feedback mechanism is employed to adjust the tip-sample distance and to maintain a constant force between the tip and the sample. The

sample is mounted on a piezoelectric scanner, which moves the sample in the *z* direction, therefore maintaining a constant force or a constant height above the sample (Figure 1).

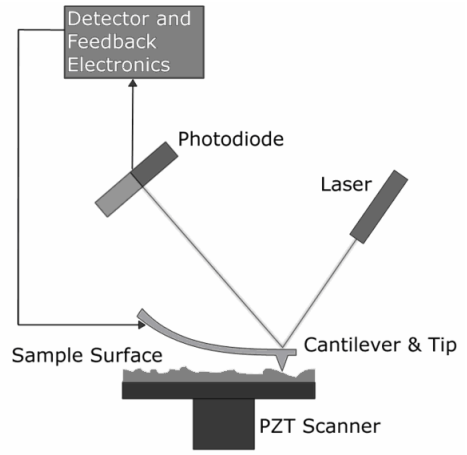

Figure 1. *Schematic representation of an atomic force microscope.*

The AFM can be operated in a number of modes, depending on the application. In general, possible imaging modes are divided into contact modes and non-contact modes in which the cantilever is vibrated.

Contact Mode. In contact mode, also known as repulsive mode, the tip makes soft "physical contact" with the sample. As the scanner traces the tip across the sample, the contact force causes the cantilever to deflect to accommodate changes in topography. In constant force mode, the tip is adjusted to maintain a constant deflection, and therefore constant height above the surface.

Lateral Force Microscopy. It measures frictional forces on a surface by measuring the "twist" of the cantilever. In this way, one can qualitatively determine areas of higher and lower friction.

Noncontact Mode. A stiff cantilever is oscillated close to the sample but without touching it. The forces between the tip and sample are very low, and the detection is based on measuring changes of the resonant frequency or amplitude of the cantilever.

Tapping Mode. In tapping mode AFM an oscillating tip is brought intermittently into contact with the surface during scanning. The cantilever is brought into oscillation, and the changes in oscillation, amplitude, or phase are detected as the vibrating tip sweeps across the surface. The movement of the sample in the z direction, is registered during x-y scanning, and a three dimensional map is constructed which is closely related to the topography of the surface. As the tip gets closer to the sample the amplitude of the tip oscillation decreases due to interactions between the tip and the surface. Therefore, a piezoelectric actuator is used to control the height of the cantilever above the sample. The height is maintained at a set cantilever oscillation amplitude as the cantilever is scanned over the sample. The advantage of tapping the surface is improved lateral resolution on soft samples such as polymers. Lateral forces such as drag, common in contact mode, are nearly eliminated.

7. 2. Ellipsometry

Ellipsometry is a versatile optical technique that uses polarised light to probe the dielectric properties of thin films and bulk materials. This technique is typically used for films with thickness ranging from sub-nanometers to a few microns. It relies on the polarization changes caused by reflection or transmission from a material to deduce its properties, such as thickness morphology, chemical compositions or electrical conductivity. It can yield information about layers that are thinner than the wavelength of the probing light, even down to a single atomic layer. The name “ellipsometry” comes from the fact that polarized light becomes elliptical polarized upon light reflection. Since it is an optical technique, it is non-destructive and contactless. An ellipsometer includes a light source (xenon lamp), a polarization generator, a polarization analyzer and a detector (Figure 2). The polarization generator and analyzer are constructed of optical components that manipulate the polarization: polarizers, compensators, and phase modulators.

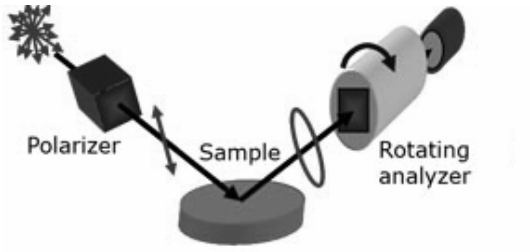

Figure 2. *Schematic representation of an ellipsometer.*

The polarization state of the light incident on the sample may be decomposed into an *s* and a *p* component (the *s* component is oscillating perpendicular to the plane of incidence and the *p* component is oscillating parallel to the plane of incidence) (Figure 3). Upon reflection, the *s* and *p* components experience a different attenuation and phase shift according to the Fresnel equations. The ellipsometer will measure the ratio of the reflected *p* and *s* components (tan ψ) and the phase difference between these two components (cos Δ), which is described by the fundamental equation of ellipsometry (Equation 7. 2):

$$\rho = r_p/r_s = \tan(\psi)e^{i\Delta} \qquad 7.\ 2$$

where, r_s and r_p, are the amplitudes of the *s* and *p* components, after reflection and normalized to their initial value, tan ψ is the amplitude ratio upon reflection, and Δ is the phase shift. The amplitude ratio and the phase shift are related to fundamental physical properties of the sample such as optical constants (refractive index - n and extinction coefficient - k) and thickness of the material.

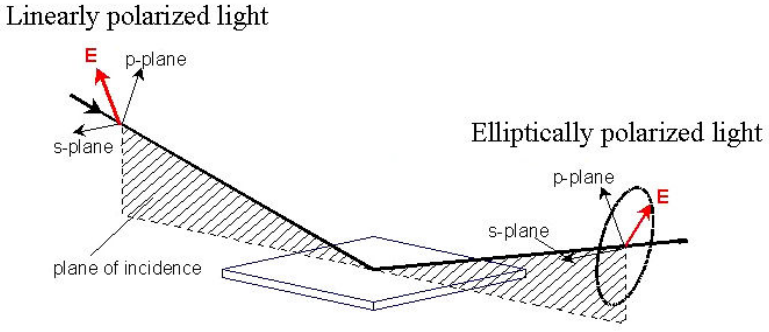

Figure 3. *Schematic of the geometry of an ellipsometry experiment.*

Since ellipsometry is an indirect method, in general the measured Ψ and Δ cannot be converted directly into the optical constants of the sample. Therefore, after the measurement, a layer model is needed to describe the sample, which considers the optical constants and thickness parameters of all individual layers of the sample and also includes the correct layer sequence. The unknown thickness and/or optical constants are determined through the use of an iterative regression fitting computer algorithm which minimises the error between the measured data and the model-generated data by adjusting the physical parameters of the model. The calculated Ψ and Δ values, which match the experimental data best, provide the optical constants and thickness parameters of the sample.

7. 3. Attenuated Total Reflectance (ATR)-FTIR spectroscopy

ATR-FTIR spectroscopy is a sampling technique used in conjunction with infrared spectroscopy. It is widely used to examine a variety of samples such as solids, powders, pastes and liquids without further preparation. An attenuated total reflection accessory operates by measuring the changes that occur in a totally internal reflected infrared beam when it comes in contact with a sample which is placed on a high refractive index crystal (Figure 4). Typical materials for ATR crystals include germanium, zinc selenide or diamond. The later has excellent mechanical properties which make it an ideal material for ATR. In the case of a liquid sample, pouring a very small amount over the surface of the crystal is sufficient. If the sample is solid, it is pressed into direct contact with the crystal.

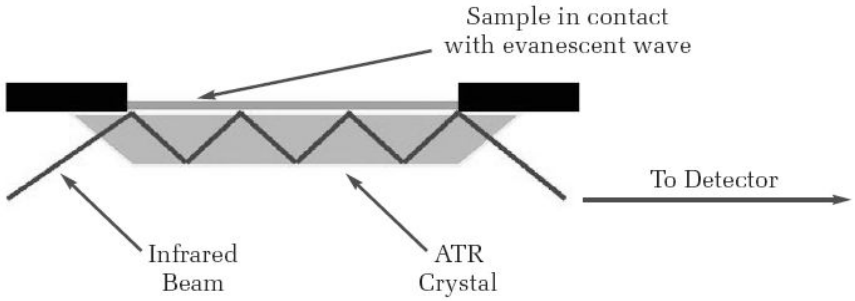

Figure 4*. Schematic representation of an ATR-FTIR spectrometer.*

An infrared beam is directed onto a high refractive index crystal at a certain angle. Due to the nature of the ATRP crystal, the refractive index of the analyzed sample will have a lower refractive index than the refractive index of the crystal. Under these conditions total internal reflection can occur at a certain angle of incidence at the interface between the two media. This internal reflectance creates an evanescent wave that extends only a few microns beyond the surface of the crystal into the sample. In the regions of the infrared spectrum where the sample absorbs energy, the evanescent wave will be attenuated. The beam is then collected by a detector as it exits the crystal and the infrared spectrum of the samples is generated.

7. 4. Contact Angle

The contact angle (θ), is a quantitative measure of the wetting properties of a solid by a liquid. The contact angle can be measured by producing a drop of pure liquid on a horizontal solid surface. It can be defined geometrically as the angle formed by a liquid at the three phase boundary where a liquid, gas and solid intersect (Figure 5a). The contact angle is affected by the chemical composition and the roughness of the surface. A surface with a water contact angle greater then 90^o is called hydrophobic. This condition is exemplified by poor wetting, and a low free energy of the solid surface (Figure 5b). On the other hand, when the contact angle of water is less than 90^o the surface is hydrophilic. This condition illustrates a better wetting, and a higher surface energy (Figure 5c).

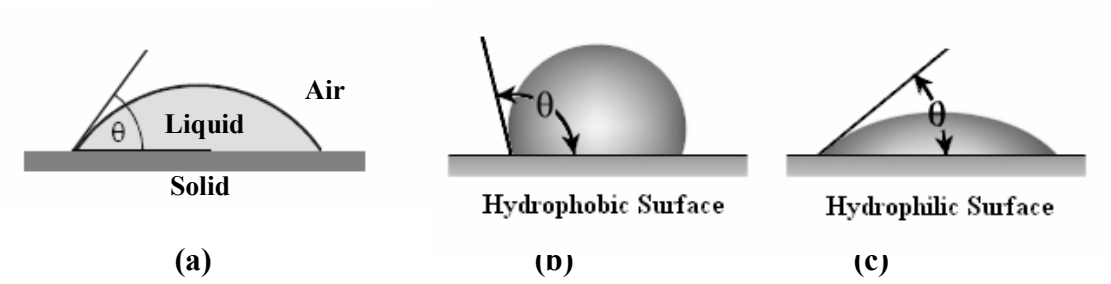

Figure 5*. Contact angle of a liquid on a surface (a); contact angles on a hydrophobic and a hydrophilic surface (b).*

The shape of the drop is controlled by the interaction forces of interfacial tension of each participating phase (gas, liquid and solid). (Figure 6). For a liquid droplet on a flat film the wettability is determined by the surface free energy of the solid substrate, which is commonly given by Equation 7. 3 known as the Young-Laplace equation:

$$\cos \theta = (\gamma_{sv}-\gamma_{sl})/\gamma_{lv} \qquad 7.\ 3$$

where, γ_{sv} is the solid-vapor interfacial energy, γ_{sl} is the solid-liquid interfacial energy , γ_{lv} is the liquid-vapor energy and θ is the equilibrium contact angle. The Young equation assumes a perfectly flat and smooth surface.

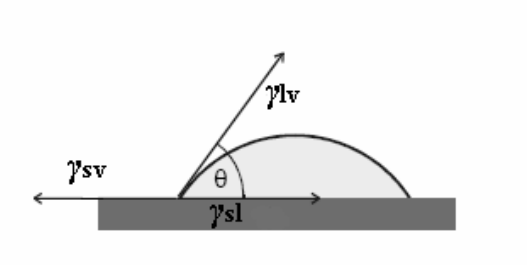

Figure 6. *Contact angle of a liquid on a fla surface and interphase-energy between gas, liquid, and solid phases.*

However, non-ideal conditions, due to roughness and chemical heterogeneity lead to deviations from the Young equation. The theories that are commonly used to correlate the surface roughness with the apparent contact angle of a liquid droplet on a solid substrate are the Wenzel and the Cassie model.

The Wenzel model. In the Wenzel model, illustrated in Figure 7a, the liquid drop fills the grooves of the surface completely. The Wenzel contact angle is given by Equation 7. 4:

$$\cos \theta_W = r \cos \theta \qquad 7.\ 4$$

where, r is the surface roughness factor and θ is the contact angle on a flat surface. The equation above, suggests that if the contact angle of a liquid on a smooth surface is less than 90°, the apparent angle on a rough surface will have a smaller value. If the contact angle on a smooth surface is higher than 90°, the contact angle on the rough surface will be larger.

The Cassie model. The Cassie model assumes that vapor pockets are trapped inside the grooves of the surface underneath the liquid drop (Figure 7b). The Cassie apparent contact angle can be correlated to the chemical heterogeneity of a rough surface by Equation 7. 5:

$$\cos \theta_C = f_s \cos \theta_s + f_v \cos \theta_v \qquad 7.5$$

where f_s is the area fraction of the solid and f_v is the area fraction of the vapor on the surface.

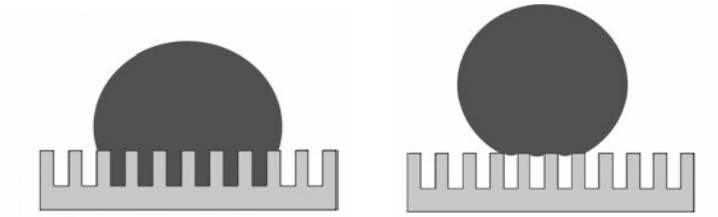

Figure 7. Graphic representation of Wenzel (a) and Cassie models (b).

Measuring methods

A) The static sessile drop method. The wettability of a surface is commonly measured by the apparent contact angle, which is the static behavior of a liquid droplet on a horizontal surface. The sessile drop method is measured by a contact angle goniometer. The profile of a liquid drop on a solid substrate is captured and analyzed by an optical system which employs a high resolution camera and software.

B) The dynamic sessile drop method. *B1) The extension/contraction method.* In this method the droplet is attached to a needle tip on the solid surface, while the contact angle is measured as the droplet amount is increased or decreased. The angle formed while increasing the volume is called the advancing angle, and the angle formed by decreasing volume is called the receding angle. *B2) The sliding method*. This method measures the contact angle of a droplet attached on a tilted solid surface. The angles formed in the front and the back of the droplet sliding down are the advancing angle and the receding angle, respectively.

7. 5. Surface Plasmon Resonance (SPR)

SPR is a real-time imaging technique that has been used to study intra-molecular interactions. It is an optical technique that uses the evanescent wave phenomenon to measure changes in refractive index very close to the sensor surface. It can be used successfully in the analysis of anibody-antigen interaction, to obtain kinetic parameters such as association and dissociation constants in the range of $10^3 – 10^7$ M^{-1}/s and $10^{-5} – 10^{-1}$ s^{-1} respectively, equilibrium binding constants in a range of 10^4 -10^{12} M^{-1} as well for concentration determination in a range of 10^3 -10^{-11} M.

When light traveling within an optically dense medium reaches the interface with a medium of lower refractive index it can be partly reflected and partly refracted. Above a certain critical angle of incidence, no light is refracted across the interface, and total internal reflection is observed. Under these conditions, an electromagnetic field component called, the evanescent wave, penetrates the interface between the two media. Due to its nature, the evanescent wave can only travel for approximately one wavelength within the medium of lower refractive index. If the light is monochromatic and p-polarized (i.e., the electrical vector component is parallel to the plane of incidence) and the interface between two media is coated with a thin layer of metal such as gold then, a sharp intensity dip appears in the reflected light at a specific angle called the SPR angle (Figure 8). A change in the refractive index will lead to a shift in the resonance angle.

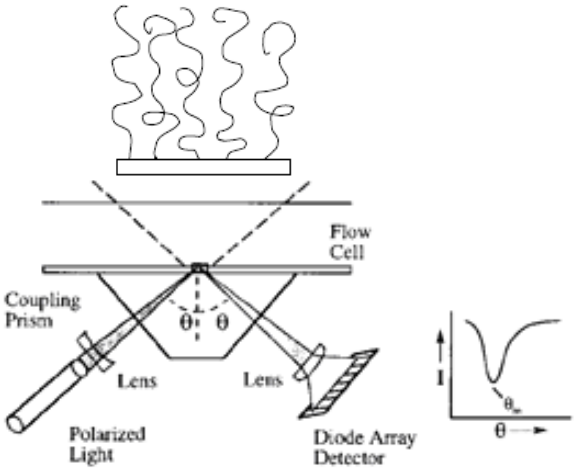

Figure 8. *Schematic representation of an SPR device.*

SPR arises through the interaction of the evanescent wave with the delocalized surface electrons (or plasmons) of the metal layer at the interface with the medium of lower refractive index. SPR occurs at a specific angle of incidence, which depends on the ratio of the refractive indices of the two media, the wavelength of the light and the physical properties of the metal surface. The later parameters, as well as the refractive index of one of the medium can be kept constant and by measuring the angle at which SPR occurs it is possible to monitor the changes in the refractive index of the other medium. In case of protein-adsorption the difference between the refractive index of the buffer and the refractive index of the adsorbed molecules can be easily converted into mass and thickness of the adsorbate as all proteins have almost identical refractive indices.

7. 6. Size Exclusion Chromatography (SEC)

SEC or gel-permeation chromatography (GPC) is a chromatographic method in which molecules in solution are separated based on their hydrodynamic volume. GPC is employed to determine the molecular weight and the molecular weight distribution of polymers. In SEC the polymer is dissolved in an appropriate solvent and is injected into a column packed with porous particles of different pore sizes. The mobile phase is generally the same solvent used to dissolve the polymer. As the polymer elutes thorough the column molecules that are smaller than the pore size can enter the particles and therefore have a longer path and longer transist time than larger molecules that cannot enter the particles. As a result smaller molecules elute at a later time (Figure 9). Since SEC is a relative and not an absolute molecular weight technique, the columns are calibrated with polymer standards of known molecular weight.

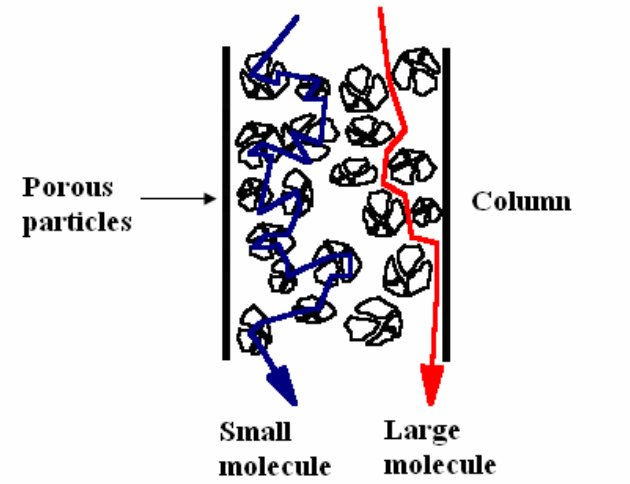

Figure 9. *Schematic of a size-exclusion chromatography column.*

7. 7. References

1. R. Wiesendanger, Scanning Probe Microscopy and Spectroscopy, (Cambridge University Press), **1994**.
2. H. Fujiwara, Spectroscopic Ellipsometry Principles and Applications, (John Wiley and Sons Ltd), **2007**.
3. E. Gizeli, C. R. Lowe, Biomolecular Sensors, (Taylor and Francis), **2002**.
4. Z. Salamon, G. Tollin, Surface Plasmon Resonance, Theory, Spatially Resolved Specroscopic Analysis, Academic Press, **1999**, 2311-2319.
5. R. P. H. Kooyman, Surface Plasmon Resonance, Instrumentation, Spatially Resolved Specroscopic Analysis, Academic Press, **1999**, 2302-2310.
6. X. Feng, L.Jiang, Adv. Mater. **2006**, *18*, 3063–3078.
7. T. Sun, L. Feng, X. Gao, L. Jiang, Acc. Chem. Res. **2005,** 38, 644-652.
8. H. R. Allcock, F. W. Lampe, J. E. Mark, Contemporary Polymer Chemistry 3rd ed. (Pearson Education, Inc) **2003**.

- http://vanha.physics.utu.fi/opiskelu/kurssit/SFYS4294/6-AFM.pdf
- http://www.afmuniversity.org/
- http://www.uta.edu/optics/research/ellipsometry/ellipsometry.htm
- http://academic.brooklyn.cuny.edu/physics/holden/ellipsometry.htm

Acknowledgments

I would like to start by thanking my supervisor, Prof. Maria Vamvakaki for giving me the opportunity to work in this project and for all the assistance she has provided me throughout these years. I would also like to thank my supervisor from the chemistry department, Prof. Demetrios Ghanotakis for supporting me as his student. Prof. Spiros Anastasiadis is acknowledged for his collaboration on the project of pH-responsive surfaces with micro- and nano-structured roughness. He is also thanked for being the interface/buffer (pun intended) between the secretary and me in these past few months. We are obliged to Prof. Nikos Chaniotakis for allowing our group access to lab resources and instrumentation. I also give many thanks to the rest of the committee for taking the time to read and judge my thesis.

Prof. Constantinidis and his group are acknowledged for providing me with all that gold, "unfortunately" it came shaped as a substrate. Many thanks to Katerina for teaching me how to work on the AFM and all her help. Our collaborator Dr. Manolis Stratakis is acknowledged for providing us with the roughened silicon substrates and all his additional assistance. I would also like to thank Prof. Narain Ravin and his group for the synthesis of the glycomonomers.

Many thanks go to Maria, Raluca, Dafni, and Dimitra (or should I say the "pupeze") for making my life in the lab more fun. I would also like to thank Maria for being my friend though all this years.

Special thanks to my parents for their constant support during these years that I have spent away from home. Since I did not listen to my mom and I did not go to medical school to become a doctor, I would like to tell her that finally it all worked out and soon she will call me doctor anyway!!!! And last but not least I would like to thank Niko (The Puss) for listening to the many complaints regarding a polymer chemist's life and for his constant help.

The Greek general secretariat for research and technology (PENED 2003, 03EΔ623) is acknowledged for financial support.